Adv Polym Sci (2006) 199: 1–82
DOI 10.1007/12_076

Published online: 16 February 2006

Polyphenylene-type Emissive Materials: Poly(*para*-phenylene)s, Polyfluorenes, and Ladder Polymers

Andrew C. Grimsdale · Klaus Müllen (✉)

Max-Planck-Institut für Polymerforschung, Ackermannweg 10, 55128 Mainz, Germany
muellen@mpip-mainz.mpg.de

Abstract This chapter reviews the synthesis of the various classes of polyphenylene-based materials that have been investigated as active materials in light-emitting applications. In particular, it is shown how the electronic properties may be controlled by synthetic design. Insoluble poly(*para*-phenylene) can be made by a variety of precursor routes. Attachment of solubilising side chains gives soluble polyphenylenes in which a high degree of torsion between adjacent benzene rings produced by steric interactions between the substituents strongly reduces their electronic interaction. The phenylene units can be made coplanar by bridging them with methine or other bridges to produce ladder-type polymers, which show excellent photophysical properties, but strong intermolecular interactions lead to problems in obtaining blue emission. Similar problems are seen for 'stepladder' polymers such as polyfluorenes with only partial bridging of the phenylene rings. These interactions may be controlled by introduction of bulky substituents. The electroluminescence efficiency of these materials can also be enhanced by use of charge-transporting substituents. Copolymerisation with lower-band-gap units enables tuning of the emission colour across the entire visible range.

Keywords Poly(*para*-phenylene)s · Ladder polymers · Photoluminescence · Electroluminescence · Light-emitting diodes

Abbreviations

Ac	acetyl
AIBN	azabis(isobutyronitrile)
Boc	*tert*-butoxycarbonyl
Bu	butyl
sec-Bu	*sec*-butyl
^{t}Bu	*tert*-butyl
Cp	cyclopentadienyl
DMSO	dimethyl sulfoxide
ECL	effective conjugation length
EL	electroluminescence
eV	electron volt
HOMO	highest occupied molecular orbital
IR	infrared
ITO	indium tin oxide
LB	Langmuir–Blodgett
LEC	light-emitting electrochemical cell
LED	light-emitting diode
LPPP	ladder-type poly(*para*-phenylene)
LUMO	lowest unoccupied molecular orbital
MALDI-TOF	matrix assisted laser desorption ionisation–time of flight mass spectrometry

Me	methyl
Me-LPPP	methyl-substituted LPPP
M_n	number-averaged molecular weight
M_w	weight-averaged molecular weight
NMR	nuclear magnetic resonance spectroscopy
PANI	polyaniline
PDAF	poly(dialkylfluorene)
PEDOT	poly(3,4-ethylenedioxythiophene)
PEO	poly(ethylene oxide)
PF	polyfluorene
Ph	phenyl
Ph-LPPP	phenyl-substituted LPPP
PIF	polyindenofluorene
PMMA	poly(methyl methacrylate)
PPP	poly(*para*-phenylene)
PPV	poly(*para*-phenylene vinylene)
PS	polystyrene
PSS	poly(styrene sulfonate)
PVK	poly(*N*-vinyl carbazole)
TGA	thermal gravimetric analysis
UV-VIS	ultraviolet–visible

1 Introduction

Polyphenylenes are one of the most important classes of conjugated polymers and have been the subject of extensive research, particularly as active materials for use in light-emitting diodes (LEDs) [1, 2] and polymer lasers [3]. These materials have been of particular interest as potential blue emitters in such devices. The discovery of stable blue-light-emitting materials is a major goal of research into luminescent polymers [4]. In this chapter we review the synthesis of polyphenylene-based materials for light-emitting applications, with a particular emphasis on how the properties of the materials may be tuned by synthetic design. The classes of material that will be covered in this review (Scheme 1) are polyphenylenes including poly(*para*-phenylene) (PPP, **1**) and soluble PPPs (**2**), in which there is only a single bond between each adjacent pair of phenylene units, ladder-type PPPs (LPPPs, **3**), in which all the phenylene units are tied together in a coplanar fashion by methine bridges, and so-called 'stepladder' polymers such as polyfluorenes (PFs, **4**) and polyindenofluorenes (PIFs, **5**), in which only some of the phenylenes are linked by methine bridges. In this introduction we present an overview of the important properties of these materials that need to be controlled in order to obtain efficient LEDs, of the general principles of how these properties may be controlled by synthetic or other methods, and of the general synthetic methods available for the preparation of these polymers. We will then present a more

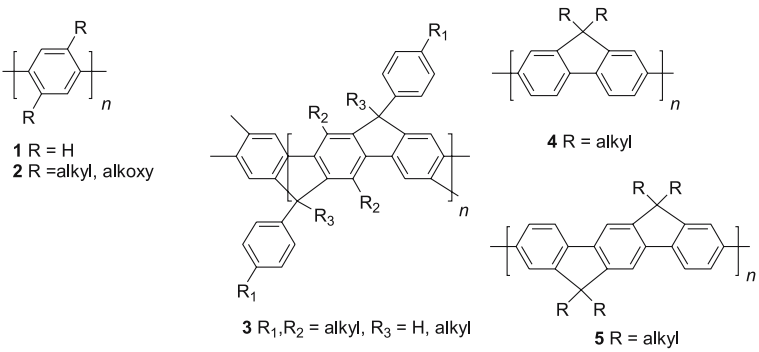

Scheme 1 Typical polyphenylene-based conjugated polymers

detailed discussion of the synthesis and optimisation of polymer properties for each class of material.

There are several properties of luminescent materials that need to be controlled in order to make efficient LEDs and lasers. The first is the colour of the emission, which is primarily determined by the energy difference (band gap) between the highest occupied molecular orbital (HOMO) and the lowest unoccupied molecular orbital (LUMO), but in the solid state is also affected by interactions between the molecules or polymer chains which can lead to red shifts in the emission due to formation of aggregates. This can be controlled by manipulating both the polymer backbone and the substituents. Polyphenylenes are intrinsically blue-emitting materials with large HOMO-LUMO gaps but, as we will show, by copolymerisation with other materials it is possible to tune the emission colour across the entire visible spectrum. Even without incorporation of comonomers it is possible to tune the emission colour over a substantial range by controlling the conjugation length through restriction of the torsion of adjacent phenylene rings. Thus substitution of PPP (**1**) with solubilising groups to give soluble PPPs (**2**) causes a blue shift in the emission as the steric interactions between the side chains induce increased out-of-plane twisting of the phenylene units, while the enforced coplanarity produced by the methine bridges in LPPP (**3**) results in a marked red shift in the emission. The 'stepladder' polymers such as PFs (**4**) and PIFs (**5**) show emission colours intermediate between those of **2** and **3**. As already mentioned, solid-state interactions between polymer chains can cause red shifts in the emission from these materials, which can be suppressed by suitable choice of substituents. This can however adversely affect the charge-transporting properties of the material (see below).

The second critical property to be tuned is the efficiency of charge injection, which is determined by the energy barrier between the HOMO and the anode (for hole injection) and between the LUMO and the cathode (for electron injection), and of charge transport which is controlled by intermolecular

or interchain interactions. Polyphenylenes are materials with intrinsically low-lying HOMOs (typically 5.8–6.0 eV), which creates a large barrier to hole injection from the most widely used anode material, indium tin oxide (ITO), which has a work function of 4.8–5.0 eV. The LUMO values are typically around 2.2–2.5 eV, which makes electron injection from air-stable metals like aluminium (work function 4.3 eV) difficult, thus requiring the use of more electropositive metals such as calcium (work function 2.9 eV) as cathodes. Obviously, one can improve the charge injection by raising the HOMO and/or lowering the LUMO energy of the polymer, but in doing so one reduces the size of the energy gap and so red shifts the emission colour. As a result, obtaining efficient blue emission is a particular problem.

The efficiency of devices can be increased by the incorporation of layers of charge-injecting (or level-matching) materials which have energy levels intermediate between that of the emissive layer and the work function of the electrode, but the use of such layers has the disadvantage of increasing the device thickness which increases the driving voltage, and also complicates device fabrication as successive layers have to be deposited in ways such that the lower layers are not disturbed by deposition of the upper ones. Blending charge- transporting materials into the emissive layer leads to problems with phase separation giving unstable device performance. Incorporation of charge-accepting units into the polymer backbone or onto the side chains avoids both these problems. This approach has been used to successfully improve both the hole- and the electron-accepting properties of phenylene-based polymers. Good charge transport in the solid state requires close packing of polymer chains permitting rapid and efficient hopping of charges between chains. As mentioned above, strong interchain interactions can cause undesirable red shifts in the emission spectrum, so that it is sometimes necessary to compromise the charge-transport properties of the material to obtain the desired emission colour.

Other desirable properties are the ability to form defect-free films, preferably by solution-processing techniques, a high solid-state photoluminescence (PL) quantum efficiency, and good stability towards oxygen and light. For some applications the ability to obtain polarised light is also desirable. All of these properties are to some extent controllable by design of the structure and the synthetic pathway. The formation of a thick, uniform defect-free film by spin coating or similar solution-processing methods is dependent upon many factors. The first is the molecular mass of the compound, as low molar mass materials tend to be crystalline and so do not form high-quality amorphous films, while very high molar mass polymers are difficult to dissolve. The second is the solubility. To obtain a good film, the material must be reasonably soluble as too dilute solutions give too thin films, and must not form aggregates in solution as these will tend to lower the film quality (uneven morphology) and may produce red shifts in the emission. The exact PL efficiency of a given material is as yet not predictable,

but the removal of fluorescence quenching defects, such as halide atoms or carbonyl groups, and the suppression of interchain interactions leading to non-radiative decay pathways, are known to assist in improving solid-state quantum efficiency of materials. The stability of a polymer towards photo-oxidation can be improved by avoiding susceptible functional groups, e.g. benzyl protons. Polarised emission is obtained by alignment of the polymer chains, which seems to be easiest for polymers which possess a liquid-crystalline mesophase [5]. Circularly polarised emission has been obtained by using chiral side chains.

The synthesis of polyphenylenes has been reviewed most recently by Kaeriyama [6] and Scherf [7]. There exist three general methods for the synthesis of polyphenylene-based materials: (a) aromatisation of poly(cyclohexa-1,3-diene) precursor polymers, which is used only to make poly(*para*-phenylene (PPP, **1**) and rod–coil copolymers containing PPP rods; (b) oxidative coupling of monomers, which is of strictly limited synthetic utility as only low molecular mass materials are obtained from such methods; and (c) transition-mediated polycondensations of substituted aromatic compounds and/or aryl organometallic compounds. This last is the main method for preparing phenylene-based polymers. The two main polycondensation methods used are the Suzuki polycondensation of aryl halides with arylboronic acids [8] and the Yamamoto polymerisation of aryl dihalides using nickel(0) reagents [9]. Generally speaking, the Suzuki method gives higher molecular masses than the Yamamoto procedure, but is synthetically more demanding. A more detailed comparison of the relative merits of the two methods will be given in the discussion of the synthesis of soluble PPPs (Sect. 2.2, below). Other coupling reactions, e.g. Stille coupling of aryl halides and aryl tin reagents [10] or Kumada coupling of aryl halides with aryl Grignard reagents [11], have also been used to make polyphenylenes, but generally give lower molecular masses than the Suzuki or Yamamoto methods.

2
Poly(*para*-phenylene)s

2.1
Poly(*para*-phenylene) (PPP)

2.1.1
PPP by Coupling of Benzene Rings

Unsubstituted PPP (**1**) is insoluble, and so direct synthesis by oxidation of benzene by the Kovacic method [12] or by nickel(0) coupling of 1,4-dihalobenzenes [9] (Scheme 2) gives insoluble and intractable powders with degrees of polymerisation of about 20 as determined by IR absorption meas-

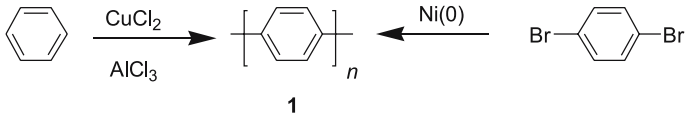

1

Scheme 2 Direct routes to PPP

urements [13]. The material obtained by the Kovacic method contains a large amount of defects due to 1,2-coupling and/or formation of condensed polyaromatic units, while the Yamamoto method gives only 1,4-coupling.

Films of oligophenylenes with an average of about nine benzene rings (**1**, $n = 9$) can be prepared from these powders by vacuum deposition [13, 14]. Due to the difficulty of obtaining pure oligomers of PPP with more than six benzene rings, the effective conjugation lengths (ECLs) for absorption and emission of PPP (i.e. the lengths beyond which increasing the length of the polymer chain produces no further red shift in absorption or emission) have not been determined. A study of oligomers with solubilising substituents (**2**, $n = 3$–17) determined the ECLs for such compounds to be 11 phenyl rings for absorption and seven rings for emission [15]. As substituted PPPs (**2**) have shorter conjugation lengths than PPP (**1**) due to the steric interactions between the substituents leading to greater out-of-plane twisting of the conjugated backbone, the ECLs for **1** can be expected to be longer. Related polymers such as ladder-type PPPs (**3**, Sect. 3.1), polyfluorenes (**4**, Sect. 4.1), and polyindenofluorenes (**5**, Sect. 4.2) in which the torsion angles between adjacent units are similar to or smaller than in PPP all show ECLs for emission of between 11 and 15 phenyl rings. The EL emission maximum from devices using vacuum-deposited films of PPP oligomers ($n \sim 9$) occurs at 446 nm [16–18]. Comparison of the EL maxima from these devices and those using high molecular weight PPP made by a precursor route (see below) suggests that the ECL for emission from **1** is greater than 10 benzene rings. Insertion of a poly(*N*-vinylcarbazole) (PVK) charge-transporting layer improves the efficiency tenfold, but at low voltages there is considerable emission ($\lambda_{max} = 550$ nm) from an excimer between PVK and the oligophenylenes [18]. As the voltage increases this decreases as the recombination zone shifts into the bulk of the oligophenylene layer, thus giving voltage-tunable EL. Leising and coworkers have used well-defined films of a hexaphenyl oligomer (**1**, $n = 6$, sexiphenyl) to make blue-emitting devices, with an emission maximum at 425 nm [19–26]. Comparison of the EL spectra of sexiphenyl films with the orientation of the oligomers variously parallel or perpendicular to the substrate shows that the latter gives brighter emission with a narrower spectrum [27]. Polarised emission has been reported from oriented films of sexiphenyl [28, 29]. The Leising group have made red- and green-emitting devices using thin films of sexiphenyl covered with appropriate dyes to convert its blue emission [23, 30–35]. White emission is obtainable by appropriate colour mixing [35].

2.1.2 Precursor Routes to PPP

Films of PPP have to be prepared via precursor routes (previously reviewed by Gin and Conticello [36]). The route most often used to prepare films of PPP (**1**) is one developed at ICI (Scheme 3) [37, 38]. This starts with a microbial oxidation of benzene to cyclohexadienediol **6**. Radical-initiated polymerisation of the diacetate **7** gives the precursor polymer **8**, which is then thermally converted to **1**. However, the material is not stereoregular as it contains about 10–15% of 1,2-linkages. This material has been used by Leising et al. to prepare blue-emitting LEDs (λ_{max} = 459 nm) with efficiencies of up to 0.05% [39–41].

A number of other diesters of **6** have been polymerised by the same method (again with 10–15% of 1,2-linkages in the polymer) and thermally converted to PPP, with the highest molecular weights being obtained with dimethyl carbonate and dipivaloyl esters [42]. Copolymers with blue-shifted PL spectra can be prepared by copolymerisation of **7** and 10 mol % of vinylbiphenyl or *N*-vinylcarbazole [43, 44]. The blue shift is due to interruption of the conjugation by the non-aromatic units.

Totally stereoregular PPP (i.e. with all 1,4-linkages) has been prepared by Grubbs and coworkers (Scheme 4) by a stereospecific nickel-catalysed polymerisation of a cyclohexadienediol disilylether **9**, followed by conversion of the resulting polymer **10** to **1** via the acetoxy-precursor **8** [45–48]. However,

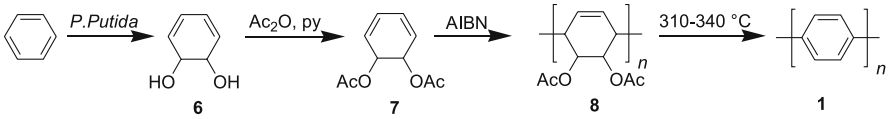

Scheme 3 ICI route to PPP

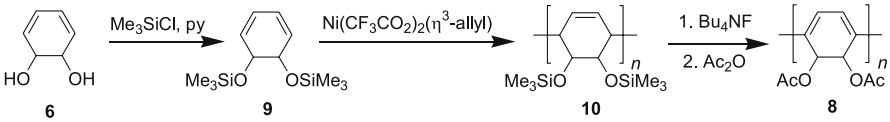

Scheme 4 Grubbs route to regioregular PPP

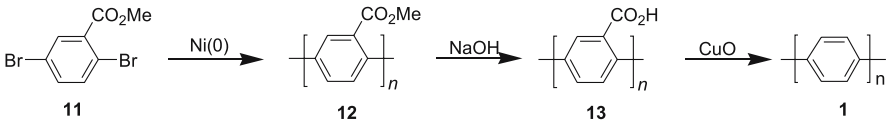

Scheme 5 Kaeriyama precursor route to PPP

to assist processing they used an acid catalyst in the final step, which badly contaminated their product, making it unsuitable for use in LEDs.

Another method for preparing all 1,4-linked PPP is that of Kaeriyama and coworkers (Scheme 5) [49, 50]. Yamamoto polycondensation of methyl 2,5-bromobenzoate **11** produced a soluble all-para polymer **12**, which was hydrolysed to the polyacid **13** and then decarboxylated to give PPP. However, the decarboxylation cannot be satisfactorily performed in the solid state, so this method is unsuitable for preparing high-quality films.

PPP films can also be prepared by electropolymerisation under either reductive or oxidative conditions, but the EL properties have been found to be highly dependent on the polymerisation conditions [51]. A study of the PL efficiency of PPP thin films of varying chain length concluded that for highly ordered PPP films a chain length of 25–30 units was optimal [52]. Oriented films of PPP have been prepared by a friction deposition method and found to show highly polarised fluorescence [53].

2.2
Poly(*para*-phenylene)s with Solubilising Substituents

2.2.1
Synthetic Routes to Substituted PPPs

Yamamoto and coworkers prepared a PPP derivative **14** by treatment of **1** (prepared by the Yamamoto method [54]) with perfluorpropylperoxide (Scheme 6). From NMR and other analysis they estimated that the average chain length was 13 benzene units with an average of two perfluorpropyl units per molecule. This material showed blue PL (λ_{max} = 450 nm), and was used to construct a device whose emission colour was found to shift from green to blue with increasing applied voltage [55].

More generally, PPP derivatives **15** with solubilising side chains, most commonly alkyl or alkyoxy groups, are prepared by transition metal catalysed polycondensations [56]. The main methods used are the Suzuki and Yamamoto polycondensations. Two variations of the Suzuki polycondensation can be used. The simpler, so-called 'AB coupling' (Scheme 7), involves conversion of a dibromobenzene **16** into a bromoarylboronic acid **17**, which is then homocoupled to give **15**. Random copolymers can be made by using a mixture of monomers.

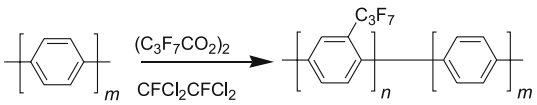

1 14

Scheme 6 Perfluorpropylation of PPP

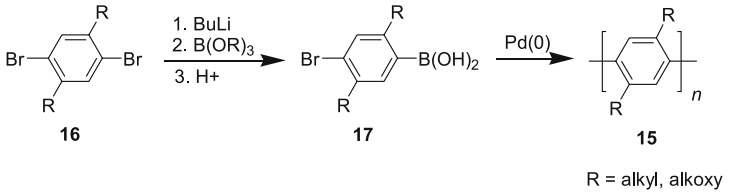

Scheme 7 Soluble PPPs by AB-type Suzuki polycondensation

In the other 'AA-BB coupling' method (Scheme 8) a phenylbisboronic acid **18** is coupled with a dihalobenzene **16.** This method has the advantage of permitting the preparation of alternating copolymers **19**, but there can be experimental difficulties as exactly equimolar amounts of **16** and **18** are required for optimal polymerisation. In particular, boronic acids are hygroscopic, may be contaminated with significant amounts of the anhydrides, and are often difficult to purify. As a result boronic esters are frequently preferred as reagents, even though their preparation involves an extra step, as they are usually easier to purify and handle.

Considerable work in optimising the Suzuki polycondensation methods for making polyphenylenes has been done, particularly by the Wegner and Schlüter groups [57–64]. For a fuller description of the scope and problems of Suzuki polycondensation, the reader is referred to the recent review by Schlüter [8].

The Yamamoto method of condensing dihalobenzenes **16** with nickel(0) (Scheme 9) has the advantage of experimental simplicity, but is limited to preparation of homopolymers and random copolymers, and requires stoichiometric amounts of expensive nickel(0) reagents. These can be generated in situ by the reduction of nickel(II) salts in the presence of suitable ligands,

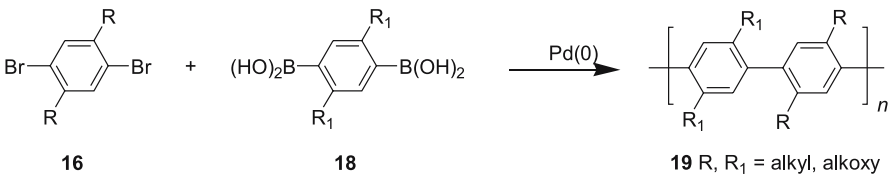

Scheme 8 Soluble PPPs by AA-BB-type Suzuki polycondensation

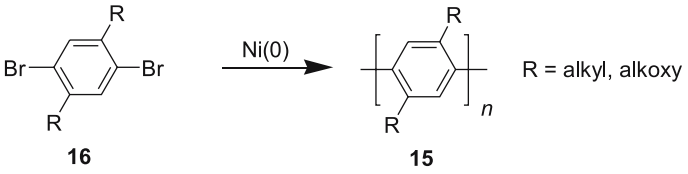

Scheme 9 Soluble PPPs by Yamamoto polycondensation

but the results from such polymerisations tend to be inferior than from the use of commercially available nickel(0) reagents. For a more comprehensive discussion of the reagents and conditions for this method, the reader is referred to the review by Yamamoto [9].

Percec and coworkers have developed a variation of this method in which hydroquinone bistriflates **20** [65–67] or bismesylates **21** [68, 69] are coupled to give alkyl, aryl, or ester functionalised PPPs **22** (Scheme 10). An advantage of this method is that the monomers are easily prepared from hydroquinone.

Poly(2,5-dialkoxy-1,4-phenylene)s can also be made by oxidation of *para*-dialkoxybenzenes (Scheme 11). Thus, 1,4-dimethoxybenzene (**23**) can be polymerised with aluminium chloride and copper(II) chloride or iron(III) chloride. The polymer **24** is only soluble in sulfuric acid, however, and so not usable in LEDs [7]. Oxidation of 1,4-dibutoxybenzene (**25**) with iron(III) chloride by contrast gives a polymer **26** which is soluble in organic solvents [70, 71].

Of these methods it is reported that the Suzuki method gives the highest degrees of polymerisation in alkyl or alkoxy PPPs [72]. In addition to alkyl and alkoxy groups, a wide range of other substituents have been used to solubilise PPPs. In polymers where the rings have two identical substituents, the question of polymer regioregularity does not arise, but in other cases there is the possibility of the units coupling in either a 'head-to-head' or 'head-to-tail' fashion (Scheme 12). The different steric interactions between the substituents on adjacent units may cause different degrees of out-of-plane twisting in the two cases, which will affect the conjugation length, while the differences in the interactions between the chains may cause differences in chain packing, which influences the morphology of the polymer film and the rates of charge-carrier and exciton migration between chains. To date

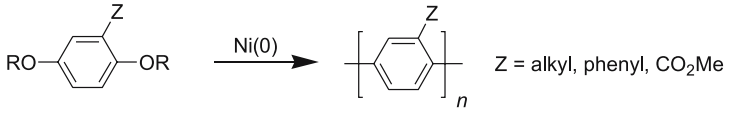

20 R = CF_3SO_2
21 R = CH_3SO_2

22

Scheme 10 Percec route to soluble PPPs

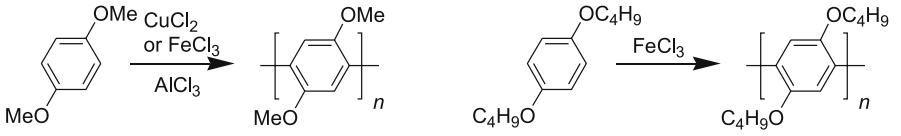

23 **24** **25** **26**

Scheme 11 Alkoxy-substituted PPPs by oxidative polymerisation

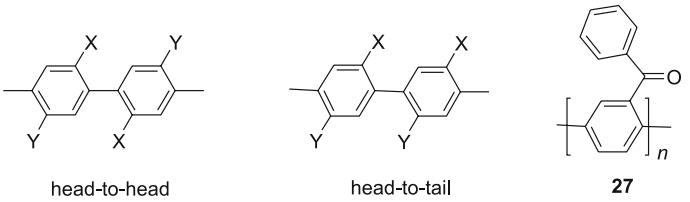

Scheme 12 Regioisomerism in substituted PPPs

the only report of the synthetic control of the regioregularity of a substituted PPP influencing the properties comes from the synthesis of poly(2-benzoyl-1,4-phenylene) (**27**) by Yamamoto polycondensation [73]. When the polycondensation was performed with 2,2-bipyridyl as a ligand, the resulting polymer was found to have a sharply red-shifted UV absorption maximum (λ_{max} = 352 nm versus 328 nm) indicating a much longer conjugation length, which was attributed to the material being much more head-to-tail regioregular.

2.2.2
Luminescent Properties of Soluble PPPs

These polymers show blue PL emission and many of them have been used by various groups to make LEDs (Scheme 13) [71, 74–89]. The EL spectra are often red shifted compared to the PL spectra and, due to formation of aggregates which show longer-wavelength, usually yellow, emission the overall EL emission colour is not always blue, but may be green or even white, particularly after operation of the device for some time. Efficiencies from single-layer devices are about 0.05% with aluminium cathodes (work function 4.3 eV), and up to 1.8% with more electropositive calcium cathodes (work function 2.9 eV), due to the smaller energy barrier between the LUMO (∼ 2.2–2.5 eV) and the electrode. By using a hole-injecting layer of PVK (work function 5.5 eV), efficiencies of up to 3% have been obtained using calcium cathodes, and of up to 0.8% using other, more air-stable metal cathodes. This suggests that the main limiting factor for emission efficiency in these materials is

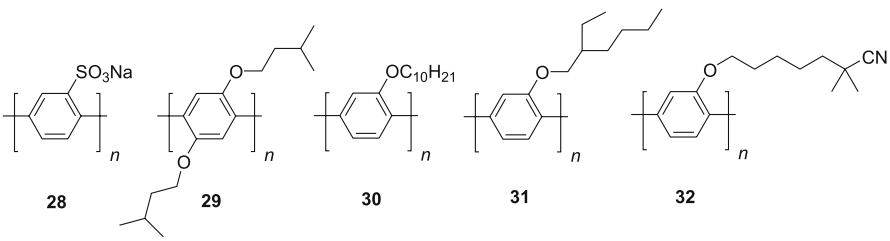

Scheme 13 Typical substituted PPPs used in blue-emitting devices

hole injection due to their very low HOMO energy levels ($\sim$ 6.0 eV) creating a large barrier to charge injection from ITO (work function 4.8–5.0 eV). No systematic study has been done on the effects of the substituents upon the EL efficiency, but Neher and coworkers reported that single-layer devices using the sulfonium-substituted polymer **28** gave efficiencies of 0.5–0.8% with an aluminium cathode, which is an order of magnitude higher than for the dialkoxysubstituted polymer **29** in identical devices [80]. Heeger and coworkers [77] have compared the PL and EL efficiencies of the mono-substituted polymers **30–32**. They showed identical PL efficiencies in solution (85%), but in the solid state the polymers **31** and **32** with branched side chains showed higher efficiencies (40% and 46%, respectively) than the polymer **30**, which has straight alkyl chains (35%). This may reflect less efficient polymer chain packing in the former, due to the bulkier substituents, leading to less exciton migration and non-radiative decay. Conversely, the EL efficiency of double-layer devices using **30** (3.0%) was higher than for **31** (2.0%) or **32** (1.4%).

Use of sulfonium or other ionic substituents also gives solubility in very polar solvents including water [90–93]. Though water is not a desirable solvent for processing materials for use in electronic devices due to the danger of corrosion of the electrodes, the ability to process from highly polar solvents such as ethanol can be advantageous in constructing multi-layer devices as many organic electronic materials have very limited solubility in such solvents, thus allowing an ethanol-soluble material to be deposited from solution on top of such a material. Use of a polyaniline (PANI) anode or blending of the PPP derivative with a hole-transporting material lowers the operating voltage [77, 78].

Polarised EL emission has been obtained from a device using polymer **29** deposited as a Langmuir–Blodgett (LB) film [79, 81]. In contrast to the blue emission obtained from spin-coated films, the emission from the LB films is mainly yellow due to the formation of aggregates, with the emission parallel to the dipping direction (λ_{max} = 536 nm) slightly red shifted compared to the perpendicular emission (λ_{max} = 524 nm). Polarised EL emission has also been obtained by rubbing alignment of a film of **33** (Scheme 14) [94]. Another way to induce alignment is to incorporate mesogenic units in the side chains. Thus, polarised PL has been obtained from films of polymer **34** containing liquid-crystalline cyanobiphenyl group substituents [95–97].

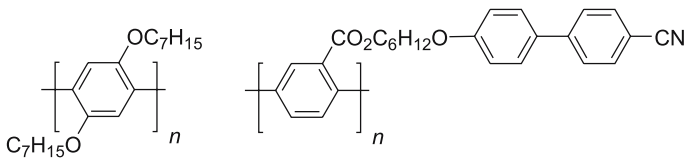

33 **34**

Scheme 14 PPPs from which polarised emission has been obtained

Circularly polarised emission is possible from polymers containing chiral groups. Scherf and coworkers have prepared a cyclophane-substituted PPP by the Suzuki route using the dibromocyclophane **35** and the corresponding bisboronic acid **36** (Scheme 15) [98, 99]. If racemic monomers were used the resulting polymer **37** was not chiral with the cyclophanes randomly distributed on either face of the polymer (atactic). If resolved enantio-pure monomers were used, then the stereoregular isotactic **38** or syndiotactic **39** polymers could be obtained depending upon which enantiomer of each monomer was used. The isotactic polymer is chiral and both enantiomers have been prepared.

Not all the substituents need to be chiral to achieve overall chirality in the polymer. Thus, the copolymer **40** (Scheme 16) containing only 5% chiral units shows a Cotton effect in the circular dichroism spectrum [100]. Circularly polarised PL has been obtained from a copolymer **41** containing both mesogenic and chiral side chains [101].

Complexation of a PPP **42** having carboxylate substituents (Scheme 17) with cyclodextrin gives a fluorescent polyrotaxane which shows a PL

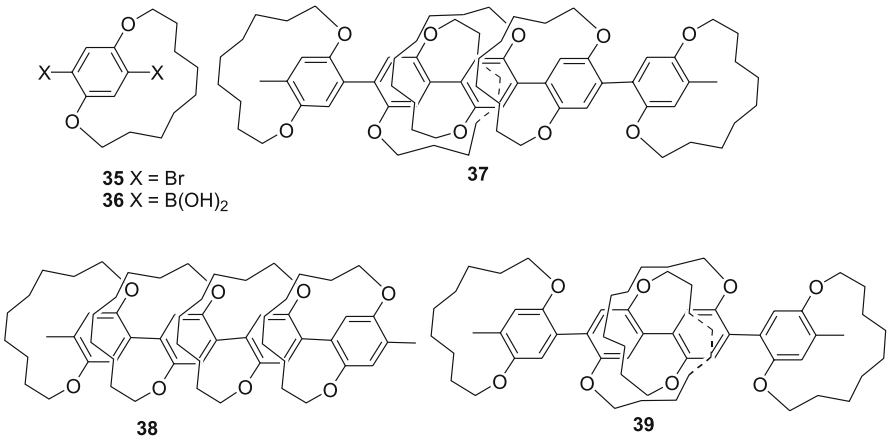

Scheme 15 Stereoisomeric cyclophane-substituted PPPs

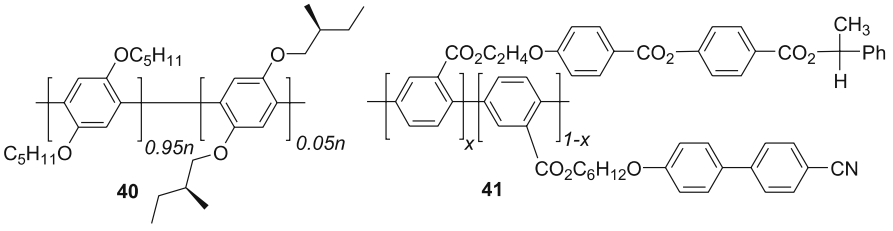

Scheme 16 Other PPPs producing circularly polarised emission

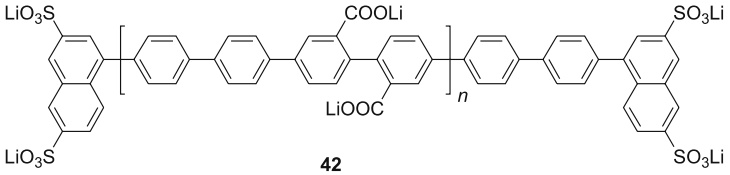

42

Scheme 17 Polycarboxylate used to make fluorescent polyrotaxane

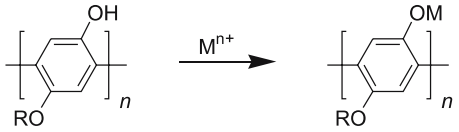

43 R = $C_{12}H_{25}$
44 R = $C_{16}H_{33}$
45 R = $C_{18}H_{37}$

M = Na^+, Co^{2+}, Cu^{2+}, Fe^{3+}

Scheme 18 Complexation of polyphenols with metal ions

maximum at λ_{max} = 410 nm compared to 430 nm for the uncomplexed chain [102]. The EL for the rotaxane is reported to be slightly red shifted compared with the PL [103].

A red shift in the PL emission from the polyphenols **43–45** has been observed upon complexation with metal ions (Scheme 18) [104]. The uncomplexed polymers show violet PL (λ_{max} = 402 nm) in THF solution. Treatment with one equivalent of sodium hydroxide solution produces a marked red shift to give blue-green emission, together with a large drop in the PL intensity. The degree of red shifting depends upon the chain length of the alkoxy substituents, with the red shifts observed for **43** (λ_{max} = 474 nm) and **44** (λ_{max} = 479 nm) being much larger than for **45** (λ_{max} = 461 nm). Similar effects are seen upon addition of methanolic solutions of metal ions to solutions of the polymers in THF. Thus, complexation of **43** with cobalt(II) or copper(II) shifts the PL maximum into the blue (λ_{max} = 436 nm), while the iron(III) complex emits in the green (λ_{max} = 509 nm). Here the length of the side chain has an even bigger effect on the size of the red shift, as complexation of **44** with copper produces blue-green (λ_{max} = 471 nm) PL, with the cobalt and iron complexes emitting in the green (λ_{max} = 471 nm) and the yellow (λ_{max} = 551 nm) regions of the spectrum, respectively. Polymer **45** shows smaller red shifts than **44** upon complexation with copper (λ_{max} = 499 nm) or iron (λ_{max} = 519 nm), but a greater shift with cobalt (λ_{max} = 489 nm). Presumably these effects reflect either changes in the planarity of the polymer chain or emission from aggregates brought about by the complexation. There is no report of whether similar effects are seen in the solid-state spectra of these materials, but this approach is an excellent example of how control-

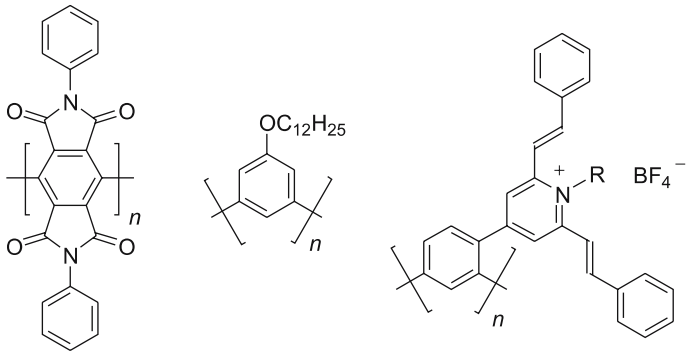

46 **47** **48** R = alkyl, phenyl

Scheme 19 Soluble PPPs with very short conjugation lengths

ling interchain interactions can profoundly influence the optical properties of a conjugated polymer.

A major feature of these materials is that steric interactions between the solubilising substituents lead to an increased phenylene–phenylene torsion from 23° in PPP to around 60–80° in polymers with substituents in the 2- and 5- positions [105]. As a result, the conjugation along the backbone is much reduced, so that their absorption and emission are blue shifted compared with PPP. Their PL emission is thus largely in the violet with a maximum typically between 400 and 420 nm. As mentioned in Sect. 2.1 above, the effective conjugation lengths for the poly(dialkoxyphenylene) **29** have been determined to be 11 phenyl rings for absorption and seven rings for emission, which are somewhat lower than for other polyphenylene-based materials [15].

An exception is the bisimide **46** (Scheme 19), which shows green PL (λ_{max} = 553 nm) that is similar to that of the monomer, suggesting that the emission comes from isolated monomer units [106]. A soluble poly(*meta*-phenylene) **47**, made by Reddinger and Reynolds by the Yamamoto method, which has an even shorter conjugation length, emits mainly in the ultraviolet (λ_{max} = 346 nm) [107]. Other *meta*-linked polymers **48**, however, show violet-green PL (λ_{max} = 445–532 nm) as the emission comes from the substituents [108].

2.2.3 Copolymers with Partial Substitution

One way to red shift the emission is to make copolymers with only partial substitution. Holmes and coworkers prepared the random copolymer **49** with 33% of unsubstituted phenylene units ($m : n = 2 : 1$) by copolymerisation of the substituted and unsubstituted bromobenzene boronic acids (Scheme 20) [75]. The PL emission was blue ($\lambda_{max} \sim 420$ nm), but the EL was

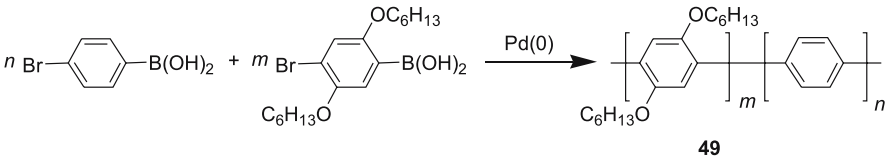

49

Scheme 20 Partially substituted PPP random copolymers by Suzuki polycondensation

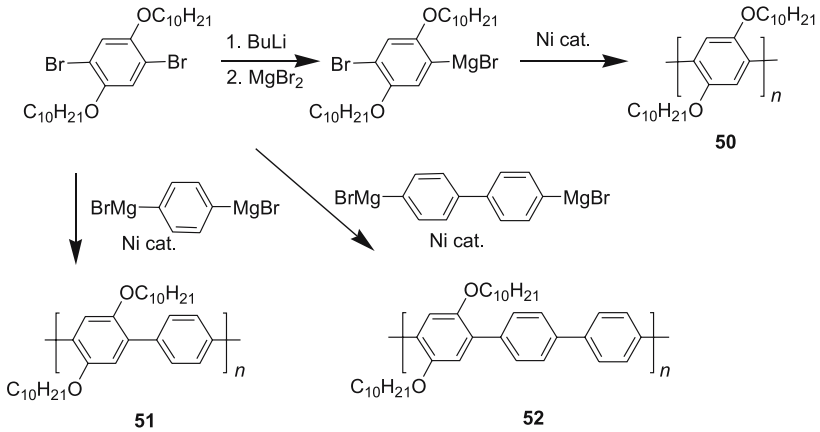

Scheme 21 PPPs with varying degrees of substitution by Grignard coupling

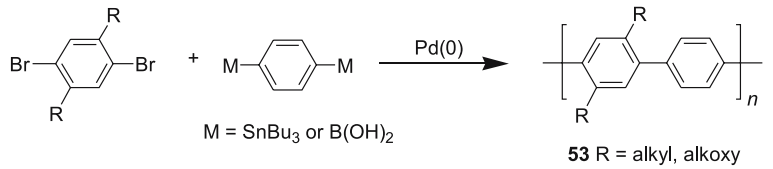

Scheme 22 Partially substituted PPP alternating copolymers by other routes

white with the emission maximum being red shifted by about 70 nm, and a broad featureless tail up to 800 nm being seen, which was attributed to emission from excimers.

Fu has prepared the homopolymer **50** and the copolymers **51–52** by Grignard coupling (Scheme 21) [88]. While **50** shows violet emission (λ_{max} = 415 nm), the PL from **51** and **52** is blue-green (λ_{max} = 450, 500 nm).

Copolymers **53** with alternating substituted and unsubstituted phenylenes have also been made by Stille [109, 110] or Suzuki coupling (Scheme 22) [72, 111, 112]. These copolymers show violet to blue (λ_{max} = 370–425 nm) fluorescence. The emission from the dialkoxy-substituted polymers is red shifted by $\sim$ 50 nm compared with their dialkyl analogues [89, 109–111]. These copoly-

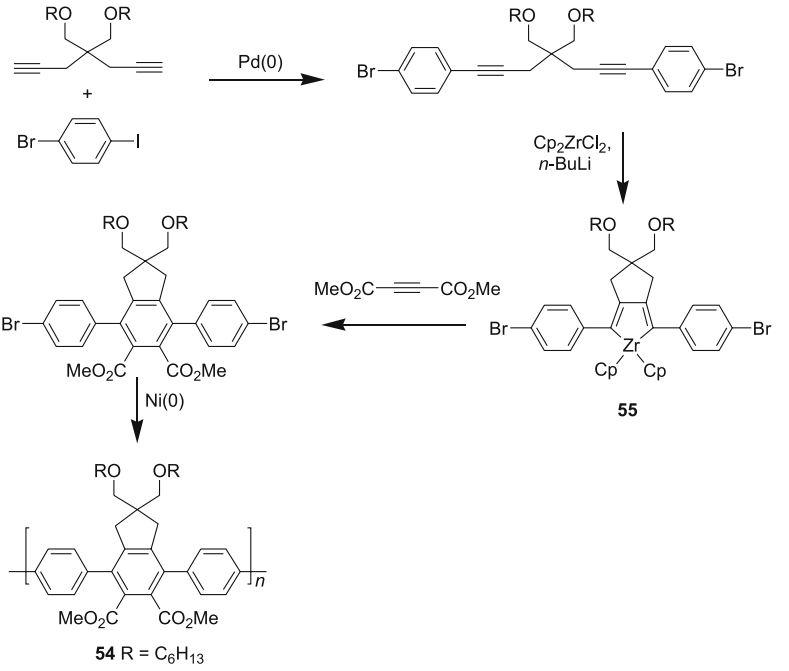

Scheme 23 Zirconocene-precursor route to substituted PPPs

mers also show less red-shifted emission due to aggregates than the corresponding homopolymers [89].

The triphenylene monomer for polymer **54** is made via a zirconcene precursor **55** (Scheme 23). This is a versatile intermediate as the zirconium can be displaced by a variety of reagents, thus permitting the synthesis of a range of monomers. The polymer shows blue emission in THF solution with a maximum in the violet at 376 nm, suggesting that there is particularly large torsion between the substituted and unsubstituted rings, and a long tail into the green, perhaps due to aggregates [113].

2.2.4
Blends of PPPs with Other Polymers

Blending also provides a method for tuning the emission from substituted PPPs. Thus, Salaneck and coworkers found that blending the violet-blue-emitting copolymer **56** (λ_{max} = 389, 443 nm) with the blue-green emitter **57** (λ_{max} = 479 nm) (Scheme 24) gave rise to blue EL (λ_{max} = 460 nm) with an optimal efficiency of 1.9% for a blend containing 10 wt % of **57** [114–116].

Edwards et al. reported that blending **27** (Scheme 12) with PVK produced a red shift in the EL with the maximum moving from λ_{max} = 433 nm to 446 nm [117]. A similar red shift in the EL emission (λ_{max} = 448 nm) has also

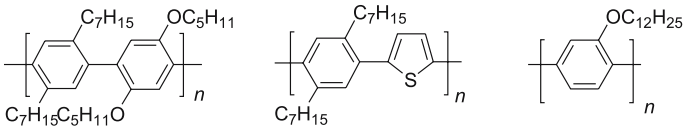

56 57 58

Scheme 24 Phenylene-based polymers used in blends in LEDs

been obtained from a blend of **15** with PVK [118]. The cause of these red shifts is not clear, but may be due to formation of an exciplex. White emission is reported from an exciplex of the dodecyloxy-PPP **58** and PVK formed when the layer of **58** is spin coated onto a layer of PVK from toluene solution due to partial dissolution of the lower layer and consequent mixing of the two polymers at the interface [85]. The spectrum is broad and covers the range from 400 to 700 nm, with maxima at λ_{max} = 495 and 533 nm. If the PPP layer is deposited instead from hexane, in which PVK is insoluble, the EL emission is blue (λ_{max} = 412 nm).

Whereas the above examples show a red shift in the emission by blending with a lower-band-gap material, a blue shift from λ_{max} = 430 nm to λ_{max} = 400 nm has been obtained in the EL emission of **29** (Scheme 13) by blending it with poly(methylphenylsilane)s, whose PL emission is in the near ultraviolet [89]. This is because the polysilanes prevent aggregation of the emitting polymer chains, and so suppress the long-wavelength emission seen from films of pure **29**. The emission colour is also stabler with none of the red shifting seen for the pristine polymer during device operation. A second effect of this better confinement of the excitons is that the EL efficiency is increased by up to 30 times due to suppression of the non-radiative decay pathways.

3
Ladder-type Poly(*para*-phenylene)s

An obvious approach to overcoming the problem of phenylene–phenylene torsion in substituted PPPs is to tether adjacent rings together with short alkyl bridges to make a ladder-type polymer. Ladder-type polymers are of considerable scientific interest as they are intermediate between linear and three-dimensional materials [119]. They can be prepared in two ways: (a) by iterative multi-centre condensation or addition (e.g. Diels–Alder cycloaddition) reactions; (b) by polymer-analogous conversion of suitably functionalised single-stranded precursors. A major feature of the second method is that the polymer-analogous reactions must proceed quantitatively to avoid formation of defects in the final polymer. Though ribbon-like polyacenes can be prepared by polycycloaddition methods [119], linear ladder-type PPPs are only accessible through the conversion of single-stranded PPPs. If methine

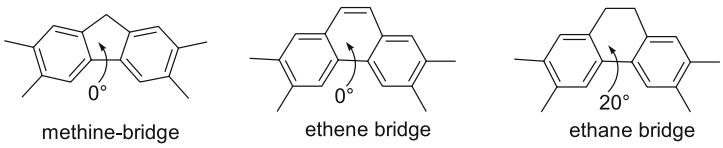

Scheme 25 Bridges and associated torsion angles in ladder polymers

or ethene bridges are used the phenylene backbone is forced to be coplanar, but use of ethane or longer alkyne bridges allows some torsion between adjacent phenylene rings (Scheme 25). For an ethane bridge the torsion angle is predicted to be about 20° [120]. Thus, some degree of control over the optical properties can be achieved by varying the type of bridge(s) used, as the more coplanar the polymer the greater the expected degree of conjugation, and thus the longer the wavelengths of the absorption and emission maxima. The methine and ethene bridges also impart greater rigidity to the structure and thus reduce the Stokes shift between the absorption and emission maxima.

3.1
Ladder-type PPPs with Methine Bridges

Scherf and Müllen prepared (Scheme 26) the ladder-type polyphenylene (LPPP, **3**) with methine bridges [121–124], via a poly(diacylphenylene-*co*-phenylene) precursor copolymer **59** obtained by an AA-BB-type Suzuki polycondensation. The key step is the polymer-analogous Friedel–Crafts ring-closing reaction on the polyalcohol **60**, obtained by the reduction of **59**. This was found to proceed quickly and smoothly upon addition of boron trifluoride to a solution of **60** in dichloromethane. The reaction appeared to be complete by both NMR and MALDI-TOF analysis, indicating the presence of less than 1% of defects due to incomplete ring closure. LPPPs with number-average molecular weights (M_n) of up to 50 000 g/mol have been obtained corresponding to about 150 phenylene rings.

A chiral LPPP **61** (Scheme 27) containing cyclophane units has been prepared by using the resolved cyclophane bisboronic acid **36** (Scheme 15) [98, 99, 125]. This is a potential candidate for obtaining circularly polarised EL.

In order to determine the effective conjugation length of **3**, oligomers with between three (**62**) and seven (**63**) benzene rings (Scheme 28) were prepared by adding a suitable amount of a monofunctional end-capping reagent to the Suzuki polycondensation shown in Scheme 26, separating the resulting oligophenylene precursors, and then performing the reduction and ring closing on them [126]. By extrapolation of a plot of their UV-VIS absorption maxima (in eV) against the reciprocal number of benzene rings, the effective conjugation length for absorption in LPPPs was estimated to be about 11 phenyl rings [120].

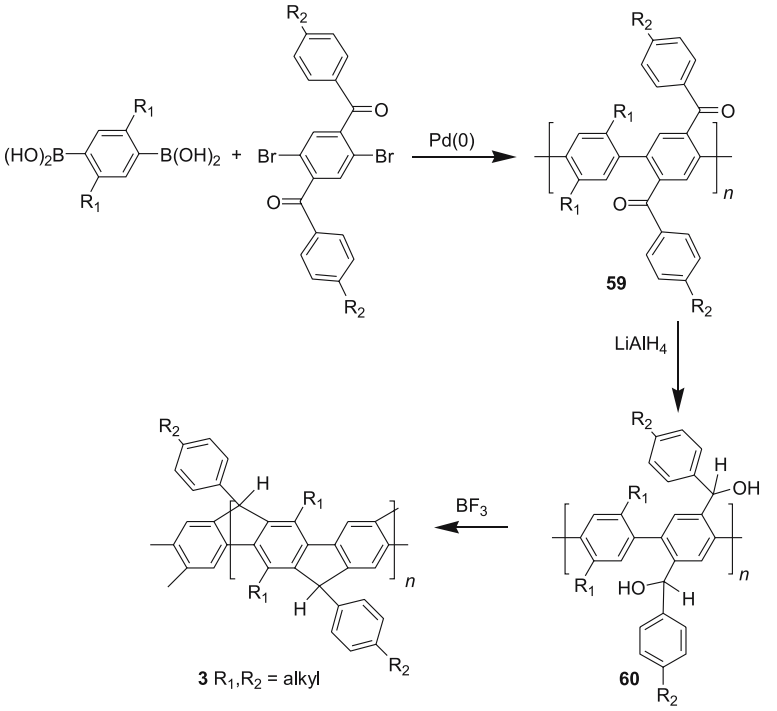

Scheme 26 Synthesis of ladder-type PPP

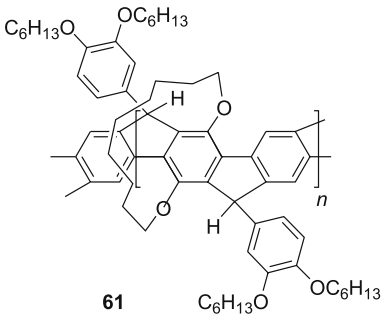

Scheme 27 Chiral ladder-type PPP

By comparison, the effective conjugation length for absorption in poly-(tetrahydropyrene)s **64** (see Sect. 4.3, below), which have an estimated 20° torsion angle between adjacent phenylene rings, was found to be about 19 phenyl rings. Thus, contrary to expectation it has been found that increased planarisation of the aromatic π-system leads to a decrease and not an increase in the effective conjugation length for absorption in PPP derivatives [120].

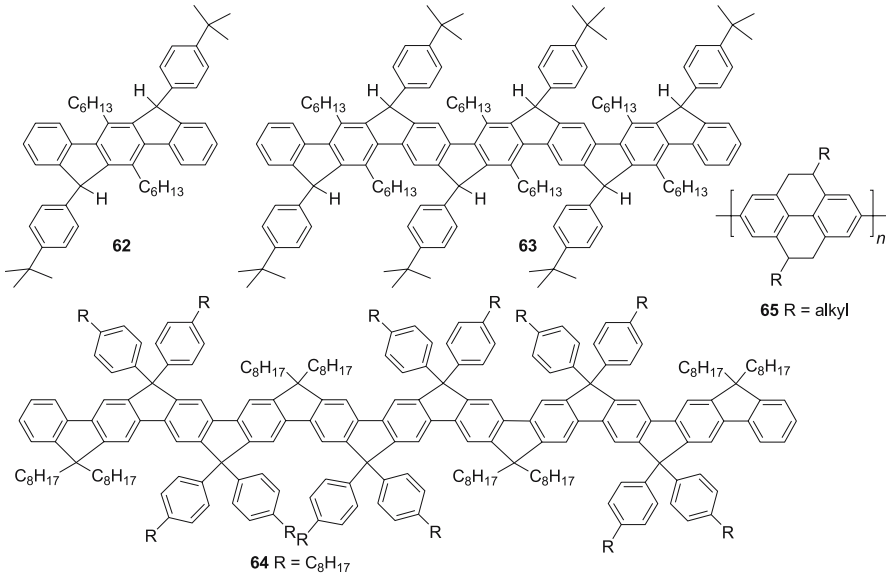

Scheme 28 Oligomers of LPPP used to determine the effective conjugation length

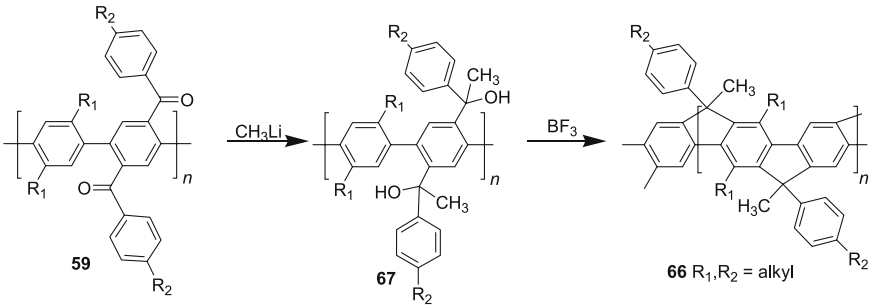

Scheme 29 Synthesis of Me-LPPP

An oligomer **65** with 11 benzene rings has been prepared [127], and its emission spectrum was found to be only slightly blue shifted compared with Me-LPPP (**66**, Scheme 29). Single molecule spectroscopy studies of **65** and **66** showed that the emission from the former at 451 nm matched that from the smallest emissive chromophores observed in the latter, but that the emission maximum from the polymer at around 460 nm comes from longer segments containing probably 14–15 benzene rings. The effective conjugation length for emission in LPPPs is thus similar to the values seen for polyfluorenes and polyindenofluorenes (see 4.1 and 4.2, below).

The planarisation of the PPP backbone in LPPP (**3**) has been found to lead to better vibrational resolution in both absorption and emission spec-

tra and to a much smaller Stokes shift [19]. The absorption maximum is at 440–450 nm, which is considerably bathochromically shifted with regard to single-stranded PPP. The absorption band also shows an unusually sharp absorption edge. The PL of **3** is an intense blue colour in solution with a maximum at 450–460 nm. The Stokes shift is thus only about 150 cm^{-1}. Such a small value is a clear indication of how the rigidity of the polymer hinders deformation in going from the ground to the excited state. A further result of this rigidity is that the PL quantum efficiencies in solution of LPPPs are very high (up to 90%), as non-radiative decay pathways are seriously reduced [128].

While the PL from solutions of LPPP is blue, in thin films the emission is dominated by a broad, featureless band in the yellow (λ_{max} = 600 nm) [20, 40, 129, 130]. The relative intensity ratio of the blue and yellow bands is strongly dependent upon the method used to prepare the films and varies with solvent and film thickness. The blue band disappears completely upon annealing a film of **3** at 150 °C. As a result, LEDs using **3** show yellow EL [131]. The efficiencies from single-layer devices are 0.4% with calcium cathodes and 0.02% with aluminium cathodes. Double-layer devices using PPV as a hole-transporting layer show 0.6% and 0.04% efficiencies with calcium and aluminium cathodes, respectively. Blue emission (λ_{max} = 450–460 nm) has been observed from LEDs using **3** but has been found to be unstable, with the yellow band rapidly appearing [129].

Originally this yellow emission band was attributed to excimers from aggregates formed by π-stacking of the polymer chains. Evidence supporting this came from photophysical experiments, including site-selective excitation experiments [132], time-resolved PL measurements [132], and photovoltaic experiments [133]. Also consistent with this hypothesis is the obtaining of pure blue EL from blends of **3** (1 wt %) in PVK [131]. The efficiency was 0.15% with a calcium cathode. The emission was found to turn white after only a few tens of minutes of device operation, which was attributed to formation of excimers due to the Joule heat produced by passing of electricity through the device. The EL efficiency of devices using such blends can be improved 2–5 times by use of an oxadiazole electron-transporting layer [134].

The stability of emission from LPPPs can be substantially enhanced by replacement of the hydrogen at the methine bridges with a methyl group to give Me-LPPP (**66**) (Scheme 29) [135]. This is achieved by treating the precursor polymer **59** with methyl lithium, followed by ring closure of the resulting polyalcohol **67** with boron trifluoride as in the preparation of **3**.

The emission from **66** is slightly red shifted compared with **3**, with an emission maximum at λ_{max} = 461 nm and a secondary peak at λ_{max} = 491 nm, so that the emission colour is blue-green. Unlike **3**, Me-LPPP shows almost identical emission from films and solutions, with PL quantum efficiencies of over 90% in solution and up to 60% in the solid state. There is a broad emission band centred at 560 nm, which has been attributed to emission from aggre-

gates [136]. This band is much weaker than the yellow band from LPPP (**3**), and the emission does not change upon annealing. LEDs using **66** produce blue-green emission with EL efficiencies of up to 4% [21, 23, 24, 137, 138]. These high emission efficiencies make Me-LPPP a particularly promising material for use in organic solid-state lasers [3]. Optically pumped lasing has been observed from films of **66** in both waveguide and 'distributed feedback' configurations by the groups of Leising and Lemmer [33, 35, 139–141].

3.2
Blends of LPPPs with Other Polymers

Blends of Me-LPPP, poly(ethylene oxide) (PEO), and lithium triflate have been used as the emissive layer in a light-emitting electrochemical cell (LEC) [142]. The emission efficiency with an aluminium cathode was 0.3%, which is somewhat lower than for the corresponding LED (1%), but the onset voltage was only 2.7 V compared with 12 V for an LED. The emission colour changed rapidly from blue to green due to an increase in the intensity of peaks at 530 and 560 nm. The change in the emission was slower in devices with very low or very high amounts of PEO, which is attributed to the decrease in interaction between **65** and PEO in such blends.

Blends of Me-LPPP (**66**) and the red-emitting polymer **68** (Scheme 30) show predominant emission from the latter even at concentrations of only 0.2% **68**. The emission is orange at 0.2% **68** with an EL efficiency of 1.6% (cf. 1% for **66** and 0.01% for **68**), but drops rapidly at higher concentrations of **68**. The PL efficiency is optimal (41% versus 30–60% for **66** and 11% for **68**) with 0.7% **68** and again drops as the concentration of **68** increases [35, 143, 144]. A blend with 0.05% **68** shows high (0.8%) efficiency white EL emission due to emission from both polymers [33, 35, 144]. Blending the polymers with poly (methyl methacrylate) (PMMA) leads to separation of the emissive polymer chains and less efficient energy transfer so that 0.08% of **68** is required for obtaining white emission, but the EL efficiency is increased to 1.2% [35, 145].

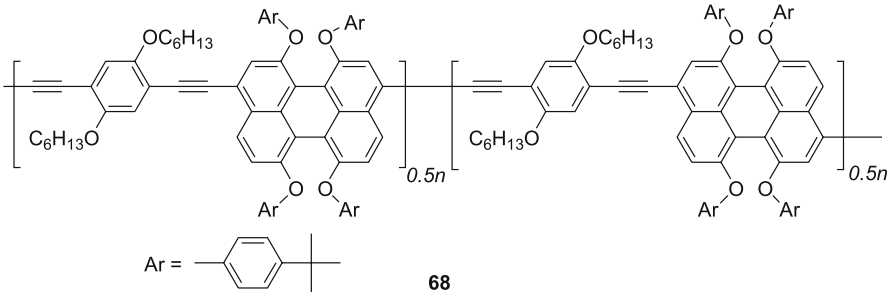

Scheme 30 Perylene-based polymer used in blends with Me-LPPP

3.3
Defect Emission from LPPPs

Lupton [146] has reported that the broad emission feature centred at 560 nm could be detected in the delayed fluorescence from both films and dilute solutions of Me-LPPP. This is not consistent with the suggestion that the long-wavelength emission from ladder-type PPPs comes from aggregates, as dilute solutions should not contain any aggregates. He therefore proposed that the long wavelength emission band originates from defects on the polymer chains.

Convincing evidence has been produced that long-wavelength emission from polyfluorenes is due to fluorenone (**69**) units (see Sect. 4.1, below), so a probable structure for the defects in LPPPs is a ketone as in **70** (Scheme 31). As the ketone in **70** has more extended conjugation than in fluorenone (**69**) one would expect the emission from it to be bathochromically shifted, which is consistent with the long-wavelength emission from LPPPs occurring at 560–600 nm, and that from polyfluorenes at about 530 nm. This is supported by comparison of experimental measurements of **3** and **66** with theoretical calculations of the properties of potential defect structures [147].

The ketone **70** presumably arises from oxidation of the methine bridge by oxygen from the air. The difference between the emission spectra in solution and the solid state would then reflect the more efficient energy transfer to the defect sites in the latter due to the increased intermolecular interactions. The much lower intensity of the defect band and the greater emission stability of Me-LPPP over LPPP can be explained as being due to the greater difficulty in oxidising the methyl-substituted methine bridge, producing a much lower level of defect sites. It is reported that when 9,9-dialkylfluorene bisboronates are substituted for benzene bisboronates in Scheme 28, the resulting polymers display blue-green emission (maxima at 460 nm), which is much stabler than that from **3** [148]. It is suggested that this is because fewer bridges are being formed in the final polymer-analogous reaction, and thus there is less chance of a defect arising from incomplete ring closure.

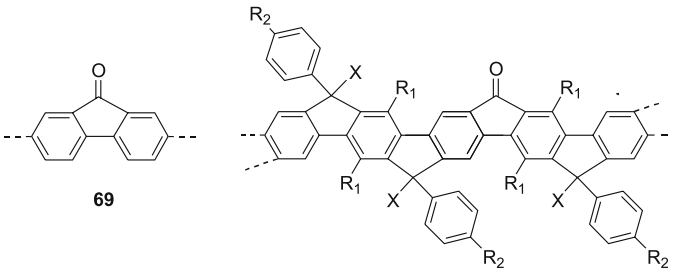

69 **70** R_1,R_2 = alkyl, X = H, CH_3

Scheme 31 Proposed emissive defects in polyfluorenes and ladder-type PPPs

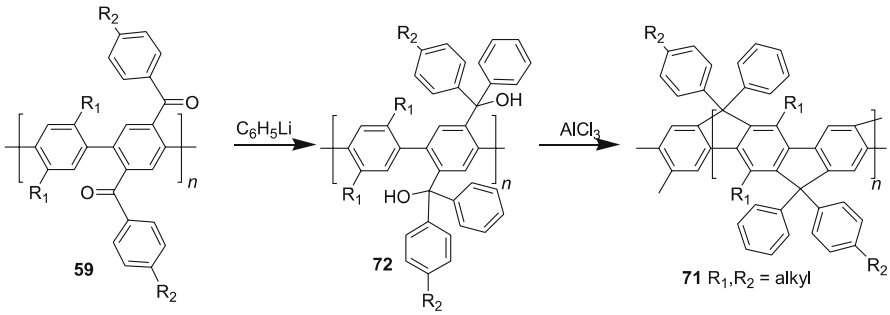

Scheme 32 Synthesis of Ph-LPPP

That even low levels of defects can produce strong emission is exemplified by the case of Ph-LPPP (**71**). The synthesis (Scheme 32) is similar to that of Me-LPPP (**66**), except that complete ring closure of the polyalcohol **71** could not be obtained using boron trifluoride [119]. As a result, other reagents had to be tested and it was found that complete ring closure could be obtained by using aluminium chloride [149].

The PL emission from **71** is very similar to that from **66** with maxima at 460 and 490 nm. However, the EL spectrum shows an additional long-wavelength band. This is not a broad featureless band as seen for the defect emission from **3** or **66**, but one with well-resolved maxima at 600 and 650 nm. Photophysical investigation of this emission showed the feature at 600 nm to be emission from a triplet exciton (phosphorescence) with a vibronic shoulder at 650 nm [150]. Elemental analysis of the polymer showed that it contained 80 ppm of palladium (cf. < 2 ppm in **66**). It was therefore proposed that residues of the palladium catalyst used to make the precursor polymer **59** reacted with the phenyl lithium and the polymer to introduce covalently bound palladium centres onto the polymer chain. These then act as sites for phosphorescent emission.

3.4
Ladder-type PPPs with Two-atom Bridges

The polymers discussed above have methine bridges. A ladder polymer **73** with dihydroxyethane bridges has been made by Forster and Scherf (Scheme 33) [151]. Yamamoto polycondensation of a dibromodibenzoylbenzene **74** gave the poly(diacylphenylene) **75**, which was coupled with samarium(II) iodide coupling to give **73**. This polymer shows strong blue-green fluorescence in solution (λ_{max} = 459 nm) and the solid state (λ_{max} = 482 nm). The red shift in the solid-state PL indicates that **73** is less rigid than the LPPPs with methine bridges, but still shows only weak geometrical changes in going

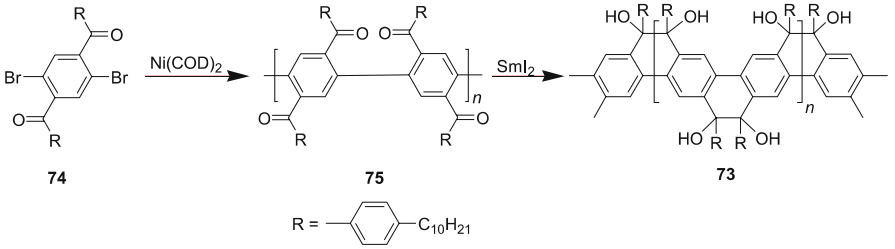

Scheme 33 Synthesis of a ladder-type polyphenylene with dihydroxyethane bridges

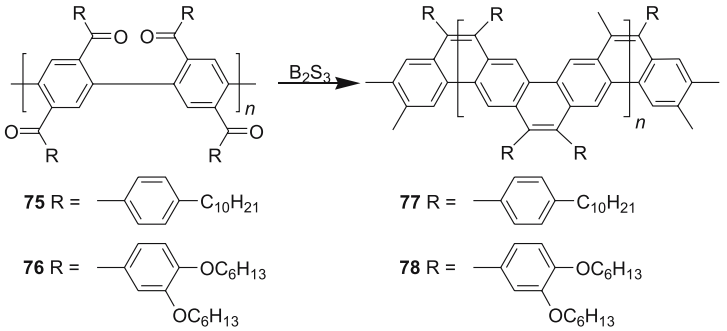

Scheme 34 Synthesis of ladder-type polyphenylene with ethene bridges

from the ground to the excited state. No long wavelength emission band is seen in the PL spectrum of **73**.

Treatment of the poly(dibenzoylphenylene)s **75** and **76** with boron sulfide gives polymers **77** and **78** with ethene bridges (Scheme 34) [152, 153]. These also show blue-green emission (λ_{max} = 478 nm and 484 nm, respectively) with some long-wavelength emission in the solid state which has been attributed to aggregates. Their EL efficiency is reported to be very low (< 0.1%) [154].

A similar polymer **79** was prepared by Goldfinger and Swager by an acid-catalysed cyclisation of a PPP precursor **80** with alkyne side chains (Scheme 35) [155]. There is no report of the emission from this material, but the absorption edge was reported to be at 478 nm, suggesting it should be a blue-green or green emitter.

Tour and Lambda [156, 157] have prepared the aza-ladder polymers **81** from the alternating copolymers **82** (Scheme 36) by treatment with acid to remove the Boc protecting groups and induce imine formation. Unfortunately these materials are only soluble in strongly protic solvents, and there is no report of their luminescent properties. The absorption maxima in protic solvents are around 400 nm, with secondary bands between 510 and 550 nm, while in the solid state maxima between 460 and 490 nm were seen, indicating that protonation has a major effect on the conjugation length.

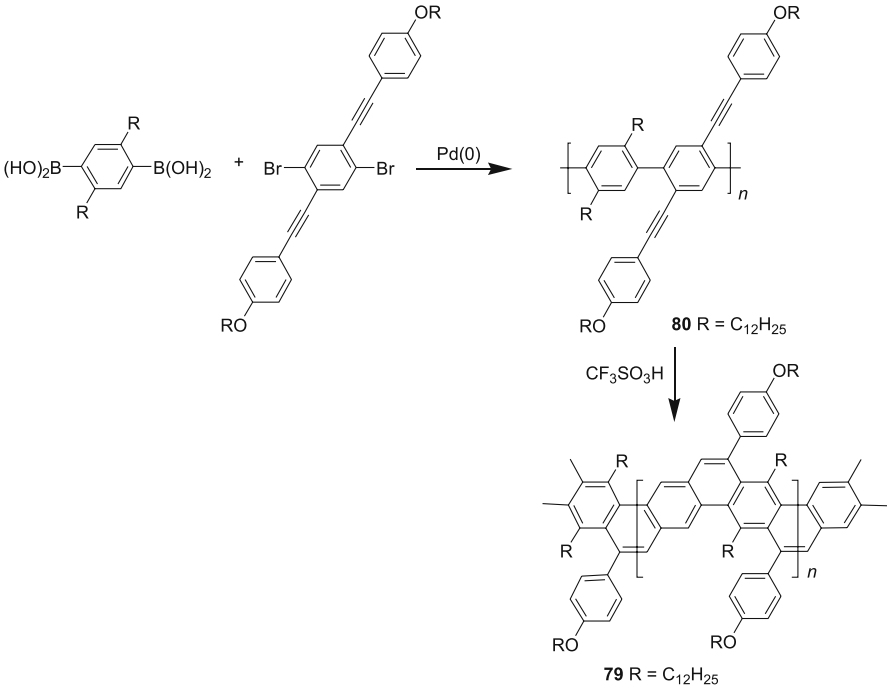

Scheme 35 Ladder-type polyphenylene by alkyne cyclisation route

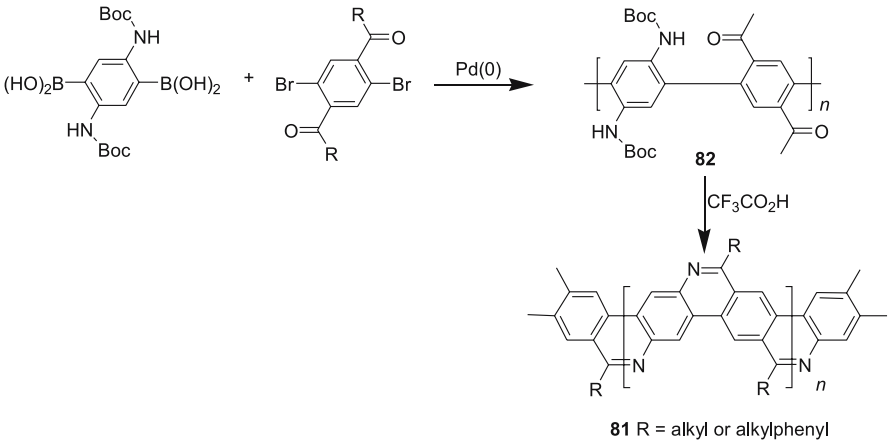

Scheme 36 Synthesis of an aza-bridged ladder polymer

3.5
Copolymers of LPPP and PPP – 'Stepladder' Copolymers

Incorporation of a dialkyldibromo comonomer into the Suzuki copolymerisation used to make the LPPP precursor **59** (Scheme 26), followed by reduction and ring closure, gives statistical copolymers **83** called 'stepladder' copolymers (Scheme 37). These contain oligo-LPPP units connected via twisted phenylene spacers. Copolymers with 40–70% of unbridged phenylene content have been been prepared [129]. The emission from these copolymers **83** is blue shifted with respect to LPPP (**3**) due to the shorter length of the LPPP segments and/or to out-of-plane twisting of the phenylene rings [40, 158]. Films of the copolymers with higher unbridged phenylene content (m = 50%+) remain blue emitting even after annealing [129]. Blue-emitting LEDs with efficiencies of nearly 1% have been made using these materials [159]. This difference in behaviour from LPPP cannot be due to any greater resistance of the copolymers towards oxidation to form defects, but must reflect less efficient exciton diffusion to defect sites due to less close packing of the polymer chains brought about by the introduction of the random twisted phenylene groups.

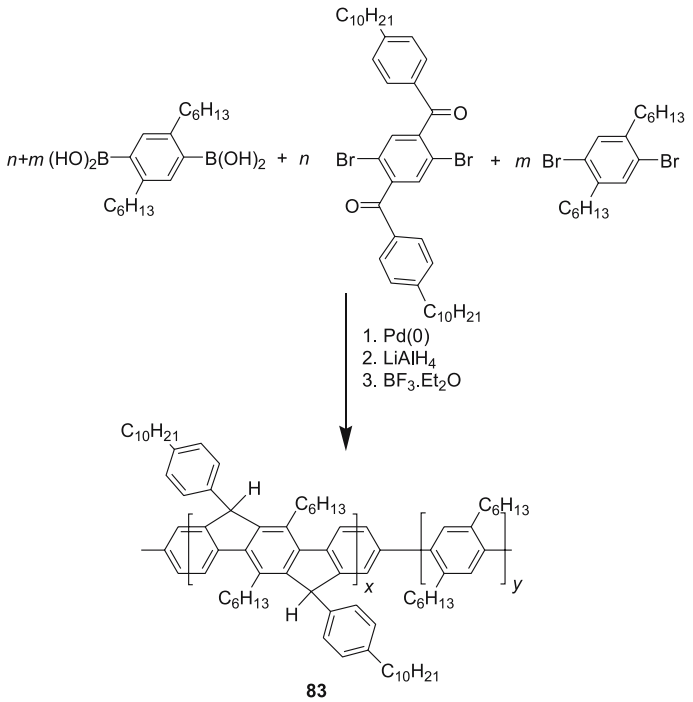

83

Scheme 37 Synthesis of random stepladder-type polyphenylenes

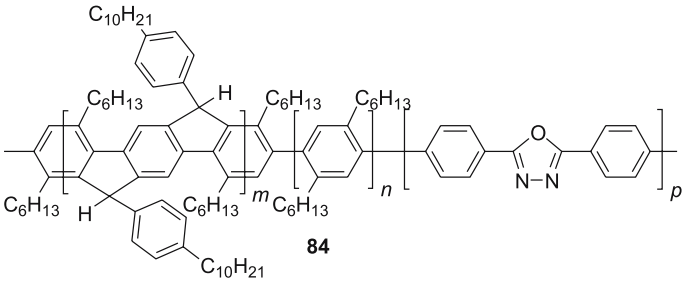

84

Scheme 38 A stepladder copolymer incorporating charge-transport moieties

A copolymer **84** (Scheme 38) containing dialkyl PPP, ladder-type PPP, and electron-transporting diaryloxadiazole segments ($m : n : p = 4 : 3 : 3$) has been prepared by a similar copolymerisation with 2,5-bis(4-bromophenyl)-1,3,4-oxadiazole added as a comonomer [160]. It emits blue light ($\lambda_{max} = 410$, 480 nm) with an efficiency of 0.4% when aluminium cathodes are used [161]. This is twice the efficiency obtained for similar devices using the copolymers **83** without the oxadiazole units.

4
Stepladder-type Poly(*para*-phenylene)s

In addition to the random stepladder polymers described in Sect. 3 above, in which the bridged and unbridged phenylene units are statistically distributed along the polymer chain, there exist regular stepladder-type polyphenylenes. Such polymers are intermediate in structure between PPP and LPPP with a defined number of bridged phenyl rings connected by single-bond linkages. Such materials have been looked at as blue-emitting materials, with the aim of achieving a balance between the excellent photophysical properties of LPPP (small Stokes shift and well-resolved vibronic structure in the emission spectrum) and synthetic accessibility.

4.1
Polyfluorenes

Polyfluorenes (PFs), the simplest regular stepladder-type polyphenylenes, in which only every second ring is bridged, have been much studied in recent years due to their large PL quantum efficiencies and excellent chemical and thermal stability, as evidenced by the number of recent reviews [162–164]. A further attractive feature of poly(9,9-dialkylfluorene)s (PDAFs) is the synthetic accessibility of the monomers, as alkylation and halogenation of fluorene proceed smoothly and in high yields.

4.1.1
Synthetic Routes to Polyfluorenes

Polyfluorenes can be made by oxidative coupling of the monomer with iron(III) chloride. Poly(9,9-dihexyl-2,7-fluorene) (**85**) with a molecular mass of 5000 ($n \sim 20$) was made in this way by Yoshino and coworkers (Scheme 39) [165, 166], and used to make low-efficiency blue-emitting ($\lambda_{max} = 470$ nm) devices [167–169]. These were the first blue-emitting LEDs reported using a phenylene-based polymer.

The disadvantages of this method are that the degree of polymerisation is low, and the high level of defects produced due to coupling other than at the 2- and 7-positions. As a result this method is generally not used to make PFs. A recent exception is the synthesis of the polymer **86** with a cyanoalkyl substituent (Scheme 39) [170]. Here, transition-metal-mediated coupling methods such as Suzuki or Yamamoto polycondensation could not be used as the nitrile deactivates the metal catalysts by binding to the metal.

Advincula et al. oxidised the polyionene **87** with iron(III) chloride to obtain an insoluble polyfluorene network **88** (Scheme 40) [171]. This shows violet PL ($\lambda_{max} \sim 410$ nm), suggesting that the polyfluorene segments are rather short. Due to its insolubility this material cannot be used to make good-quality films for use in LEDs, but the incorporation of a conjugated backbone within a network is one possible way to obtain isolated chains and so avoid the problems associated with interchain interactions, e.g. excimer formation.

Most syntheses of PFs use Suzuki polycondensations or Yamamoto Ni(0) couplings of dibromomonomers. A group at Dow [172–177] have developed a Suzuki cross-coupling route leading to high molecular weight PDAFs (Scheme 41), e.g. poly(9,9-dioctylfluorene) (**89**) with $M_n > 100\,000$ g/mol was obtained after less than 24-h reaction time. Bradley and coworkers [178] used **89** made by this method to make a blue ($\lambda_{max} = 436$ nm) LED with relatively high (0.2%) efficiency being obtained when a hole-transporting layer was used.

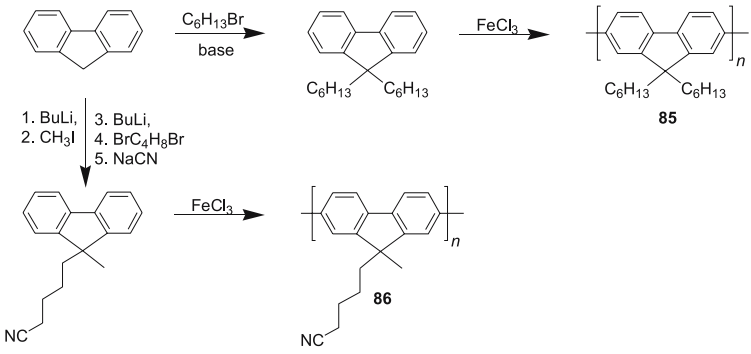

Scheme 39 Synthesis of polyfluorenes by oxidative polymerisation

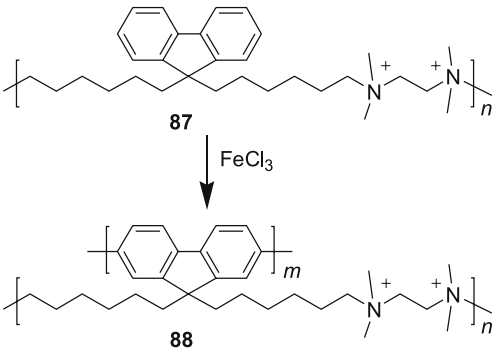

Scheme 40 Synthesis of a polyfluorene network by oxidative coupling

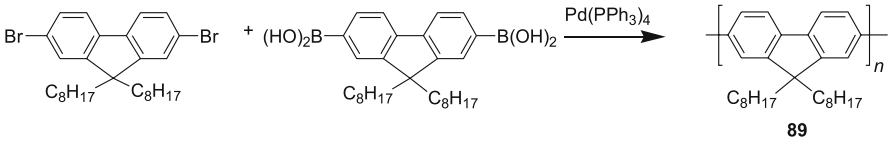

Scheme 41 Dow route to high molecular weight polyfluorenes

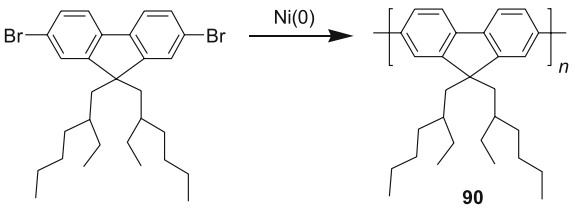

Scheme 42 PDAFS by Yamamoto polycondensation

Yamamoto-style polycondensations have also been used to make high molecular weight PFs. For example, Scherf and coworkers prepared poly[9,9-bis(2-ethylhexyl)fluorene] (**90**) with M_n of over 100 000 g/mol by coupling the dibromofluorene monomer with bis(cycloocta-1,7-dienyl)nickel(0) and bipyridine (Scheme 42) [179].

4.1.2 Optical Properties of PDAFs

The emission from PDAFs is violet-blue with a primary emission maximum at about 425 nm, and a secondary peak at about 445 nm. Well-defined oligomers of **85** have been prepared, and as a result the effective conjugation length for PDAFs has been determined to be about 12 units (24 phenyl

rings) for absorption and six units for emission [180–182], indicating that the geometries of the ground and excited states are different.

PDAFs with unbranched alkyl substituents, e.g. **85** and **89**, show two thermotropic nematic liquid crystalline phases [183, 184]. Longer alkyl chains lower the transition temperatures, so that whereas for **85** the phases occur at 162–213 °C and 222–246 °C, with isotropisation occurring at 290–300 °C, for **89** the nematic phases are between 80–103 °C and 108–157 °C with isotropisation at 278–283 °C, and for the dodecyl-substituted polymer **91** (Scheme 43) they are observed at 62–77 °C and 83–116 °C with isotropisation at 116–118 °C [184]. Annealing films of the polymers at a temperature just above the second liquid crystalline transition followed by rapid cooling preserves the liquid-crystalline order [183, 184]. Deposition of such a film of **89** upon a rubbing-aligned polyimide alignment layer has been used to obtain polarised PL and EL [5, 185]. A rubbing-aligned layer of PPV has also been used as an alignment layer to obtain polarised EL from films of **89**, but the emission spectrum is slightly red shifted due to some absorption by the PPV layer in the region of the main emission peak at 433 nm [186–188].

By contrast, the polymer **90** with branched alkyl chains shows only one nematic phase. Thus, **90** shows a phase transition at 167 °C upon heating with the reverse transition upon cooling being seen at 132 °C. Annealing of a film of **90** at 185 °C upon a rubbing-aligned polyimide layer followed by rapid cooling produced a film which showed polarised EL with a dichroic ratio of up to 20 [179, 185, 189, 190].

Circularly polarised PL and EL emission has been obtained from polymers, e.g. **92** and **93** (Scheme 43), bearing chiral side chains [191–194].

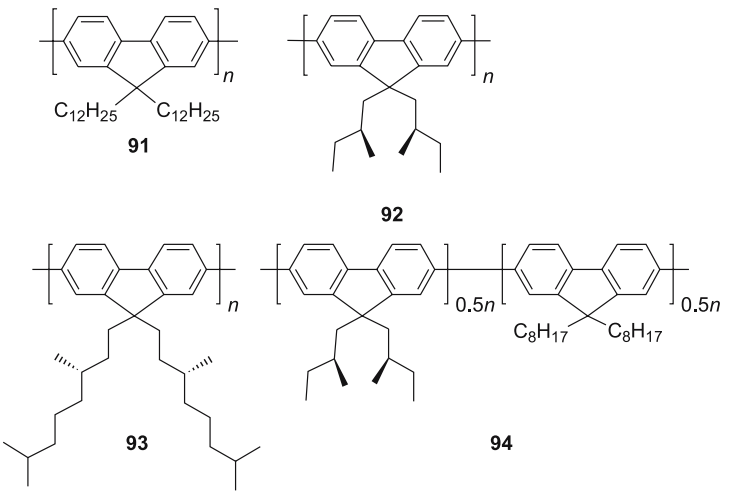

Scheme 43 Polyfluorenes with linear and branched alkyl chains

The copolymer **94** also showed circularly polarised emission, but the degree of dissymmetry was much reduced [191–193]. This was attributed to the dioctylfluorene units preferring a planar conformation of the backbone while the chiral-substituted units adopt a helical structure. A combination of a helical backbone conformation and liquid crystallinity is thought essential for obtaining a high degree of circular polarisation.

4.1.3
PFs with Substituted Alkyl Side Chains

PDAFs are highly soluble in non-polar solvents, e.g. toluene, but insoluble in highly polar solvents, e.g. ethanol. Solubility in such solvents can be obtained by introduction of charged groups onto the side chain. The polycation **95** made by reduction of the polyamide **96** (prepared by Yamamoto polycondensation of the dibromomonomer) and quaternisation of the resulting polyamine **97** (Scheme 44) is soluble in ethanol, methanol, and water, but insoluble in non-polar solvents such as THF [195].

Hydrolysis of the polyester **98** with potassium *tert*-butoxide and potassium hydroxide in THF to make the polyacid **99** (Scheme 45) gave a material which was insoluble in water, even at high pH, but soluble in pyridine. ^{1}H NMR performed in d_5-pyridine showed that complete hydrolysis had occurred [195].

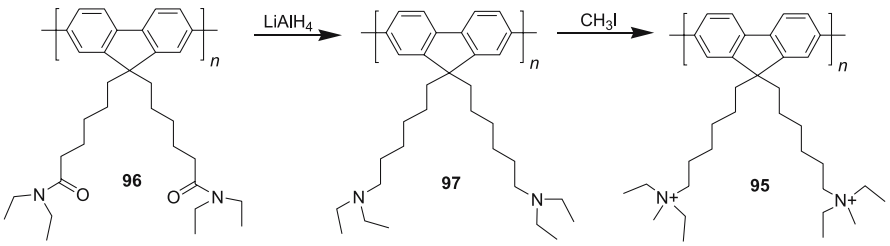

Scheme 44 Synthesis of a water-soluble polyfluorene

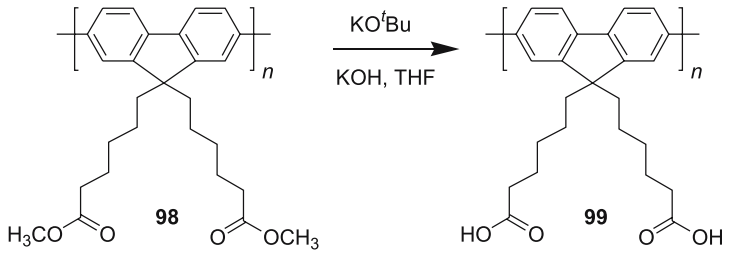

Scheme 45 Preparation of a fluorene-based polyacid

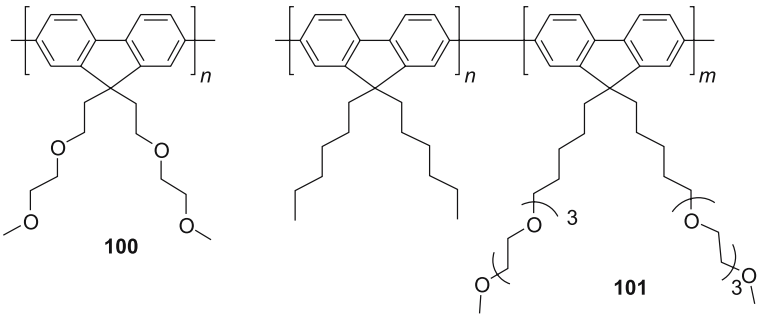

Scheme 46 Polyfluorenes with ethylene oxide side chains

Polymers **100** [196] and **101** [197] (Scheme 46) with ethylene oxide side chains have been prepared by Ni(0) coupling. The oxygenated side chains enable them to bind with metal ions, making them suitable as emissive materials for blue-emitting LECs as well as LEDs. Their emission in both LED and LEC devices rapidly changes from blue (λ_{max} = 430 nm) to blue-green due to the appearance of long-wavelength emission centred at 530 nm. When **100** is blended with PEO in a LEC, phase separation occurs, resulting in highly efficient (2.4%) white emission with an emission maximum at λ_{max} = 550 nm [198]. By use of colour filters, pure red, green, or blue emission can be obtained.

4.1.4
Defect Emission from PDAFs

As with LPPP the blue emission from PDAFs is unstable, with the appearance of a strong emission band around 530 nm after annealing or upon running an EL device [163, 164, 199, 200]. Initially this long wavelength emission band was believed to be due to emission from excimers [201, 202]. In support of this, absorption and PL studies of **85**, **89**, and **91** showed that annealing resulted in a red shift in the absorption edge, which was greatest for **91**, which was attributed to the formation of a more planar extended ground state conformation [184].

However, it was also noted that polymers end-capped with fluorenone units showed a similar emission band at around 530 nm to that seen from annealed films of PDAFs [201], suggesting that emission from fluorenone defect sites **69** was an alternative explanation for this emission. Consistent with this, the emission from the fluorenone-containing polymer **102** (Scheme 47) made by Bunz and coworkers is blue (λ_{max} = 428, 447 nm) in solution, but in the solid state is orange (λ_{max} = 533 nm), with all the emission coming from the fluorenone units [203]. Furthermore, it has been observed that when fluorene groups were used as end-capping groups for PFs, they were readily oxidised to

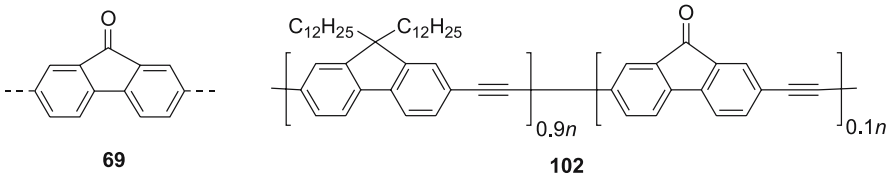

69 102

Scheme 47 The solid-state emission from the fluorenone-containing copolymer **102** matches the long-wavelength emission from polyfluorenes attributed to an emissive defect **69**

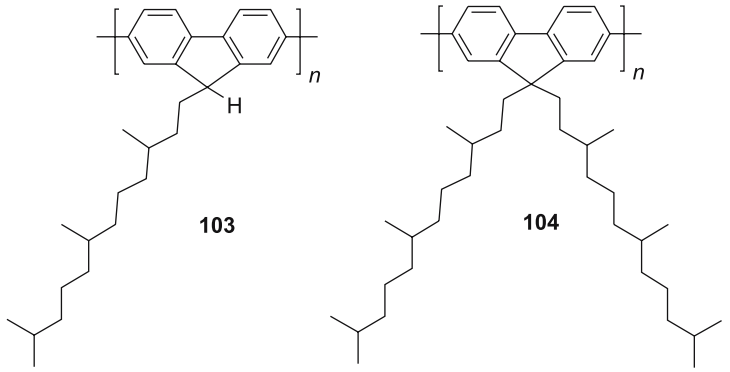

103 104

Scheme 48 Mono- and dialkylated polyfluorenes used to test ketone-defect hypothesis

fluorenones during annealing in air. This suggested that the appearance of the yellow emission band might be at least partially due to oxidation of fluorene units in the polymer to fluorenone [201].

Scherf and coworkers [204] prepared the polymer **103** (Scheme 48) with only one alkyl substituent at the 9-position by the Yamamoto method, and found that even pristine material contained fluorenone units as shown by a carbonyl stretching band at 1721 cm^{-1} in the IR absorption spectrum, and that the solid-state PL and EL spectra of **103** were dominated by a low-energy emission band centred at 533 nm due to fluorenone emission. A band at exactly the same position was seen from the corresponding dialkylfluorene polymer **104** after photooxidation in air or 30-min continuous operation of an LED. They accordingly suggested that the long wavelength emission band in PDAFs is due to energy transfer to ketone defect sites. The greater contribution of this band to the EL than the PL spectrum they attributed to the fluorenone units acting as electron-trapping sites, thus favouring recombination at the defect sites. Further support for this view came from time-delayed PL measurements of polymer **93** in solution by Lupton et al. [205].

To account for the formation of the defect sites in pristine **103**, they proposed that, during the polymerisation, some of the alkylfluorene units were reduced by the nickel(0) to monoalkylfluorenyl anions **105**, which

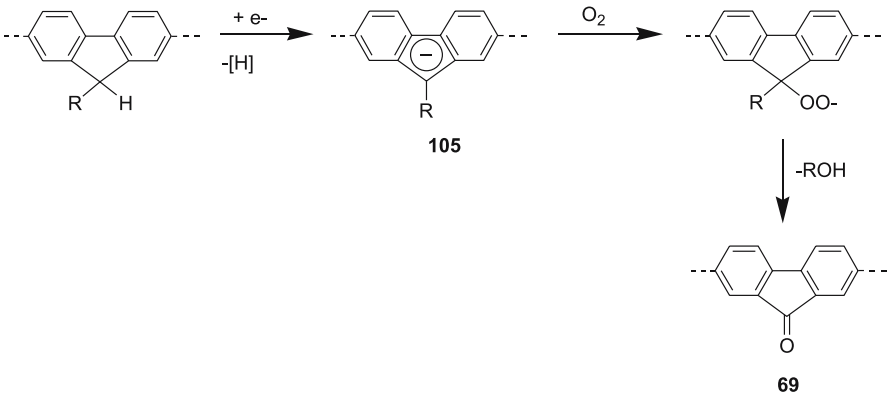

Scheme 49 Proposed mechanism for formation of ketone defects **69**

were then oxidised by atmospheric oxygen to the ketones **69** during the workup (Scheme 49). The oxidation of the 2-bromofluorenyl anion by atmospheric oxygen has been used to prepare 2-bromofluorenone in high yield, thus demonstrating the susceptibility of fluorenyl anions to attack by oxidation [206].

The defect hypothesis was challenged by Zeng et al., who reported that a pronounced emission band at 520 nm appeared upon annealing **85** under a nitrogen atmosphere, which they suggested ruled out oxidation [207]. However, in this experiment they did not use totally anaerobic (glove box) conditions. List and coworkers have found that heating a film of **104** at 200 °C in a dynamic vacuum ($< 10^{-4}$ mbar) produced no long wavelength emission band, even when the sample was simultaneously illuminated, while heating in air produced a strong band at 530 nm [208]. This demonstrates conclusively that the emission band at 530 nm from PFs is due to the formation of ketone defects by oxidation during synthesis and/or handling. This does not mean that the demonstrated interchain interactions produced during annealing of PDAFs play no part in the appearance of the long-wavelength emission, as increased interchain interactions (aggregation) would enhance exciton migration to the defect sites.

Considerable effort has gone into developing stable blue emission from PDAFs. Fractionation of **89** to remove low molecular mass material has been reported to reduce the long-wavelength emission [209]. This is at first sight a somewhat surprising result, as the probability of a polymer chain containing a defect increases with increasing chain length. However, it is possible that the oligomers in the low molecular mass fraction assist in interchain charge and energy migration, and so removing them would reduce exciton migration to defect sites. Meijer and coworkers have shown that if a dialkylfluorene monomer is treated with base to remove residual monoalkylfluorenes before

polymerisation then the resulting polymers display much stabler blue emission [210]. Since the materials were pure by all standard analytical methods before this extra purification, the amount of the monoalkylated impurities must have been less than 1 mol %.

Stable blue emission has been obtained by Neher and coworkers from blends of the copolymer **106** with hole-transporting molecules, e.g. **107** (Scheme 50) [211]. This was attributed to the dopants acting as hole traps, thus reducing the amount of charge trapping at the defect sites, and thus the emission therefrom.

A group at IBM prepared (Scheme 51) polymers **108** end-capped with vinyl groups by addition of bromostyrene as an end-capping reagent to a Yamamoto polycondensation [212]. These polymers can be thermally cross-linked at 150–200 °C to produce insoluble materials which show stable blue emission [212]. This is attributed to a reduction in chain mobility, due to the cross-linking, which hinders exciton migration to the defect sites.

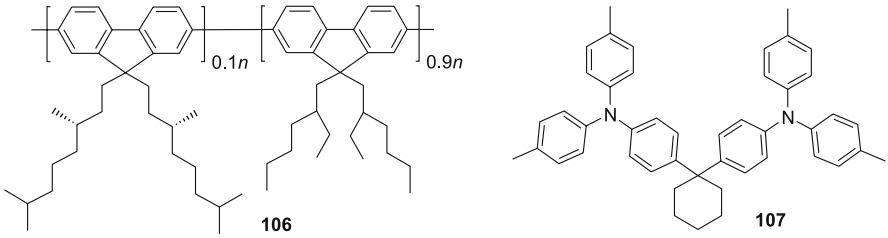

Scheme 50 Polyfluorene and typical hole-transporting material blended with it to obtain stable blue emission

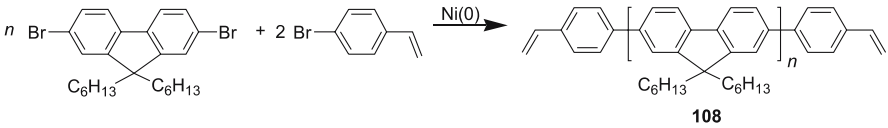

Scheme 51 Preparation of a polyfluorene end-capped with a cross-linkable group

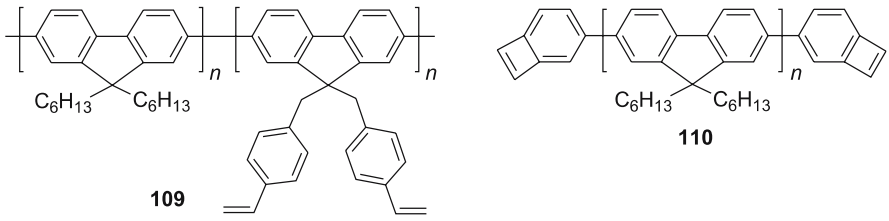

Scheme 52 Other cross-linkable polyfluorenes

By contrast, cross-linking of polymers **109** with styryl groups as side chains (Scheme 52) [212] does not produce efficient suppression of the long-wavelength emission. This suggests that reducing chain-end mobility is important in reducing interchain interactions. No suppression in defect emission is observed in thermally cross-linked polymers **110** end-capped with cyclobutene groups [213]. It is not clear why this is so, but it may be that more oxidation occurs at the higher conversion temperature (250 °C) used in this process or that the cross-linking is less efficient.

Other approaches that have been found to improve the stability of blue emission from PDAFs are to attach bulky substituents such as cyclohexyl groups [214] or polyhedral siloxanes [215–217] to the ends of the alkyl chains. These presumably work by reducing exciton migration to defect sites.

4.1.5
Colour Control by Copolymerisation

Miller and coworkers have prepared copolymers **111** (Scheme 53) of dihexylfluorene with anthracene by the Yamamoto method. These show stable blue emission (λ_{max} = 455 nm) even after prolonged annealing [182, 218]. As the ratio of anthracene (15%) to fluorene (85%) units was too low to produce significant steric repulsion between the polymer chains, they attributed the absence of long-wavelength emission to trapping of the exciton at the anthracene sites and subsequent emission therefrom [218, 219]. Similar copolymers **112** with dioctylfluorene are reported to show PL and EL maxima at respectively 446 nm and 435 nm [220]. The reason for this difference is not apparent.

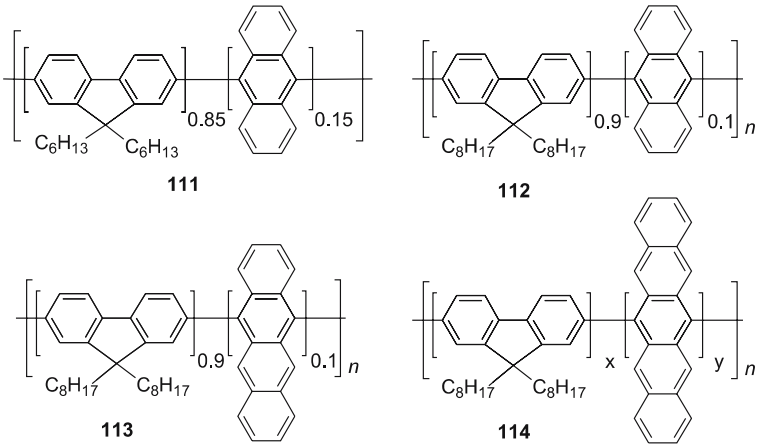

Scheme 53 Copolymers of fluorene with acenes

Copolymers **113** and **114** containing tetracene and pentacene units show emission from the acene units to give green (λ_{max} = 520 nm) and red (λ_{max} = 623 nm) PL and EL, respectively [220]. However, due to rapid degradation of the acenes by oxidation their emission rapidly turns blue and the emission efficiency drops markedly. The pentacene copolymer **114** shows a lower turn-on voltage and higher efficiency with 1 mol % as opposed to 10 mol % of pentacene.

Similar exciton trapping has also been observed in copolymers containing perylene **115** (an equal mixture of 3,9- and 3,10-linked units) or cyanostilbene **116** units (Scheme 54) made by Yamamoto copolymerisation [219, 221]. Thus, the perylene copolymer **115** (m = 15%) showed green emission (λ_{max} = 540 nm), while by altering the amount of stilbene the emission from **116** could be tuned between λ_{max} = 466 nm (m = 5%) and λ_{max} = 510 nm (m = 50%).

Such exciton trapping has been exploited by Müllen and coworkers, who prepared copolymers of dioctylfluorene- and perylene-based dyes (1–5 mol %) by Yamamoto copolymerisation (Scheme 55) [222–224]. These materials were designed so that by efficient Förster energy transfer from the fluorene to the dye units, efficient emission across the whole visible spectrum could be obtained. Perylene dyes were chosen as the chromophores due to their high solid-state PL quantum yields, and their excellent thermal and photochemical stability.

Four different dyes were used, with emission maxima in the green (λ_{max} = 525 nm), yellow (λ_{max} = 540 nm), orange (λ_{max} = 584 nm), and red (λ_{max} = 626 nm), respectively. In the copolymers with the green-emitting **117** and yellow-emitting **118** dyes, the conjugation is maintained between the fluorenes and the chromophore. It should be noted that these dyes are inseparable 1 : 1 mixtures of 3,9- and 3,10-dibromo compounds, but there is no reason to believe that this has any adverse effect upon their optical or electronic properties. By contrast, in the copolymers with the orange-emitting **119** and red-emitting **120** dyes, the imide groups interrupt the conjugation.

Since the efficiency of energy transfer between the fluorene and the dye is dependent upon the overlap of the fluorene emission spectrum and the absorption spectrum of the dye, it was anticipated that energy transfer to the

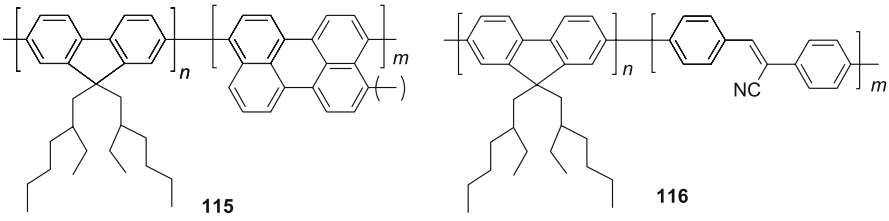

Scheme 54 Copolymers of fluorene with green- and red-emitting chromophores

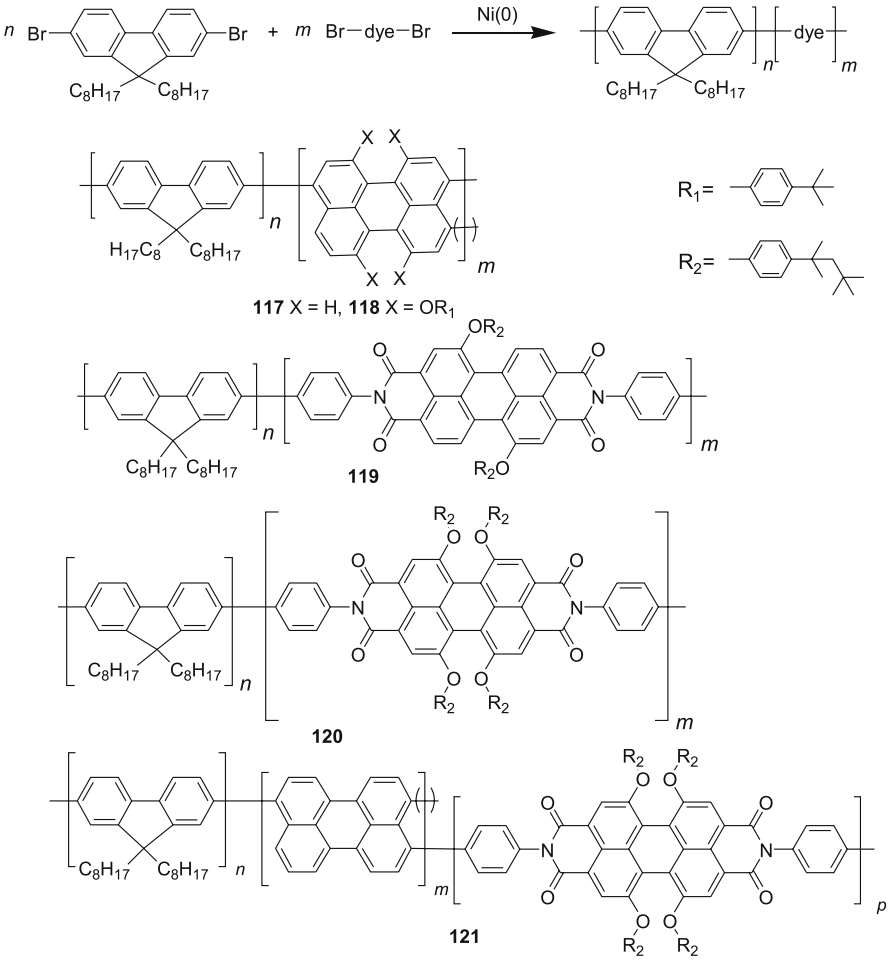

Scheme 55 Synthesis of copolymers of fluorene- and perylene-based dyes

orange and red dyes would be less efficient than to the green and yellow ones. Calculations based upon the spectral overlap indicated that the rate constant for energy transfer to the red dye was an order of magnitude smaller than for transfer to the green dye. Accordingly, a copolymer **121** was made containing both green (3 mol %) and red (3 mol %) emitting chromophores in order to determine if sequential energy transfer might be more efficient. The molecular weights of the copolymers were a little lower than for the homopolymer **89** (32 000–75 000 versus 85 000 g/mol), and their polydispersities were higher (3.6–4.9 versus 2.8).

The PL spectra of these materials in solution showed emission from both components roughly proportional to their relative mole ratios, but in films energy transfer occurred so that the PL spectrum was dominated by emis-

sion from the dyes. The PL quantum efficiencies of the copolymers **117–120** were only slightly lower (33–51%) than for **89** (55%), but that for **121** was very low (7%). This must be due to aggregation or some other fluorescence-quenching process. In the EL spectra only emission from the dyes was seen, which is due to a combination of energy transfer from the fluorene and the dyes acting as charge traps. The EL spectra closely resembled the PL emission from the dyes except for the copolymer **119** with the orange-emitting dye, where the EL spectrum was broader and red shifted compared with the PL spectrum. External efficiencies of 0.2–0.6% were obtained from these devices, which are comparable with other polyfluorene-based devices. The emission colours are stable, unlike devices using a blend of dye and **89**, where phase separation results in a loss of half the luminescence intensity within a few minutes, accompanied by a change in emission colour as the emission from the host polymer **89** reappears as the energy transfer becomes less efficient. As all the copolymers contain at least 95 mol % of dioctylfluorene units their blends with each other and with **89** should be stable, thus enabling stable emission of practically any colour desired, including white, to be obtainable.

Efficient energy transfer was also obtained from a copolymer **122** in which the perylene was attached as an end-capping group (Scheme 56) [224]. By using a ratio of fluorene to monobromo dye of 18 : 1 in a Yamamoto poly-

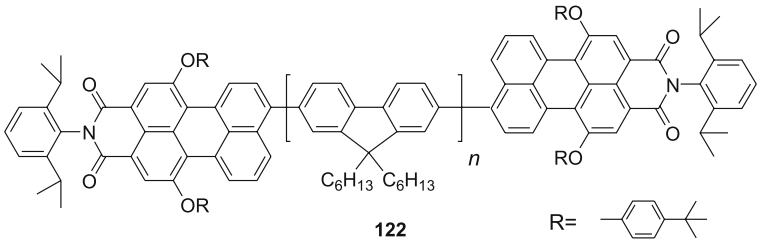

Scheme 56 Polyfluorene end-capped with a perylene dye

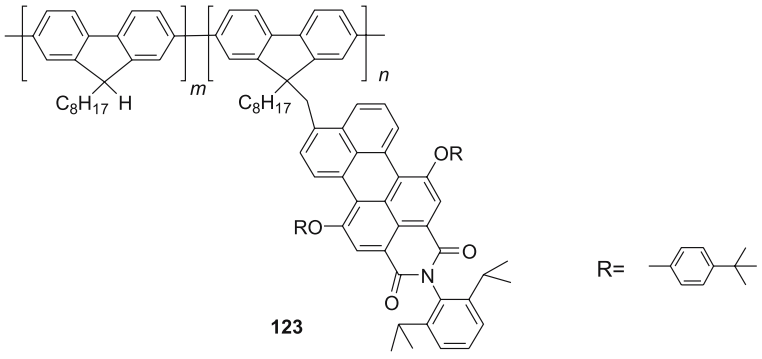

Scheme 57 Polyfluorene with dyes as side chains

condensation, a polymer with $M_n = 21\,000$ and a polydispersity of 2.1 was obtained, corresponding to a degree of polymerisation of about 40. As with the random copolymers **117–121**, no energy transfer was seen in solution, but in the solid state the emission was almost entirely from the dye moieties ($\lambda_{max} = 613$ nm). A problem with using the dye as an end-capping group is that due to a competing debromination reaction, complete end-capping in Yamamoto reactions is usually not obtained. In this case it was estimated that only 40 mol % of the polymer chains contained two dye units.

Due to the low mole ratio of dye units present, the above copolymers, with perylene dyes in the main chain or as end groups, show energy transfer only in the solid state. If the dyes are attached on the side chain, then copolymers containing much higher mole ratios of chromophore are accessible. The copolymer **123** (Scheme 57) in which 33% of the fluorene units have dyes attached ($m : n = 2 : 1$) showed energy transfer in solution as well as in a thin film [224]. The emission colour differed slightly between the two states, with the emission maximum appearing at $\lambda_{max} = 561$ nm in solution with a shoulder at 599 nm, and at $\lambda_{max} = 599$ nm in the solid state. This is probably due to interaction of the chromophores in the solid phase.

4.1.6
Dendronised Polyfluorenes – Towards Stable Blue Emission

In order to suppress long interchain interactions without losing solubility, bulky substituents can be attached. The IBM group prepared PDAFs end-capped with Fréchet-type dendrons of generations one (**124**, Scheme 58) to four [225]. By using a fluorene to end-capper ratio of 9 : 1 they obtained polymers with about 80 fluorene units. They found that the polymers with third- or fourth-generation dendrimer end groups showed no long-wavelength emission, even after annealing at 200 °C.

They have also prepared polymers with Fréchet-type dendrons of generations one to three as side chains by Yamamoto polycondensation (Scheme 59) [226]. A molecular weight of 51 000 was obtained for the homopolymer **125** with a first-generation dendrimer attached, but only oligomers ($M_n < 10\,000$ g/mol) were obtained from polymerisation of the fluorenes

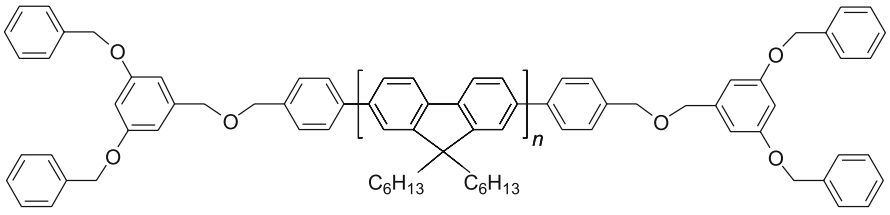

124

Scheme 58 Polyfluorene end-capped with a Fréchet-type dendron

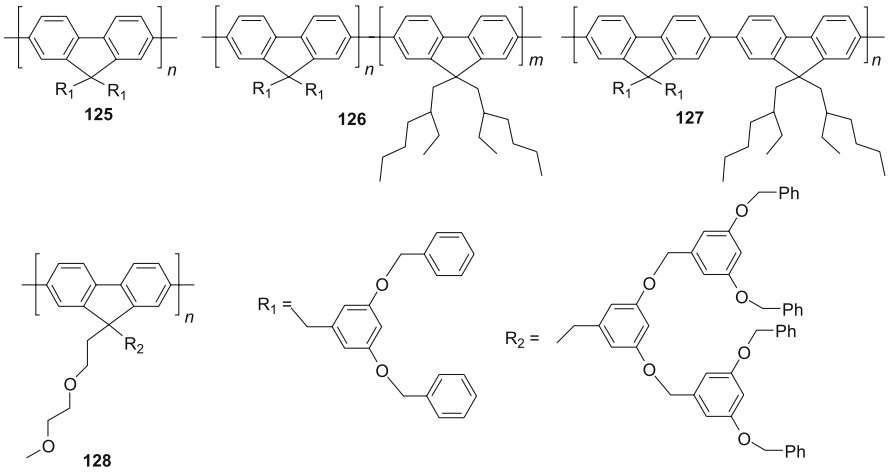

Scheme 59 Polyfluorenes with Fréchet dendrons as side chains

with higher-generation dendrimers attached. Random copolymers with ethylhexylfluorene, e.g. **126**, were made by the same method and showed much higher molecular weights (M_n = 26 000–68 000 g/mol), but the relative amount of dendrimer incorporated decreased with increasing generation from $m : n = 1 : 1.5$ for the first-generation dendrimer to 1 : 0.07 for the third-generation dendrimer. This shows that, as might be expected, the bulkier monomers are much less reactive under Yamamaoto conditions. Alternating copolymers, e.g. **127**, were made by Suzuki coupling. The molecular weights were lower (M_n = 4000–16 000 g/mol) with a degree of polymerisation for the monomers with first- and third-generation dendrimers of only three (six fluorene units). The second-generation dendrimer monomer was more reactive, showing a degree of polymerisation of eight. The PL and EL spectra of the polymers with second- or third-generation dendrimer side chains showed no long-wavelength emission, but the lifetime of the LEDs was short, as only very thin films could be deposited by spin coating. The highest PL efficiencies were obtained from the polymers and copolymers with second-generation dendrimer substituents. Pure blue PL (λ_{max} = 423, 447 nm) has also been reported from the polymer **128** with a single second-generation dendrimer side chain [227].

Müllen and coworkers have prepared a polymer **129** with a first-generation polyphenylene dendron on the side chain (Scheme 60) [228]. Unlike Fréchet dendrimers, such dendrimers are rigid and shape-persistent. Interestingly, the bulky side chains produced no blue shift in the absorption or emission of the polymer compared with PDAFs such as **89**, indicating that there is no increased steric repulsion between adjacent fluorene units. LEDs using this polymer display device characteristics (turn-on voltage, emission efficiency,

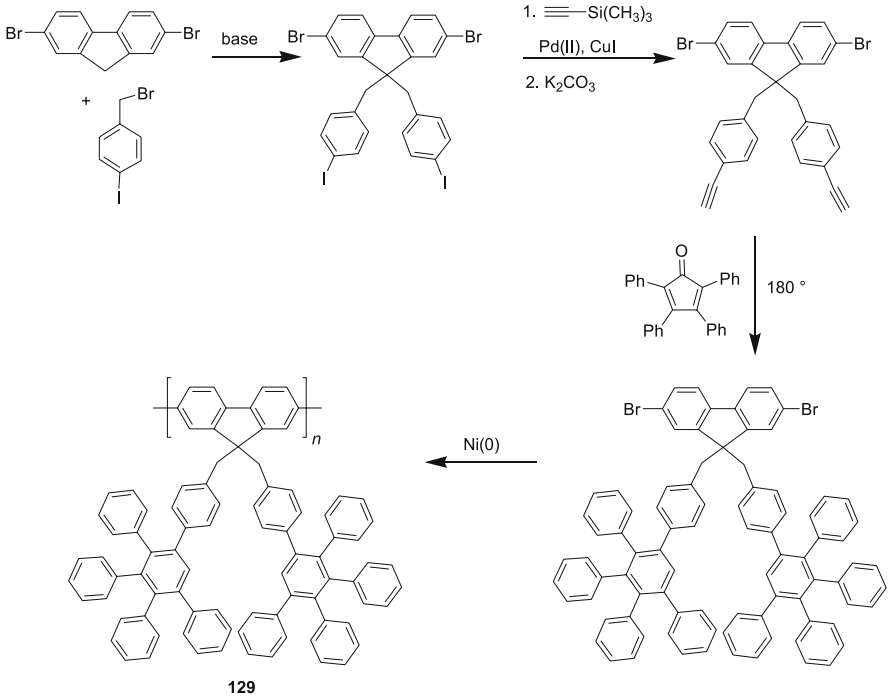

Scheme 60 Synthesis of a polyfluorene with a polyphenylene dendron on the side chain

and brightness) comparable to those for the PDAFs such as **89**, but with no long-wavelength emission being seen at driving voltages below 12 V.

Though the emission stability of **129** is much better than for PDAFs, long-wavelength emission is seen with time, possibly due to the susceptibility of the benzyl linkages to oxidation. Accordingly, a new class of polyfluorenes with aryl substituents at the 9-position has been developed (Scheme 61) [228]. Aryl substituents are much less susceptible to oxidation to fluorenone than alkyl groups and their bulk reduces interchain interactions, and hence exciton diffusion to any defect sites that may be formed.

As aryl groups, unlike alkyl groups, generally cannot be directly substituted onto the 9-position of fluorenes, the monomers were prepared by addition of aryl lithium reagents to the biphenyl-2-carboxylic acid methyl ester **130**, followed by ring closure of the resulting carbinols in hot acetic acid, using a small amount of concentrated sulfuric acid. This produced a dark-blue or lilac colour due to the formation of the cation, followed by the appearance of a white precipitate of the desired 9,9-diarylfluorenes **131**. These were then polymerised using nickel(0).

The diphenylfluorene polymer **132** (Scheme 62) was virtually totally insoluble. Characterisation by MALDI-TOF of a soluble fraction, obtained by prolonged Soxhlet extraction with toluene, suggested that it consisted mainly of

oligomers up to the hexamer ($n = 6$), though chains of up to 15 fluorene units were detected [229]. The insoluble fraction contained chains with degrees of polymerisation of up to 25, which suggests that some chain addition occurred even after the material was no longer soluble in the reaction medium.

By contrast, the materials **133** with di-*tert*-butylphenyl and **134** with first-generation dendron side chains were processable from toluene [228]. The degrees of polymerisation for these polymers were rather low, with the dendronised polymer **134** having M_n of only 10 000 g/mol ($n = 10$), probably due to the bulkiness of the substituents. Polymer **134** was also found to be exceptionally thermally stable, with no significant mass loss being observed in thermal gravimetric analysis (TGA) until 570 °C (cf. 463 °C for **89** [224]). Substituted first-generation and unsubstituted second-generation dendrimers have been attached to fluorene by a modification of the above route in which an ethynyl-substituted benzene is attached to the fluorene 9-position and the dendrimers then built up from it [230]. The degree of polymerisation of **134** can be increased (M_n = 32 000 g/mol, $n = 32$) by using a dichloro instead of a dibromo monomer in the Yamamoto polymerisation [231].

Stable blue PL emission has been obtained from films of both **133** and **134**, with no sign of an emission band at 530 nm even after annealing for 24 h in

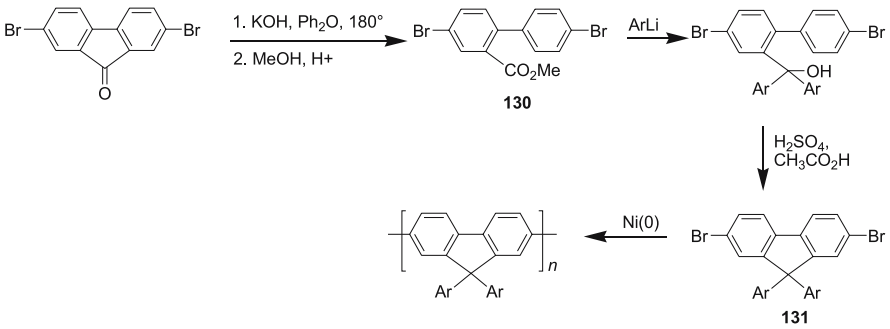

Scheme 61 Synthetic route to poly(9,9-diarylfluorene)s

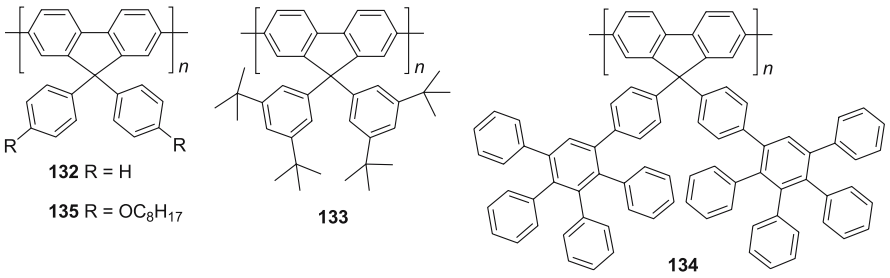

Scheme 62 Poly(9,9-diarylfluorene)s

air at 100 °C. This shows that aryl substituents are much stabler towards oxidation than alkyl groups, as annealing of **89** under these conditions produces a strong defect emission band. Drop-cast films of **133** showed a slight red shift in the PL spectrum upon annealing, which may be attributed to changes in the chain packing, as no such change was seen from spin-cast films, which illustrates the importance of processing conditions in determining the properties of films of conjugated materials. Stable blue emission has also been obtained from the polymer **135** bearing 4-octyloxyphenyl substituents [232]. This was prepared by addition of phenol to dibromofluorenone, followed by alkylation and polymerisation (cf. Scheme 70, below).

Both **133** and **134** show blue EL with no significant defect emission even after several minutes operation [223, 233]. When devices using **134** were run continuously at 8 V for 30 min, a slight increase in long-wavelength emission was observed [233]. This partially disappeared upon reversing the bias, which was attributed to a shift in the recombination zone within the device. By subtracting the original spectrum from that of the aged device it was found that the extra emission corresponded to the defect emission band at 530 nm, which suggests that some oxidation of **134** was occurring, possibly due to incomplete encapsulation of the device. When the device was run in pulsed mode, however, stable blue blue EL with a luminance of 191 cd/m^2 was obtained with no sign of degradation even over prolonged periods [233].

Comparative photophysical studies of **90** and **129** suggest that in dendronised polyfluorenes the bulkiness of the substituents hinders exciton migration due to increased chain separation [234]. Delayed PL studies [235] of **90** and **134** found that both polymers display a defect emission band at 530 nm, and a band at 480 nm previously attributed to interchain aggregates [205]. This is an interesting result as interchain aggregates had previously been assumed to arise from π-stacking of the polymer chains. Calculations of

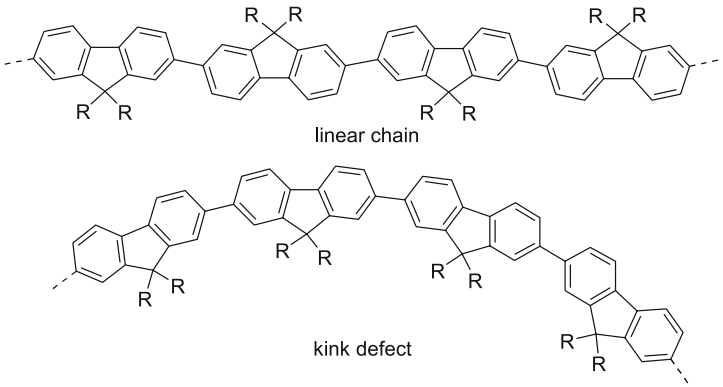

Scheme 63 Possible conformations of polyfluorene chains

oligomers of **89** and **90** show that by adopting a planar conformation the dioctylfluorene units in **89** can π-stack with a separation of 5 Å, while the fluorenes with the ethylhexyl substituents in **90** cannot approach within 7 Å of each other, which precludes π-stacking [236]. The separation of dendronised fluorene units can be expected to be even greater than for the units in **90**. Thus interchain interactions in these polymers must arise not from cofacial π-stacking, but at point defects on the chains. These defects can arise because fluorene is not linear, but is bent, with an angle between the bonds to the 2- and 7- positions of about 20°. Normally in polyfluorene chains the fluorene units align with successive units having their substituents pointing in opposite directions so as to give overall a linear chain. However, 'kink' defects can form where the chain bends due to successive fluorene units aligning with the 9-substituents on the same side (Scheme 63). A bent conformation has been detected for an end-capped fluorene trimer in a polymer matrix [237]. In theory the chain can even loop back on itself. At such points two chains might be able to interact without interference from the side chains.

4.1.7
Polyfluorenes with Improved Charge Injection

A second problem with PDAFs is that of charge injection. The energy levels of the HOMO and LUMO orbitals of **89** have been determined to be 5.8 eV and 2.12 eV by cyclic voltammetry [238]. This means that there are large barriers to charge injection from electrodes such as calcium (work function 2.9 eV) and ITO (4.7–5.0 eV). The value for the HOMO-LUMO gap of 3.7 eV determined by electrochemistry is much larger than the optical band gap of 2.95 eV calculated from the onset of absorption, which suggests that one or both of the electrochemically derived orbital energy levels are inaccurate. As the efficiency of devices using calcium electrodes seems to be limited by hole injection [239], most probably it is the LUMO value which is at fault (too high).

A number of approaches have been adopted to overcome the problem of obtaining efficient charge injection. Satisfactory electron injection seems to be obtained by use of calcium as cathode, and a composite LiF/Ca/Al cathode is reported to give better electron injection than a simple calcium cathode [240], but there usually remains a large barrier to hole injection due to the difference between the HOMO and ITO energy levels. As a result, hole-injecting layers are used in PDAF devices in order to obtain good efficiency (Scheme 64) [241]. Poly(3,4-ethylenedioxythiophene) (**136**) doped with poly(styrene sulfonate) (PEDOT : PSS) [178] is most commonly used, but recently poly(4,4′-dimethoxybithiophene) (**137**) has been reported to be a superior hole-injection material [239]. Scott and coworkers at IBM found that the efficiency of devices using emissive layers of cross-linked polymer **108** could be increased by factors of 400 and 800 respectively by use of electron- and hole-injecting layers, though the latter device also showed some

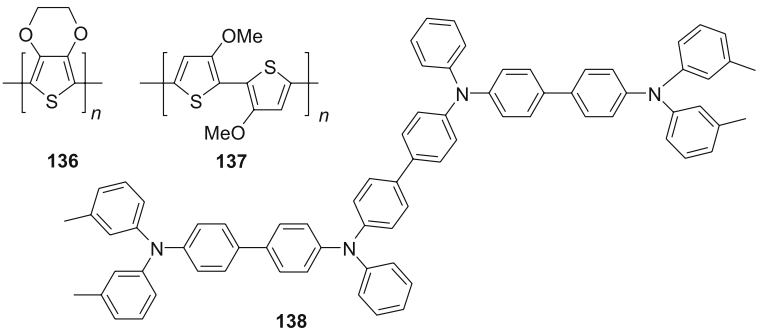

Scheme 64 Materials used to improve hole injection or transport in polyfluorenes

red-orange emission from the triarylamine hole-transporting layer [242]. A triple-layer device with both hole- and electron-injecting layers was even more efficient, with efficiencies of over 1% being obtained, although again some weak emission from the hole-transporting layer was observed.

A second method is to blend charge-transporting materials into the emissive polymer, though this raises the problems of phase separation. Neher and coworkers have examined blends of the copolymer **106** (Scheme 50) with hole-transporting small molecules [211]. Not only did this increase the efficiency and luminance of the devices, but as mentioned above it also suppressed the green emission from the ketone defects. The highest efficiency (0.87 cd/A) and luminance (800 cd/m^2) (cf. 0.04 cd/A and 70 cd/m^2 for undoped **106**) were obtained by incorporation of 3 wt % of the oligomeric triarylamine **138** (Scheme 64). No phase separation leading to device degradation was observed by them during the characterisation of their devices, but the long-term stability of such blends is uncertain.

Another approach is to incorporate charge-transporting groups into the polymer, either as end groups, as units in the polymer chain or as side chains. The IBM group [243] have compared the efficiency, using both calcium and aluminium cathodes, of triblock polymers (Scheme 65) containing an anthracene–dialkylfluorene copolymer as the emissive block with hole-transporting poly(vinyl triphenylamine) (**139**) or electron-transporting poly(vinyl oxadiazole) (**140**) blocks at each end with the simple copolymer **111** (Scheme 53).

In single-layer devices with calcium cathodes the EL efficiency of the hole-transporting triblock **139** was nearly double that of **111** (0.35% versus 0.02%), but that of the electron-transporting triblock **140** was slightly lower (0.014%). This shows that with calcium electrodes, hole injection is the limiting factor for efficiency. With aluminium electrodes, electron injection by contrast became the limiting factor so that the highest efficiency (0.01%) was obtained with **140**, although the efficiency of **139** (0.008%) was still much higher than

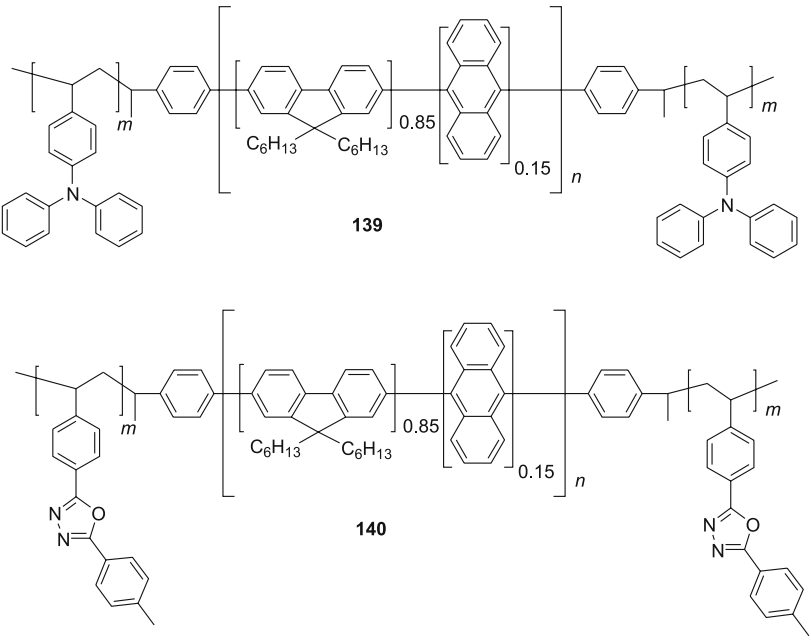

Scheme 65 Triblock copolymers containing both emissive and charge-transporting blocks

of **111** (0.001%). The triblock **139** showed a strong orange-red-emission band due to emission from the triphenylamine units in the EL, but not in the PL spectrum. The highest efficiency (0.54%) was obtained from a double-layer device of **139** with a hole-transporting layer and a calcium cathode. Again some emission from the triphenylamine units was seen, though it was much weaker than in the single-layer device.

Scherf, Neher and coworkers prepared liquid-crystalline polyfluorenes, **141** and **142** (Scheme 66), by adding bromo-substituted triarylamines as end-capping reagents to a Yamamoto polymerisation [244]. By varying the amount of end-capper they were able to control the molecular weight and polydispersity of the polymer, so that for **141** 2 mol % of end-capper gave a polymer with M_n = 102 000 and M_w/M_n = 1.4, while 9 mol % of end-capper produced a polymer with M_n = 12 000 and M_w/M_n = 2.6. NMR analysis showed that the end-capping was incomplete so that 2 mol % of end-capper produced 1.8% of triarylamine end groups and 9 mol % resulted in 8.3% incorporation of the end groups. Films of these polymers deposited on an aligned polyimide layer showed polarised emission with better efficiencies (up to 0.75 cd/A) than for the homopolymer **90**. Even better efficiencies (up to 2.7 cd/A) have been obtained from devices using an emissive layer of **141** (2 mol % end-capper) and a series of three cross-linked hole-transporting layers of varying work function [245].

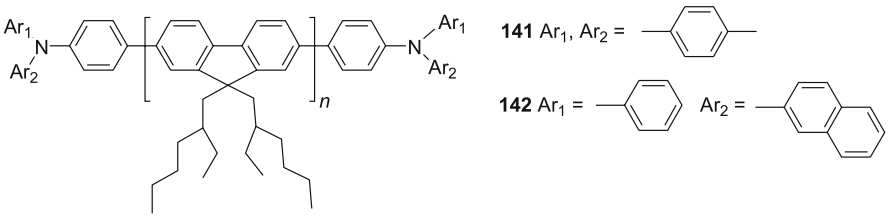

Scheme 66 Polyfluorenes end-capped with hole-transporting groups

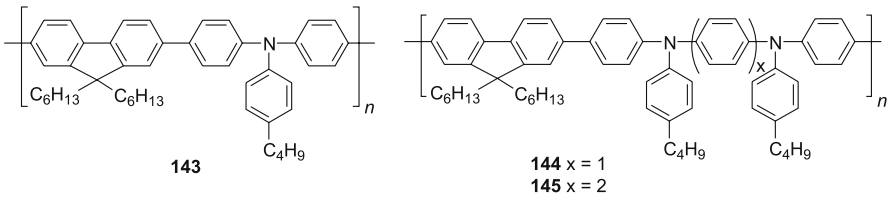

Scheme 67 Copolymers of fluorene with hole-transporting triarylamines

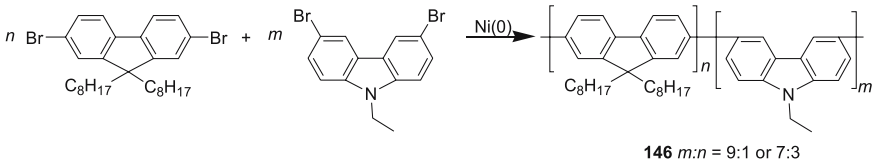

Scheme 68 Synthesis of a fluorene–carbazole copolymer

The Dow group have prepared alternating copolymers of dialkylfluorene with hole-transporting triphenylamines (Scheme 67), e.g. **143**, by Suzuki coupling of fluorene bisboronic acids with dibromotriarslamines [174–177, 241]. Blue emission has been reported from some of these polymers, e.g. **144** [246] (λ_{max} = 486 nm) and **145** [174] (λ_{max} = 481 nm). It would appear, however, that these materials are primarily intended to be used as hole-transporting rather than emissive materials.

Xia and Advincula have prepared copolymers **146** containing hole-transporting carbazole units by Yamamoto copolymerisation (Scheme 68) [247]. Cyclic voltammetry showed that the HOMO energy level increased from 5.8 eV to 5.6 eV with 10 mol % carbazole and to 5.5 eV with 30 mol % carbazole. They also found that films of these copolymers showed stabler blue PL than the homopolymer **89** with the green ketone emission band appearing only slowly upon annealing at 200 °C.

The IBM group have investigated the incorporation of charge-transporting groups into the copolymer **110** [182]. Introduction of hole-transporting triphenylamine units produced a slight red shift (λ_{max} = 462 nm) in the EL spectrum, while electron-accepting diphenylsulfone units caused a small blue shift (λ_{max} = 445–449 nm) in the emission, in both cases with a decrease

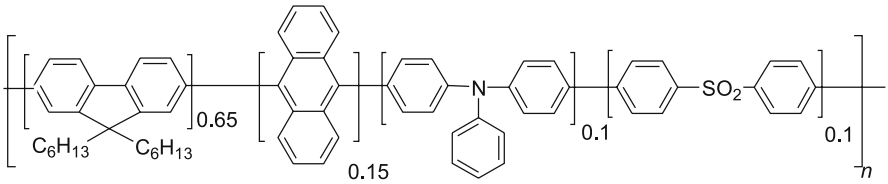

147

Scheme 69 Copolymer of fluorene with both hole- and electron-transporting units

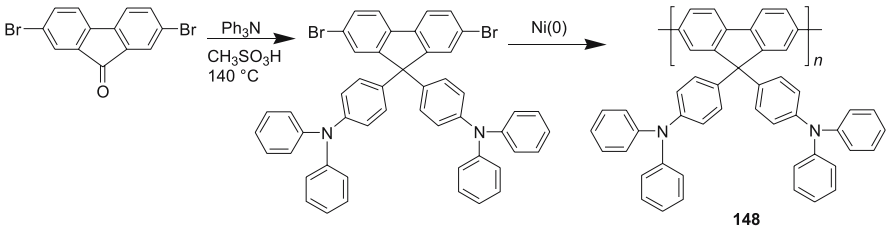

148

Scheme 70 Synthesis of polyfluorene with triphenylamine substituents

in the EL efficiency. By contrast, the copolymer **147** (Scheme 69) containing 10 mol % of both groups showed stable blue EL (λ_{max} = 460 nm) with nearly twice the efficiency of **110**.

Müllen and coworkers have recently prepared the polymer **148** in which hole-transporting triphenylamine units are attached at the 9-position (Scheme 70) [248]. The triphenylamine substituents are introduced by Friedel–Crafts alkylation of triphenylamine with 9-fluorenyl cations produced from dibromofluorenone under the reaction conditions. The degree of polymerisation is not very high (n = 14) due to the limited solubilising power of the substituents. The HOMO of **148** has been determined by cyclic voltammetry to be at 5.5 eV, so the barrier to hole injection from ITO is much smaller than for PDAFs. Polymer **148** shows stable blue EL (λ_{max} = 428 nm), but the overall EL efficiency is lower than for PDAFs despite the better hole-accepting properties, probably because of the lower PL efficiency of **148** (22% versus 55% for **89** [178]). The use of a PVK hole-injecting layer does not improve the efficiency as it does with PDAFs, indicating that hole injection into **148** is superior.

Müllen and coworkers have also prepared the blue-emitting (λ_{max} = 450 nm) polyketal **149**, films of which can be converted by exposure to dichloroacetic acid vapour to the orange-emitting (λ_{max} = 580 nm) polyfluorenone **150** (Scheme 71) [249]. The carbonyl groups enhance the electron-accepting properties of **150**, and this polymer shows useful electron-transporting properties, though the acidic residues from the conversion are a potential source of problems for electronic applications [250].

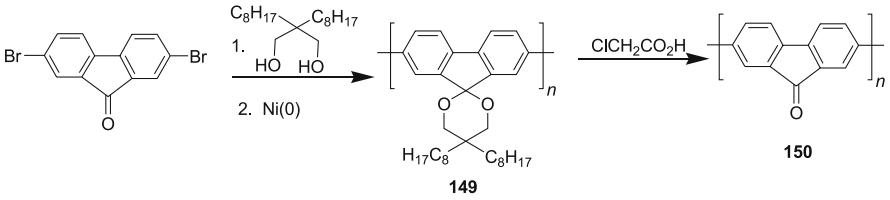

149 150

Scheme 71 Precursor route to polyfluorenone

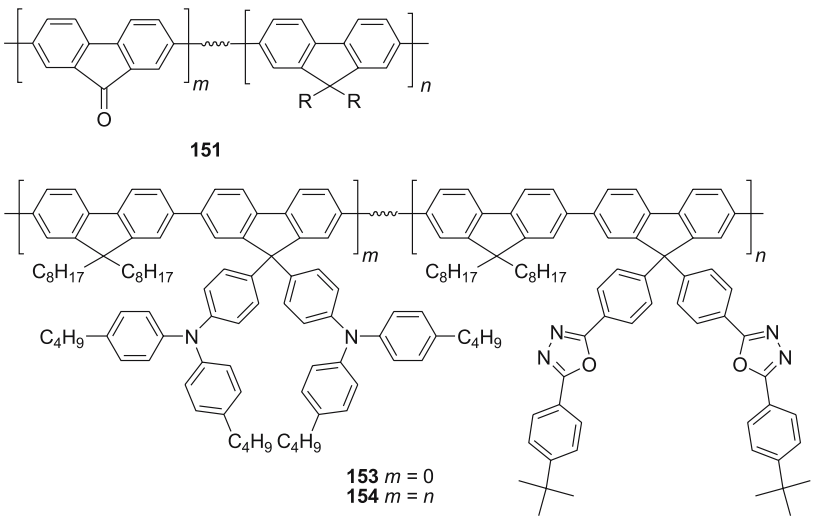

151

153 $m = 0$
154 $m = n$

Scheme 72 Fluorene copolymers with electron-accepting units

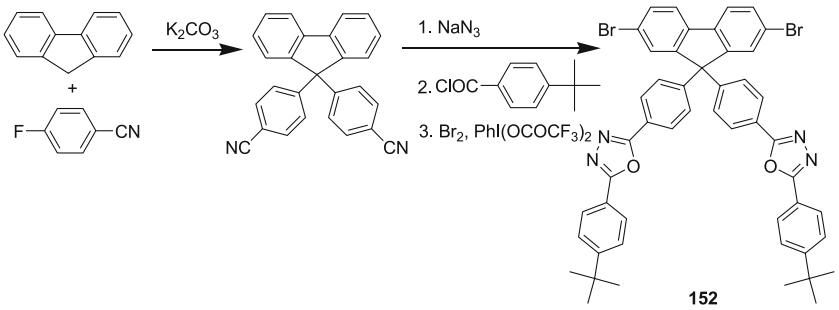

152

Scheme 73 Synthesis of a fluorene with oxadiazole substituents

Copolymers **151** (Scheme 72) containing fluorenone units have been used as green EL materials (λ_{max} = 535 nm) with the optimal efficiency of 0.19% being obtained for the copolymer with 3 mol % of fluorenone [251].

Recently, Shu, Jen and coworkers [252] prepared a fluorene **152** with two electron-accepting oxadiazole substituents by nucleophilic substitution

of 4-fluorobenzonitrile with the fluorenyl anion, and subsequent conversion of the nitriles to oxadiazoles via tetrazole intermediates (Scheme 73). The alternating copolymer with dioctylfluorene **594** (Scheme 72) showed better colour stability and higher efficiency in a single-layer device (0.52%) than poly(dioctylfluorene) (**560b**) (0.2%) due to its improved charge-accepting ability. The copolymer **595** ($m : n = 1 : 1$) with both hole- and electron-accepting substituents displayed even better efficiency (1.21%) [253].

4.1.8
Alternating Copolymers of Fluorenes and Other Arylenes

Copolymers with alternating fluorene and phenylene units (Scheme 74) can be readily prepared by Suzuki cross-coupling. The biphenylene copolymers **155** show violet-blue EL ($\lambda_{max} = 416$ nm) [254, 255], while the phenylene copolymers **156** are blue emitting ($\lambda_{max} = 420$ nm) [254–260]. Substitution of the phenylene ring with alkyl groups as in **157** produces a marked blue shift in the PL emission ($\lambda_{max} = 404–409$ nm) [207, 259], presumably due to increased torsion of the phenylene units. By contrast, the alkoxy substituents as in **158** produce almost no effect on the PL and EL maxima ($\lambda_{max} = 420–425$ nm) [207, 261, 262]. The reported EL spectrum of **158** shows no long wavelength emission band, and annealing of a film produces much less green emission than for PDAFs [207], suggesting that this material is stabler.

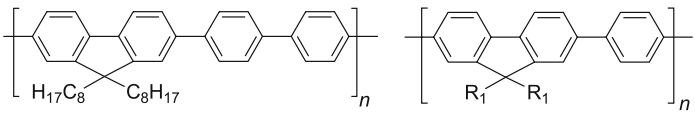

155

156 $R_1 = C_6H_{13}$ or C_8H_{17}, $R_2 = H$
157 $R_1, R_2 = C_6H_{13}$
158 $R_1 = C_6H_{13}$, $R_2 = OC_{10}H_{21}$

Scheme 74 Alternating copolymers of fluorene and other arylenes

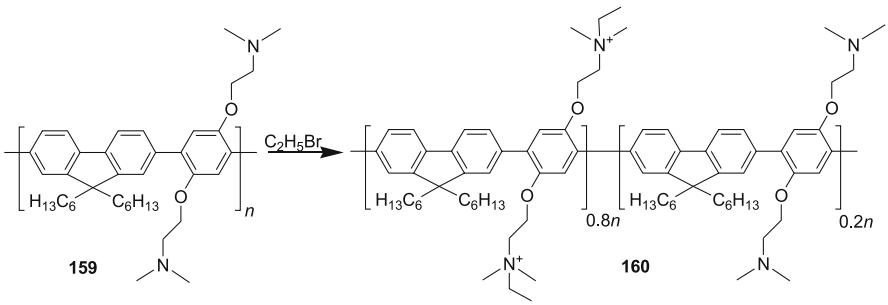

159 **160**

Scheme 75 Preparation of a water-soluble fluorene copolymer

Quaternisation of the amino side chains on the copolymer **159** (Scheme 75) with ethyl bromide causes a complete inversion in the solubility, with the 80% quaternised polymer **160** being soluble in DMSO, methanol, and water, but insoluble in chloroform and THF [263]. The emission shows some solvent dependence, with the maximum appearing at λ_{max} = 409 nm in water and methanol, and at λ_{max} = 419 nm in DMSO. A further effect of the quaternisation is that the PL quantum efficiency drops. The efficiency is much higher in methanol than in water (86% versus 25%), which was attributed to aggregation in aqueous solution.

A similar water-soluble copolymer **161** (Scheme 76) has been made by Bazan and coworkers [264] and used in a novel biosensor application [265, 266], in which energy transfer between **161** and a fluorescent dye attached to a strand of probe DNA occurs only in the presence of a DNA sequence complementary to that of the probe.

The carboxylate substituents on the phenylene in **162** (Scheme 77) produce a red shift in the PL (λ_{max} = 443 nm) but a drop in PL efficiency (20% versus 78–81% for **156**) [259]. Jen and coworkers have prepared the copolymers **163** (λ_{max} = 447 nm) and **164** (λ_{max} = 477 nm) with electron-accepting dicyanobenzene units by Suzuki polycondensations [267]. The alternating copolymer **163** shows only marginally higher EL efficiency than the PDAF homopolymer **85** (0.057% versus 0.044%), but the other copolymer **164** with only 25% of dicyanobenzene units ($m = n$) shows an EL efficiency over 10 times higher (0.50%) in double-layer devices with a PEDOT hole-transporting layer and calcium cathodes [267].

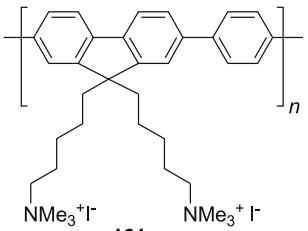

161

Scheme 76 Water-soluble polyfluorene for biosensor applications

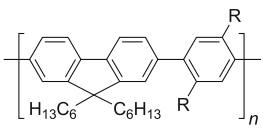

162 $R_1 = C_6H_{13}$, $R_2 = CO_2C_2H_5$
163 $R_1 = C_6H_{13}$, $R_2 = CN$

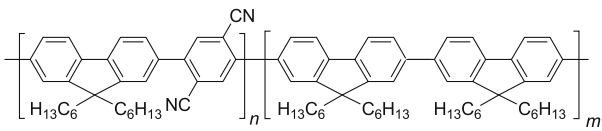

164

Scheme 77 Alternating fluorene–arylene copolymers with electron-accepting substituents

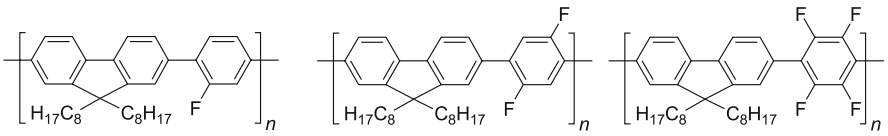

Scheme 78 Fluorophenyl–fluorene copolymers

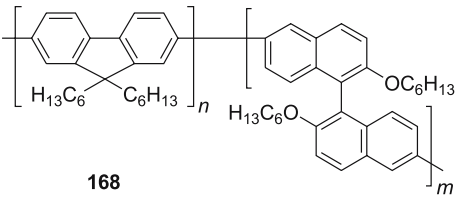

Scheme 79 Copolymer of fluorene and binaphthyl

A Japanese group have prepared the copolymers **165–167** (Scheme 78) [260]. The bulky fluorine substituents produce a blue shift in the PL emission due to increased steric repulsion, so that the PL maxima in solution shift from λ_{max} = 400 nm for **165** to λ_{max} = 398 nm and 382 nm for **166** and **167**. This blue shift is accompanied by a drop in the PL efficiencies (measured in solution) from 34% for **165** and **166** to 29% for **167** (cf. 78–81% for **156**).

Jen and coworkers have prepared a copolymer **168** ($n : m = 3 : 1$) of dihexylfluorene and binaphthyl by Suzuki copolymerisation (Scheme 79), which showed two EL maxima at λ_{max} = 420 and 446 nm in two-layer devices, whose relative intensity depended upon the device structure [268, 269]. External efficiencies of up to 0.79% were obtained.

An industrial group have reported obtaining efficient red, green, and blue emission from polyfluorene-based alternating copolymers prepared by Suzuki polycondensation, but without publishing their structures [270, 271].

4.1.9
Polymers Containing Spirobifluorene Units

Spirobifluorenes have been investigated by Salbeck [272] and found to be promising materials for use in blue LEDs, and so some effort has been made to incorporate these units into polymers (Scheme 80). Blue ($\lambda_{max} \sim 425$ nm) EL emission has been obtained from poly(spirobifluorene oligophenylene) copolymers **169** (m = 0–2) prepared by Suzuki cross-coupling [273]. These materials have somewhat limited solubility and so have not been fully characterised. By contrast, the polymer **170** bearing solubilising alkoxy groups is soluble in organic solvents [274]. No green PL emission was observed from a film of **170** that had been annealed in air at 200 °C for 3 h.

An alternating fluorene–spirobifluorene copolymer **171** has been prepared by Huang and coworkers by Suzuki coupling and found to show stabler blue emission than PDAFs with long-wavelength emission only being detected after the polymer film was heated to 150 °C [207, 275]. Blue emission with efficiencies of 0.12% and 0.54% was obtained from single- and double-layer (with a copper phthalocyanine hole-transporting layer) devices [275].

Meerholz and coworkers [276] have used Suzuki cross-coupling of a spirobifluorene bisboronate with various dibromo-comonomers to prepare cross-linkable copolymers **172–174** (Scheme 81) which respectively produced blue (λ_{max} = 457 nm), green (λ_{max} = 507 nm), and red (λ_{max} = 650 nm) EL. Illumination of films of these materials with ultraviolet light in the presence of a photoacid induced cationic polymerisation of the oxetane rings to cross-link the materials. Comparison of the EL properties of cross-linked **172** with a similar non-cross-linkable polymer showed that the cross-linking had no significant effect upon the luminescence of the materials. They used these materials to make a pixelated red, green, blue display in which each of the materials was patterned by irradiation through a mask.

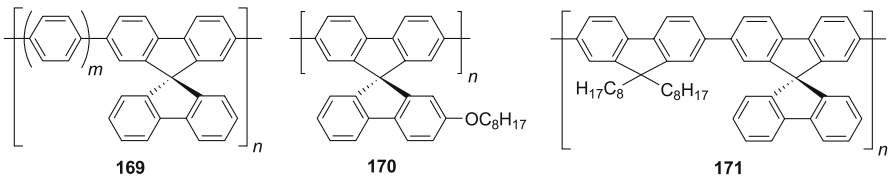

169 **170** **171**

Scheme 80 Polymers containing spirobifluorene units

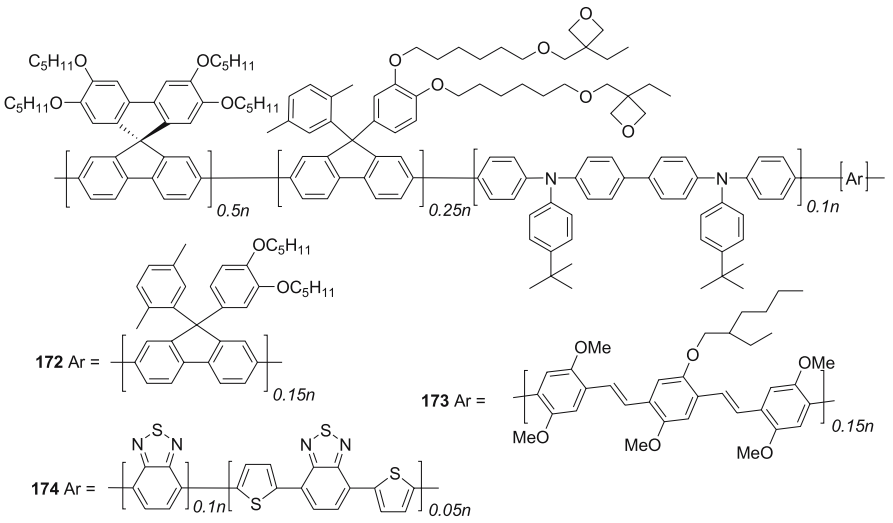

Scheme 81 Cross-linkable copolymers containing spirobifluorenes

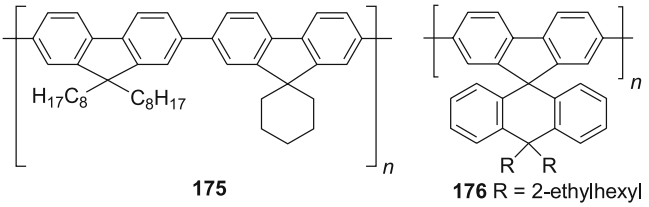

Scheme 82 Polymers containing spiro-functionalised fluorenes

Spiro-functionalisation with groups at C9 has also been examined as a means to stabilise blue emission from polyfluorenes. While polymers with spirocycloalkyl groups, e.g. **175** (Scheme 82), display green emission upon annealing [277], the polymer **176** with aryl groups at C9 produces stable blue PL and EL emission even after annealing [278].

4.2 Poly(indenofluorene)s

Poly(tetraalkylindenofluorene)s (PIFs, Scheme 83), which are intermediate in structure between PDAFs and LPPP, have been prepared by Müllen and coworkers by Yamamoto coupling [279]. In solution they showed strong blue PL with maxima around 430 nm, which made them attractive candidates for use in blue LEDs. By extrapolating the absorption and emission maxima of oligomers the effective conjugation lengths were determined to be $n = 5–6$ (15–18 benzene rings) for emission and $n = 6–7$ for absorption. Unfortunately, as with PDAFs, obtaining stable blue emission in the solid state has presented difficulties. The tetraoctylpolymer **177** is a green emitter in the solid state, with the PL and EL spectra being dominated by a broad emission band at 560 nm [280]. By contrast, films of the polymer **178** with ethylhexyl substituents show blue PL (λ_{max} = 429, 450 nm). The EL from **178** is initially blue, but rapidly red shifts, with a simultaneous loss of emission intensity, so that the devices have a half-life (time for the intensity to drop to half of its initial value) of less than 1 h. By contrast, the green emission from **177** is

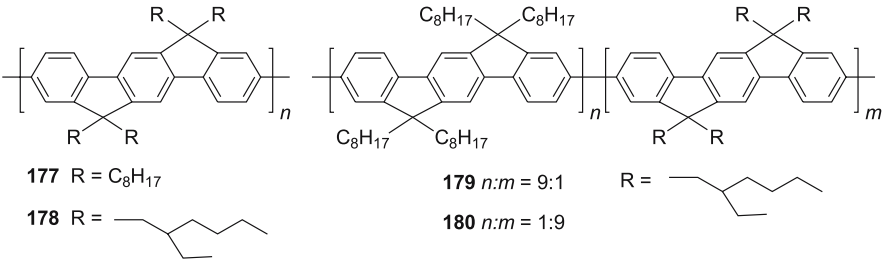

Scheme 83 Alkylindenofluorene-based polymers

stable, with an estimated half-life of 5000 h. Copolymers **179** and **180** show intermediate behaviour.

The source of this green emission might be either excimers or defects. The amount of green emission in the solid-state spectra has been shown to correlate well with the presence of long ordered structures due to π-stacking in the film morphology revealed by atomic force microscopy studies [280]. These results are consistent with the green emission arising from aggregates. Certainly the greater solid-state PL efficiency for **178** (36%) and the copolymers **179** (40%) and **180** (50%) compared with **177** (24%) is consistent with the bulkier branched side chains reducing interchain interactions and so reducing the possibility of non-radiative decay. An alternative explanation would be that the emission arises from ketone defects **181** (Scheme 84), which would be expected to show green emission intermediate between the defects **69** (530 nm) and **70** (565 nm) proposed for PDAFs and LPPPs, respectively. The above EL results would then be explicable in terms of the relative ability of excitons to diffuse to defect sites in the polymer films. To resolve this, the ketone **182** has been prepared as a model compound for such defects. The emission properties of **182** match those of defects detected by time-resolved PL measurements of **177–178** [281].

The phase behaviour of PIFs **177** and **178** resembles that of the corresponding PDAFs **89** and **90**, but with higher phase-transition temperatures. Thus, the octyl polymer **177** shows two nematic phases with transition temperatures at 250 and 290 °C (reverse transitions at 270 and 140 °C), while the ethylhexyl polymer **178** has only a single nematic phase with a transition at 290 °C (220 °C for the reverse transition) [279].

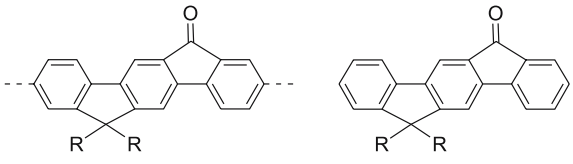

181 **182**

Scheme 84 Proposed emissive defect in polyindenofluorenes

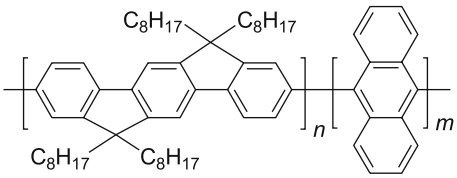

183

Scheme 85 Indenofluorene–anthracene copolymer which produces stable blue emission

As with PDAFs, copolymers with anthracene **183** (Scheme 85, $n : m$ = 85 : 15) show stable blue EL (λ_{max} = 445 nm), probably due to exciton confinement [282].

Since aryl substituents have been shown to greatly enhance the stability of blue emission from PDAFs, the effect of such substituents in PIFs has also been investigated. The synthesis of the tetraarylmonomers (Scheme 86) follows a route similar to that used for the diarylfluorenes **131** (see Sect. 4.1, above). Suzuki coupling of a dibromoterephthalate [157] with commercially available 4-trimethylsilylbenzeneboronic acid gives the terphenyl **184** in high (92%) yield. Treatment of this with four equivalents of an aryl lithium followed by electrophilic displacement of the silyl group with bromine and then ring closure produces tetraarylindenofluorene monomers **185** in good (70%) yield. These were then polymerised with nickel(0) [230].

Due to the limited solubilising power of the substituents, only oligomers (n = 2–6) of the *tert*-butylphenyl polymer **186** (Scheme 87) were obtained. The octylphenyl groups in **187** provided much better solubility, so that this polymer was obtained with M_n = 66 400 g/mol, M_w/M_n = 3.86 (measured against a polyphenylene standard), corresponding to a degree of polymerisation of about n = 66 (~ 200 phenylene rings).

The PL emission from **187** is blue both in solution (λ_{max} = 428 nm) and in thin films (λ_{max} = 434 nm), with no sign of the green-emission band seen for **177**. Some unoptimised LEDs have been constructed using **187**, which have rather high operating voltages (16 V) due to problems with preparing good-quality films. The EL spectrum has its maximum at 434 nm in the blue but with a long tail extending into the red region of the spectrum, so the emission is blue-white in colour. The emission is much stabler than from **177**–**179** above with only a slight increase in the long-wavelength emission being seen after several minutes operation of a device at 16 V. This suggests that improved devices with lower operating voltages might show stable blue EL

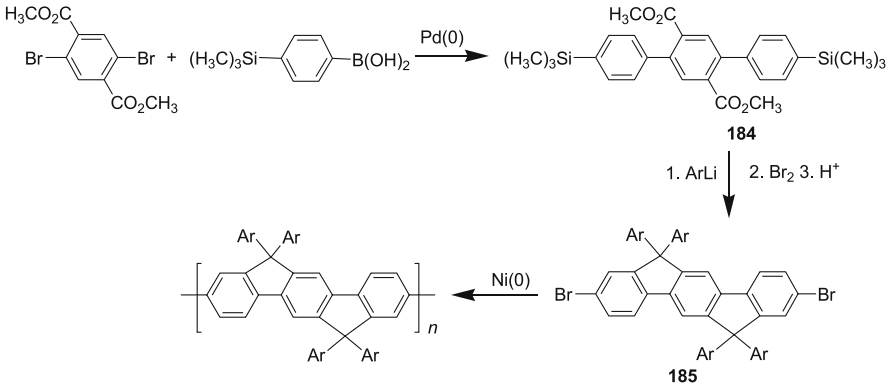

Scheme 86 Route to poly(tetraarylindenofluorene)s

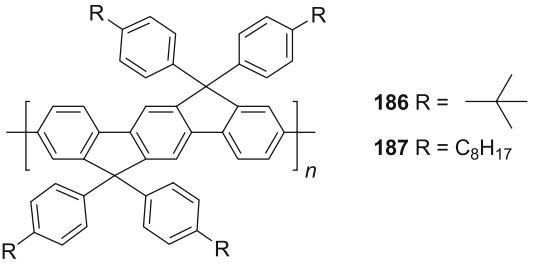

Scheme 87 Poly[tetra(4-alkylphenyl)indenofluorene]s

emission. Blending 0.3 wt % of the ketone **182** into **187** has been found to totally suppress the blue emission [281], thus demonstrating that even very low levels of emissive defects can profoundly affect the emission properties of conjugated polymers.

4.3 Poly(ladder-type pentaphenylene)s

A modification of the synthesis of the tetrarylindenofluorenes **186** shown in Scheme 86 has been used to prepare ladder-type pentaphenylenes (Scheme 88) [283]. The dibromoterephthalate was coupled with two equivalents of a fluorene boronate instead of a benzene boronic acid to give a pentaphenylene **188.** Reaction with an aryl lithium, followed by ring closure with boron trifluoride, gave the ladder-type pentamers **189**, which were brominated to prepare dibromomonomers that were then polymerised using nickel(0).

The polymer **190** produces blue PL and EL with an emission maximum at 445 nm and a very small Stokes' shift, and so closes the gap in emission colour between PIFs and LPPPs. The optical properties are very similar to those of

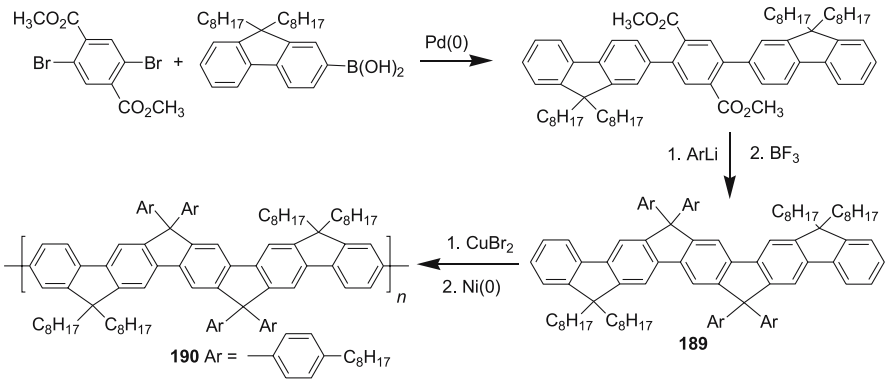

Scheme 88 Synthesis of poly(ladder-type pentaphenylene)s

LPPP **3**, but the blue emission is much more stable. Polymer **190** also has a remarkably large persistence length of 25 nm [284], indicating a highly rigid structure.

4.4 Other 'Stepladder'-type Polyphenylenes

PFs, PIFs, and poly(ladder-type pentaphenylene)s have methine bridges, and so are structurally related to LPPP **3**. Stepladder polymers have also been prepared with other types of bridges.

4.4.1 Poly(tetrahydropyrene)s

Poly(tetrahydropyrene)s **65** (Scheme 28), like polyfluorenes, have a bridged biphenyl unit, but with two ethane bridges the angle between the two phenylene rings is about 20°. Poly(2,7-dioctyl-4,5,9,10-tetrahydropyrene) (**191**) has been synthesised by Müllen and coworkers (Scheme 89) [285] by Yamamoto coupling of the dibromomonomer **192**. The monomer was prepared by a photocyclisation of a 2,2′-bis(1″-alkenyl)biphenyl **193**, followed by bromination. The molecular mass of the polymer (M_n = 20 000 g/mol) corresponds to about 46 monomer units (92 phenylene rings).

The emission from **191** is blue in solution (λ_{max} = 425 nm) and in thin films (λ_{max} = 457 nm) [285] and **191** has been used to make a blue-green-emitting LED (λ_{max} = 457 nm) with an efficiency of 0.10–0.15% [7, 286]. The large red shift between the solution and solid-state emission may be due to aggregation. Interestingly, the effective conjugation length for absorption in **191** is about 20 benzene rings [120], which is longer than for LPPP (**3**) (11 rings), but comparable with the values for PDAFs (24 rings) and PIFs (18–21 rings).

The monomer **192** is a mixture of *cis*- and *trans*-diastereomers, which can be separated, thus making stereoregular polymers accessible. Such polymers might show different properties, due to different stacking of the polymer chains.

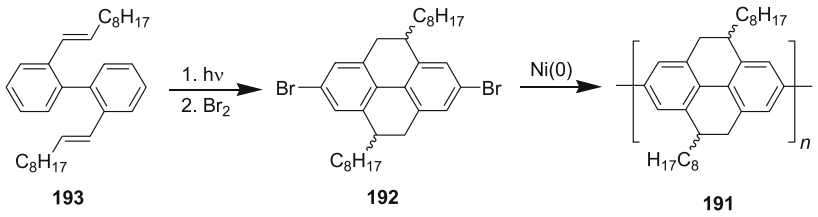

Scheme 89 Synthesis of poly(2,7-dioctyl-4,5,9,10-tetrahydropyrene)

4.4.2 Polycarbazoles

Carbazole is isoelectronic with fluorene, but the nitrogen bridge significantly alters the chemical behaviour. Whereas electrophilic substitution of fluorene occurs preferentially at the 2- and 7-positions, the strong electronic effect of the nitrogen directs substitution to the 3- and 6-positions of carbazole. As a result 3,6-carbazole polymers are much more synthetically accessible than 2,7-carbazole polymers. The chemistry and applications of carbazole-based polymers have been the subject of two major recent reviews to which the reader is referred [287, 288].

Poly(*N*-alkyl-3,6-carbazole)s **194** are readily obtained by condensation of *N*-alkyl-3,6-dibromocarbazoles with electrogenerated nickel(0) (Scheme 90) [289–291]. These polymers show blue (λ_{max} = 470 nm) PL [291] and EL [292].

Poly(*N*-alkyl-2,7-carbazole)s are harder to prepare than the 3,6-polymers **194** as the 2,7-halocarbazole monomers cannot be obtained by halogenation of carbazole. Morin and Leclerc have developed a short efficient route to 2,7-dichlorocarbazole **195** (Scheme 91) [293]. Suzuki condensation of 4-chlorobenzeneboronic acid with 2-bromo-5-chloronitrobenzene occurs preferentially with the more reactive bromide to give 4,4′dichloro-2-nitrobiphenyl, which is then reductively ring closed with triethyl phosphite to give **195** in 55% overall yield. They also prepared 2,7-iodocarbazole **196** by a longer and much less efficient route in which the ring closure was achieved by heating a 2-azidobiphenyl. Müllen and coworkers have synthesised 2,7-dibromocarbazole **197** in 51% overall yield by nitration of 4,4′-dibromobiphenyl followed by ring closure with triethyl phosphate [294].

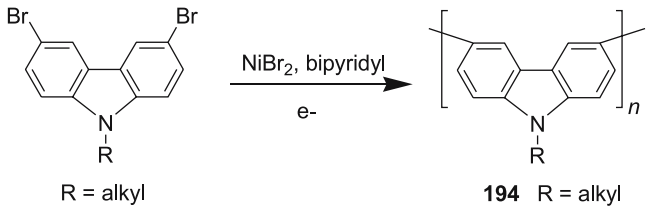

Scheme 90 Poly(*N*-alkyl-3,6-carbazole)s by electropolymerisation

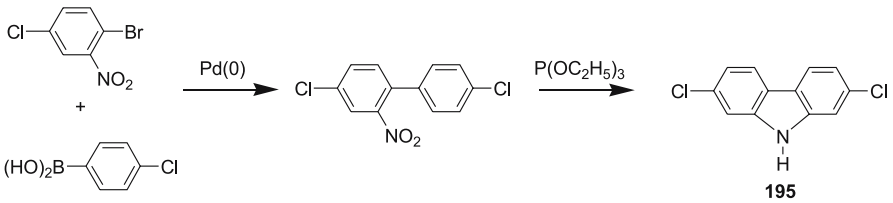

Scheme 91 Synthesis of 2,7-dichlorocarbazole

Poly(*N*-alkyl-2,7-carbazole)s (**198**) have then been made by alkylation of **195–197**, followed by polymerisation with Ni(0) (Scheme 92) [293, 295] or magnesium [296]. A ditosylate monomer **199** has also been used [297]. Due to the lower number of solubilising groups the polymers **198** are less soluble than the corresponding PDAFs, so that to obtain high molecular weight materials large branched chain solubilising groups are needed [296, 298].

Polymers **198** produce blue PL in both solution (λ_{max} = 417 nm) and as a thin film (λ_{max} = 437, 453 nm) [293, 295]. Unlike the structurally very similar PDAFs (Sect. 4.1) these polymers show no long-wavelength emission in the solid state. This is further evidence that the green-emission band seen in PDAFs does not arise from an aggregate, as chains of **198** should be able to π-stack at least as well as those of poly(dioctylfluorene) (**89**). The copolymer **200** with dioctylfluorene was made by Suzuki coupling of a diiodocarbazole and a dioctylfluorene-2,7-bisboronate (Scheme 93) [293]. This copolymer also shows stable blue PL in the solid state (λ_{max} = 450 nm). Suzuki coupling has also been used to prepare other copolymers containing dialkoxyphenylene (**201**), binaphthyl (**202**), and alkylpyridine (**203**) units, which produce stable blue emission [295, 299].

Blue-emitting LEDs have been prepared using **198** with octyl and ethylhexyl substituents, but with only modest efficiencies [300]. Electrochemical

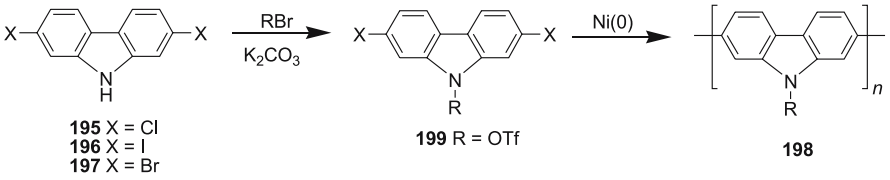

Scheme 92 Synthesis of poly(*N*-alkyl-2,7-carbazole)s

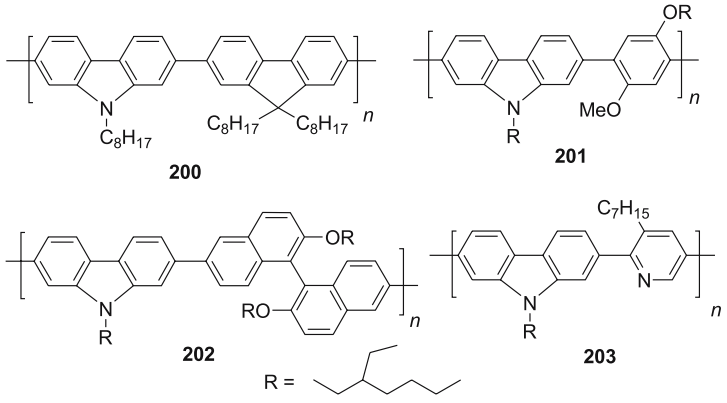

Scheme 93 Blue-emitting alternating copolymer of carbazole with other arylenes

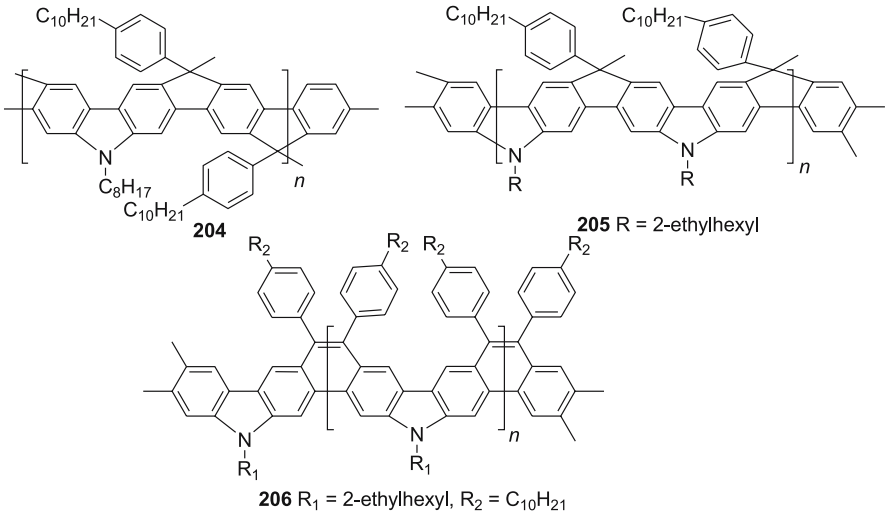

Scheme 94 Carbazole-based ladder polymers

measurements suggest that these materials are unstable under electrolytic conditions, probably due to the high electron densities at the unsubstituted carbazole 3- and 6-positions promoting coupling reactions, which implies that devices using them are likely to have short lifetimes [296]. This problem might be overcome by incorporating carbazoles into ladder structures in which the carbazoles are bridged via the 3- and 6-positions (Scheme 94). Scherf and coworkers have prepared the ladder-type polymer **204** by a modification of the synthesis of Me-LPPP using a carbazole bisboronate in place of a benzene bisboronate [301]. This polymer displays blue-green PL with a maximum at 470 nm, which is very slightly red shifted compared to Me-LPPP. Müllen and coworkers have prepared the ladder-type polycarbazoles **205** and **206**, which are also blue-green emitters in dilute solution, with emission maxima at 471 nm and 467 nm, respectively [302]. At higher concentrations polymer **205** shows broad, red-shifted emission due to aggregation.

5
Polyphenylene-based Block Copolymers

Polyphenylene-based block copolymers come in two varieties: rod–coil copolymers with a rigid rod-like PPP segment attached to a (usually non-luminescent) flexible coil or coils, and rod–rod copolymers in which the PPP rod(s) are attached to another conjugated block. To date most polyphenylene-based block copolymers reported have been rod–coil copolymers. Here the coils may contain charge-transporting units, for example the triblock copoly-

mers **138** and **139**, or may act as solubilising or phase-forming units. Phase separation between the rod and coil units in rod–coil copolymers has been shown to produce ordered nanostructures, which may have profound effects upon the film morphology and the electronic properties of these materials [303].

5.1 Rod–Coil Block Copolymers

There exist two approaches to the synthesis of rod–coil block copolymers: first, the 'grafting from' approach where one component is used as a macroinitiator for the preparation of the other, and, secondly, the 'grafting onto' method where the second component is covalently attached to a suitably end-functionalised first component. The first approach was used to prepare block copolymers of polystyrene (PS) with PPP **207** (Scheme 95) by François and coworkers [304–308] and by Advincula and coworkers [309]. In this synthesis, cyclohexadiene was added to 'living' polystyrene to give a precursor polymer **208**, which was then aromatised to **207** using chloranil in refluxing xylene.

The ultraviolet absorption spectrum of **207** reveals that the PPP units are at most 11–12 benzene rings long, which is shorter than the length of the poly(cyclohexadiene) block in the precursor **208**, indicating that PPP blocks contain defects [304–306]. As in the synthesis of PPP via a poly(cyclohexadiene), 1,2- as well as 1,4-linkages are formed during the polymerisation of the cyclohexadiene. Light-scattering experiments showed that the copolymer forms micelle-like structures with aggregates of PPP blocks surrounded by a shell of polystyrene coils [304, 307]. As a result, films of **207** show an unusual honeycomb-like morphology [308, 310]. As a result of the aggregation of the PPP units, **207** exhibits different optical properties

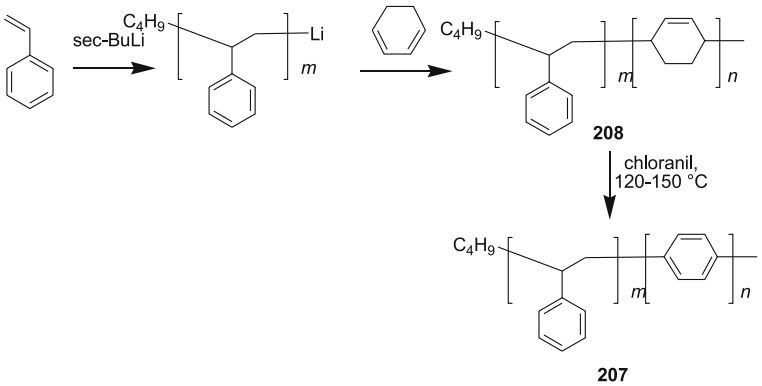

Scheme 95 Synthesis of PPP-PS block copolymers by 'grafting from' method

to PPP (**1**) and the blue EL emission width is much narrower than the PL emission [311, 312].

In the above case, the coil was used as the macroinitiator for the synthesis of the rod. The reverse case has been used by Müllen and coworkers to make the PDAF-PEO copolymer **209** (Scheme 96) [313]. Here addition of bromobenzene to the Suzuki polycondensation of a 2-bromofluorene-7-boronic acid **210** partially end-capped the growing chain at one terminus with a phenyl group, with the remaining chains bearing a terminal hydrogen at this position, while the other terminus completely retained its bromine substituent. The incomplete end-capping is due to the well-known tendency for aryl boronates to fall off under the coupling conditions. Suzuki coupling of this monobromo-PDAF with 4-formylbenzeneboronic acid produced a PDAF **211** end-capped completely at one chain terminus with an aldehyde functionality. This had a molecular weight by GPC and NMR analysis of about 3500 g/mol corresponding to a degree of polymerisation of 8. Reduction of **211** with borohydride, followed by titration with potassium naphthalide, gave the alkoxide **212** which acted as the macroinitiator for the anionic polymerisation of ethylene oxide to give the desired copolymer **209**. NMR analysis suggested that the length of the PEO coil was about 5–6 units, while GPC suggested that it was about 10 units.

Müllen and coworkers have also used the alternative 'grafting onto' approach to make a number of rod–coil copolymers, by making end-capped conjugated rods and attaching non-conjugated coils (Scheme 97). Thus, they produced an end-capped PPP **213** by the same methodology as above [314]. The degree of polymerisation in **194** was also low ($n \sim 10$). Addition of a 'living' polystyrene chain to **213** gave the PPP-PS copolymer **214**, while condensation of **213** with a commercially available amino-terminated poly(ethylene oxide) produced a PPP-PEO copolymer **215**.

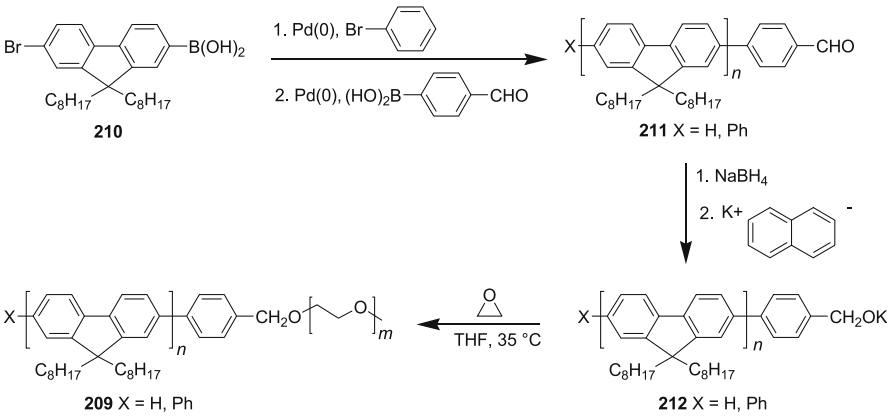

Scheme 96 Synthesis of polyfluorene–poly(ethylene oxide) rod–coil copolymer

The doubly end-capped polyfluorenes **216** and **217**, with phenol or carboxylic acid functional groups at the chain termini, have been made by addition of 13 mol % of suitable end-capping reagents to the Yamamoto polymerisation of a dibromofluorene followed by conversion of the protected functionalities (Scheme 98) [315]. The materials appeared to be totally end-capped by ^{1}H NMR analysis.

Polystyrene chains have been grafted onto the bisacid **217** (M_n = 7140 g/mol, M_w/M_n = 236, n = 18) by activation with *N*,*N*′-carbonyldiimidazole, followed by reaction with a hydroxy-terminated polystyrene (M_n = 9300 g/mol, M_w/M_n = 1.07, m = 87) to give the coil–rod–coil triblock copolymer **218** (M_n = 26 400 g/mol, M_w/M_n = 2.39) (Scheme 99) [315].

The addition of an acid-terminated PEO chain (M_n = 5860 g/mol, M_w/M_n = 1.06, m = 112) to the bisphenol **216** (M_n = 11 300 g/mol, M_w/M_n = 1.79, n = 29) under the same conditions was found to give a mixture of the diblock **219** (M_n = 17 230 g/mol, M_w/M_n = 2.10) and triblock **220** (M_n = 23 170 g/mol, M_w/M_n = 2.37) copolymers, which were separable owing to their differential solubility in methanol (Scheme 100) [315].

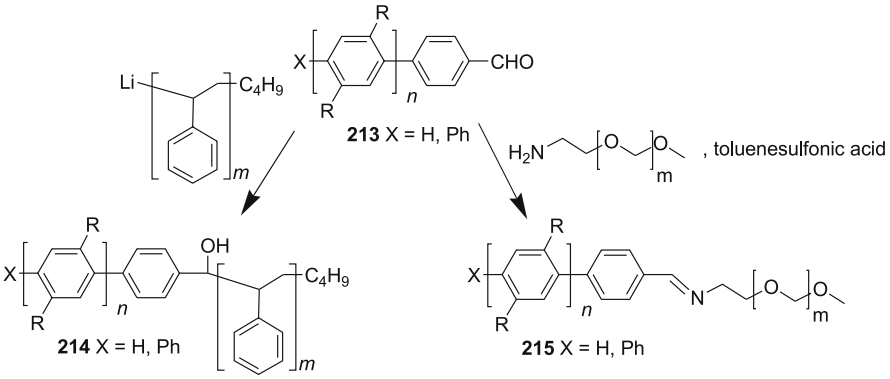

Scheme 97 PPP-based rod–coil copolymers by 'grafting onto' method

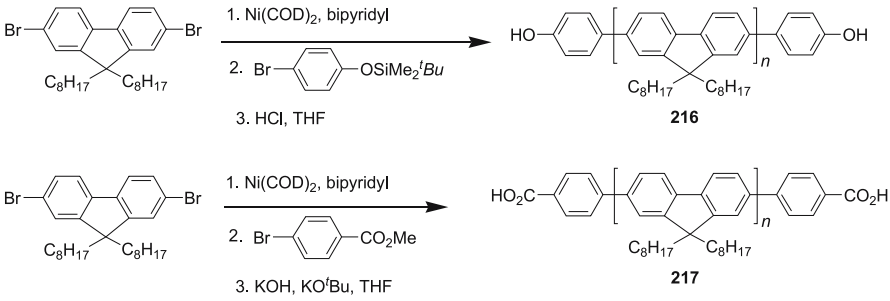

Scheme 98 Synthesis of doubly end-capped polyfluorenes as units for rod–coil copolymers

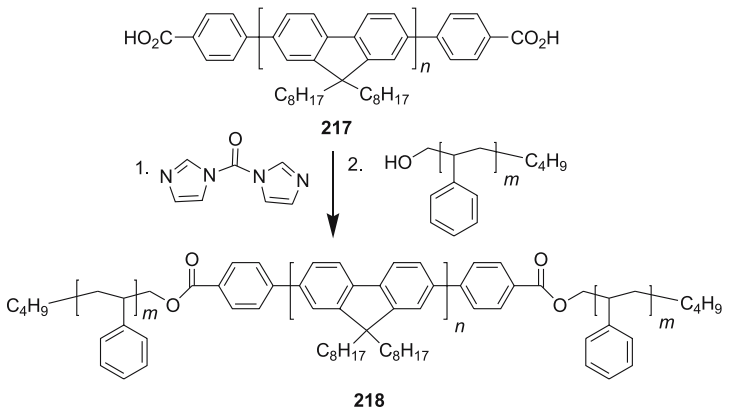

Scheme 99 Synthesis of polyfluorene–polystyrene coil–rod–coil triblock copolymers

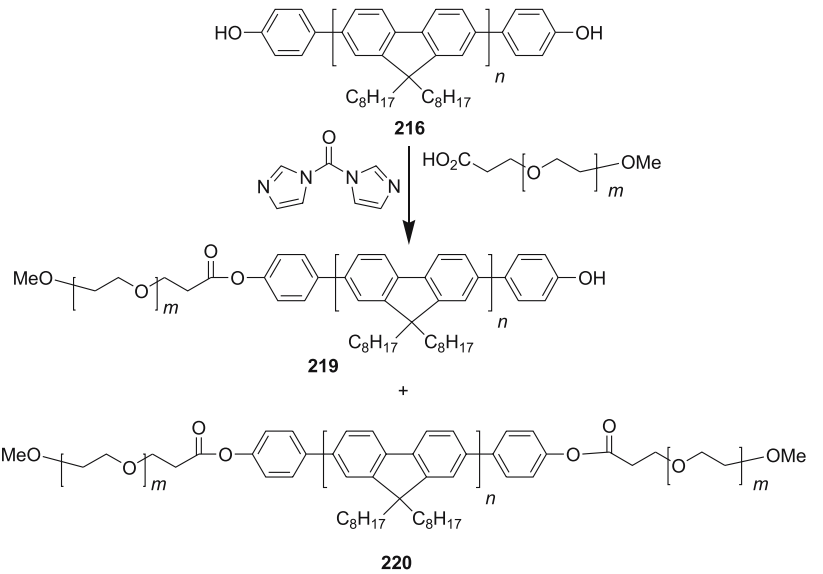

Scheme 100 Synthesis of polyfluorene–poly(ethylene oxide) di- and triblock copolymers

Scherf and coworkers have prepared di- and triblock copolymers of polyfluorene and polyaniline (Scheme 101) by attaching suitable end groups in both Suzuki and Yamamoto polymerisations. Addition of 10 mol % of 4-nitrobromobenzene as an end-capping reagent to an AA-BB Suzuki polycondensation of a fluorene bisboronate and a dibromofluorene (Scheme 41), followed by reduction with hydrogen, gave a mixture of **221** and **223** (M_n = 7700 g/mol, M_w/M_n = 2.9, $n \sim 19$). MALDI-TOF analysis of the nitro-end-capped material showed that some of the mono-end-capped chains had

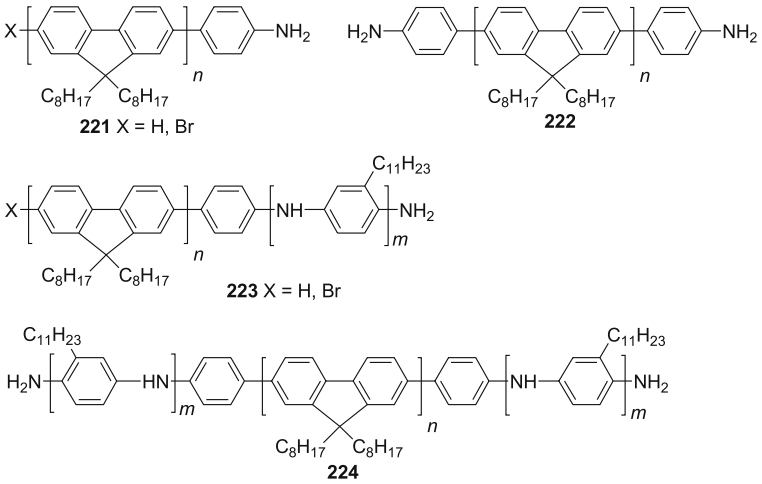

Scheme 101 Polyfluorene–polyaniline block copolymers and precursors

a bromine while others had a hydrogen at the other terminus but a quantitative analysis was not possible. These compounds were oxidatively coupled with 2-undecanylaniline to give a mixture of the PF-PANI diblock **223** and triblock **224** copolymers (M_n = 14 400, M_w/M_n = 4.3) [316]. NMR analysis of the end-capped polyfluorenes suggested that the end-capping introduced about 1–1.2 end groups per polymer chain, so that the final product was largely the diblock copolymer **223**. From the UV-VIS spectrum, the PANI blocks appeared to be about 6–7 units long. By contrast, addition of 15 mol % of 4-bromoaniline to a Yamamoto polycondensation of a dibromofluorene (Scheme 42) produced complete end-capping to give only **222** (M_n = 10 400 g/mol, M_w/M_n = 3.58, $n \sim 25$) [317]. Oxidative coupling of this with undecanylaniline then gave the triblock copolymer **224** (M_n = 36 900 g/mol, M_w/M_n = 1.55). Elemental analysis suggested that the PANI blocks were about 7–8 units long.

The optical properties of the PPP copolymers **214** and **215** do not differ from the homopolymer, but the PDAF copolymers **213** and **218–220** show slight differences in their solid-state PL spectra from the homopolymer **89**, which suggests that there is a higher degree of order in the films [313–315]. Studies of the morphology of some of these rod–coil copolymers have shown that they form extended one-dimensional fibrillar structures due to π-stacking of the rods [236, 318]. The ratio of the block sizes in PDAF-PEO copolymers has been shown to strongly influence the packing behaviour, with fibrillar structures being observed only for copolymers with an average volume ratio of PEO of 0.3 or below [319]. However, no study of the effects of the coils on the luminescence properties of these polymers has been reported yet.

Though their synthesis has not been published, it is probable that the triblock copolymers **138** and **139** [243] were prepared by a similar grafting onto procedure.

There also exist syntheses of rod–coil copolymers which do not fit neatly into either of the above categories. Miller and coworkers have prepared coil–rod–coil triblock copolymers in a one-pot method by using end-capping agents in the Yamamoto polymerisation of dibromodihexylfluorene, which also act as initiators for the formation of the coils [320]. This method can be thought of as a combination of the two approaches. Thus, nickel(0) polymerisation of dibromodihexylfluorene and living radical polymerisation of styrene in the presence of the end-capper/initiator **225** proceeded together in the same pot to produce **226** (M_n = 36 000 g/mol, M_w/M_n = 1.52), which by NMR analysis incorporated the styrene and fluorene monomers in a mole ratio of 7 : 3 (Scheme 102).

Similarly, nickel(0) polymerisation of the fluorene and ring-opening polymerisation of caprolactone in the presence of **227** proceeded to give **228** (Scheme 103). By increasing the mole ratio of caprolactone to fluorene monomer in the reaction mixture from 8 : 1 to 25 : 1, the molecular mass of the polymer could be increased from M_n = 17 000 g/mol to 36 000 g/mol, with an accompanying drop in the polydispersity from M_w/M_n = 2.39 to 1.65. NMR analysis showed that the relative amount of the fluorene in the polymer was only about 65–75% of the mole fraction of the fluorene monomer in the reaction mixture.

The copolymer with PMMA **229** (Scheme 104), however, had to be made in a step-wise 'grafting onto' procedure, as the initiator for the atom transfer radical polymerisation (ATRP) of methyl methacrylate was not stable under Yamamoto reaction conditions.

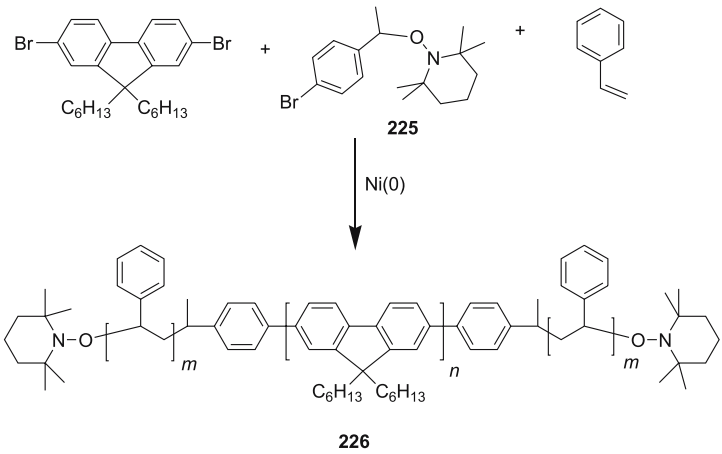

Scheme 102 One-pot synthesis of polyfluorene–polystyrene triblock copolymers

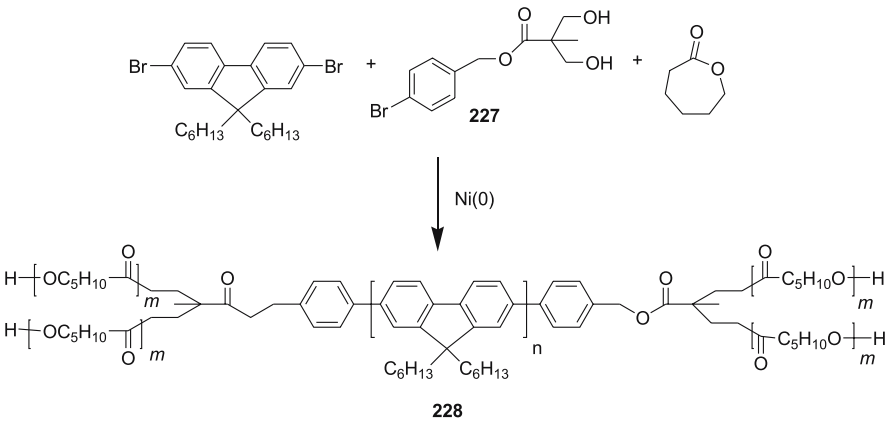

Scheme 103 One-pot copolymerisation of dioctylfluorene and caprolactone

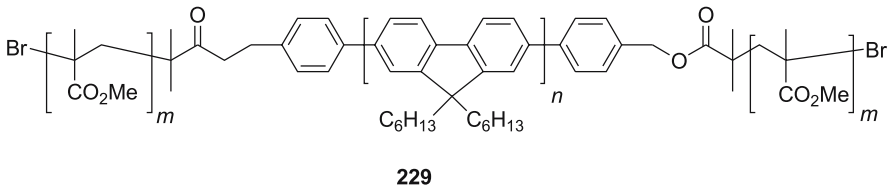

Scheme 104 Polyfluorene–PMMA triblock copolymer made by two-step process

5.2 Rod–Rod Block Copolymers

The only example of rod–rod copolymers with polyphenylene-based rods are the polymers **230** and **231**, in which two polyfluorene blocks are separated by a short arylene vinylene unit (Scheme 105). These were prepared by Suzuki polycondensation of a fluorene monoboronic acid **232** in the presence of the bromo-substituted oligo(arylene vinylene) units **233** and **234** [321]. From the molecular masses of the polymers, the total number of fluorene units in both **230** and **231** is about 18.

The PL in solution comes from the fluorene blocks (λ_{max} = 425 nm), but in the solid state energy transfer to the arylene vinylene units produces emission only from them ($\lambda_{max} \sim 525$ nm and ~ 490 nm for **230** and **231**, respectively). As the polymers are surely contaminated with the fluorene homopolymer, inter- as well intrachain energy transfer must be occurring. These polymers are promising candidates for polymer lasers [322].

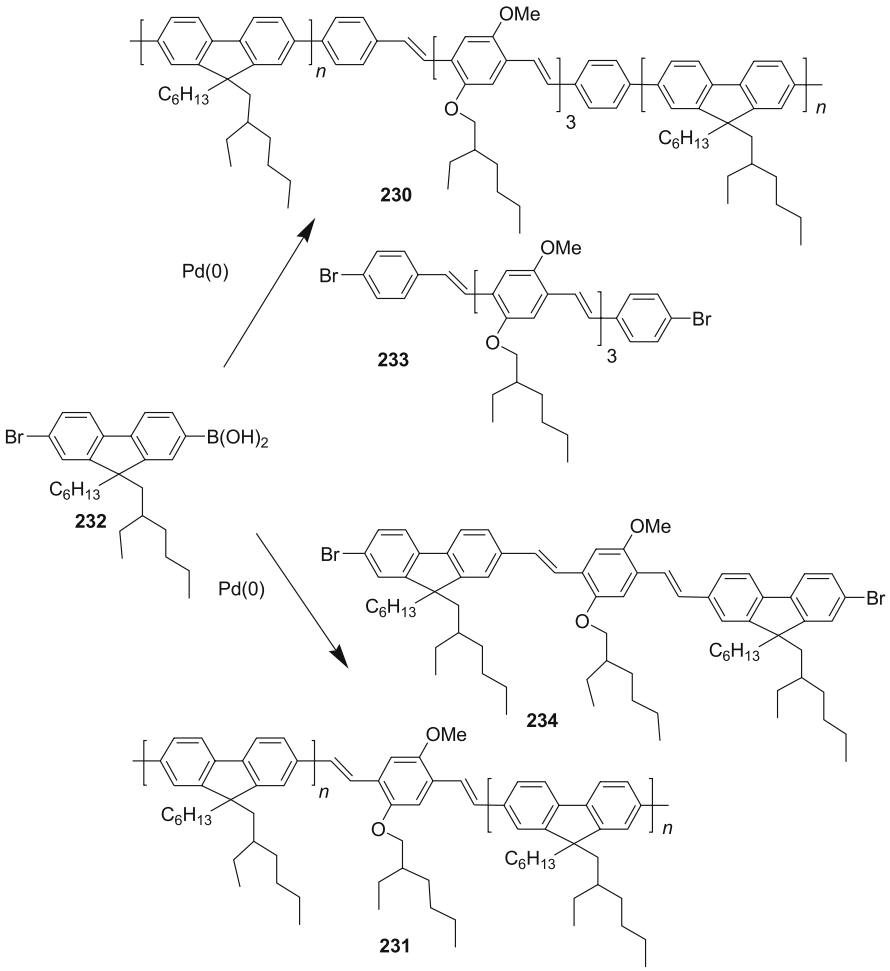

Scheme 105 Fluorene–(arylene vinylene) block copolymers

6 Conclusion

As shown in this review, the properties of polyphenylene-based materials, so as to maximise their potential as active materials in LEDs or polymer lasers, can be controlled by deliberate synthetic design. By incorporating bridges between some or all of the phenylene units to make ladder or stepladder polymers the effective conjugation length of the polymer may be controlled, while the interactions between the chains and the injection of charges may be regulated by careful selection of substituents. By these means it is possible to minimise interchain interactions, which lead to loss of luminescence

efficiency and/or undesirable red shifts in the emission spectrum. The goal of obtaining stable blue emission now appears to be attainable if steps are taken to minimise the formation of emissive defects in the polymers and the diffusion of excitons to them. The emission colour can also be tuned efficiently over the whole visible spectrum by incorporation of suitable chromophores. With ongoing interdisciplinary research efforts, the fabrication of polyphenylene-based high-efficiency full-colour LED-based displays with long lifetimes may soon be possible. The prospects for polyphenylene-based lasers also appear good, though much work remains to be done in this field.

Acknowledgements We gratefully acknowledge the financial support given to our research into emissive polyphenylenes by the Bundesministerium für Bildung und Forschung. We also thank Prof. Ullrich Scherf for communicating to us some of his unpublished results and manuscripts.

References

1. Kraft A, Grimsdale AC, Holmes AB (1998) Angew Chem Int Ed 37:403
2. Mitschke U, Bäuerle P (2000) J Mater Chem 10:1471
3. McGehee MD, Heeger AJ (2000) Adv Mater 12:1655
4. Kim DY, Cho HN, Kim CY (2000) Prog Polym Sci 25:1089
5. Grell M, Bradley DDC (1999) Adv Mater 11:895
6. Kaeriyama K (1998) Plast Eng 48:33
7. Scherf U (1999) Top Curr Chem 201:163
8. Schlüter AD (2001) J Polym Sci A Polym Chem 39:1533
9. Yamamoto T (1992) Prog Polym Sci 17:1153
10. Stille JK (1986) Angew Chem Int Ed Engl 25:508
11. Tamao K, Kodama S, Kumada M, Minato A, Suzuki K (1982) Tetrahedron 38:3347
12. Kovacic P, Jones MB (1987) Chem Rev 87:357
13. Miyashita K, Kaneko M (1994) Macromol Rapid Commun 15:511
14. Miyashita K, Kaneko M (1995) Synth Met 68:161
15. Remmers M, Müller B, Martin K, Räder H-J, Köhler W (1999) Macromolecules 32:1073
16. Lee CH, Kang GW, Jeon JW, Song WJ, Seoul C (2000) Thin Solid Films 363:306
17. Song W-J, Seoul C, Kang G-W, Lee C (2000) Synth Met 114:355
18. Kang G-W, Lee C, Song W-J, Seoul C (2001) Proc SPIE 4105:362
19. Graupner W, Grem G, Meghdadi F, Paar C, Leising G, Scherf U, Müllen K, Fischer W, Stelzer F (1994) Mol Cryst Liq Cryst 256:549
20. Grem G, Martin V, Meghdadi F, Paar C, Stampfl J, Sturm J, Tasch S, Leising G (1995) Synth Met 71:2193
21. Leising G, Köpping-Grem G, Meghdadi F, Niko A, Tasch S, Fischer W, Pu L, Wagaman MW, Grubbs RH, Althouel L, Froyer G, Scherf U, Huber J (1995) Proc SPIE 2528:307
22. Meghdadi F, Leising G, Fischer W, Stelzer F (1996) Synth Met 76:113
23. Leising G, Ekström O, Graupner W, Meghdadi F, Moser M, Kranzelbinder G, Jost T, Tasch S, Winkler B, Athouel L, Froyer G, Scherf U, Müllen K, Lanzani G, Nisoli M, DeSilvestri S (1996) Proc SPIE 2852:189

24. Leising G, Tasch S, Meghdadi F, Athouel L, Froyer G, Scherf U (1996) Synth Met 81:185
25. Meghdadi F, Tasch S, Winkler B, Fischer W, Stelzer F, Leising G (1997) Synth Met 85:1441
26. Koch N, Pogantsch A, List EWJ, Leising G, Blyth RIR, Ramsey MG, Netzer FP (1999) Appl Phys Lett 74:2909
27. Yanagi H, Okamoto S (1997) Appl Phys Lett 71:2563
28. Era M, Tsutsui T, Saito S (1995) Appl Phys Lett 67:2436
29. Andrew A, Matt G, Brabec CJ, Sitter H, Badt D, Seyringer H, Sariciftci NS (2000) Adv Mater 12:629
30. Niko A, Tasch S, Meghdadi F, Brandstätter C, Leising G (1997) J Appl Phys 82:4177
31. Tasch S, Brandstätter C, Meghdadi F, Leising G, Froyer G, Athauel L (1997) Adv Mater 9:33
32. Leising G, Meghdadi F, Tasch S, Brandstätter C, Graupner W, Kranzelbinder G (1997) Synth Met 85:1213
33. Leising G, Tasch S, Brandstätter C, Graupner W, Hampel S, List EWJ, Meghdadi F, Zenz C, Schlichting P, Rohr U, Geerts Y, Scherf U, Müllen K (1997) Synth Met 91:41
34. Niko A, Tasch S, Meghdadi F, Brandstätter C, Leising G (1998) Opt Mater 9:188
35. Leising G, List EWJ, Zenz C, Tasch S, Brandstätter C, Graupner W, Markart P, Meghdadi F, Kranzelbinder G, Niko A, Resel R, Zojer E, Schlichting P, Rohr U, Geerts Y, Scherf U, Müllen K, Smith R, Gin D (1998) Proc SPIE 3476:76
36. Gin DL, Conticello VP (1996) Trends Polym Sci 4:217
37. Ballard DGH, Courtis A, Shirley IM, Taylor SC (1983) J Chem Soc Chem Commun: 954
38. Ballard DGH, Courtis A, Shirley IM, Taylor SC (1988) Macromolecules 21:294
39. Grem G, Leditzky G, Ullrich B, Leising G (1992) Synth Met 51:383
40. Grem G, Leising G (1993) Synth Met 55–57:4105
41. Tasch S, Brandstätter C, Graupner W, Hampel S, Hochfilzer C, List EWJ, Meghdadi F, Leising G, Schlichting P, Rohr U, Geerts Y, Scherf U, Müllen K (1997) Mater Res Soc Symp Proc 471:325
42. McKean DR, Stille JK (1987) Macromolecules 20:1787
43. Kim HK, Suck J-K, Zyung T (1996) Polym Mater Sci Eng 75:255
44. Kim HK, Kim K-D, Zyung T (1997) Mol Cryst Liq Cryst 295:27
45. Gin DL, Conticello VP, Grubbs RH (1992) J Am Chem Soc 114:3167
46. Gin DL, Conticello VP, Grubbs RH (1994) J Am Chem Soc 116:10507
47. Gin DL, Conticello VP, Grubbs RH (1994) J Am Chem Soc 116:10934
48. Gin DL, Avlyanov JK, MacDiarmid AG (1994) Synth Met 66:169
49. Chaturvedi V, Tanaka S, Kaeriyama K (1992) J Chem Soc Chem Commun: 1658
50. Chaturvedi V, Tanaka S, Kaeriyama K (1993) Macromolecules 26:2607
51. Komaba S, Amano A, Osaka T (1997) J Electroanal Chem 430:97
52. Argyrakis P, Kobryanskii MV, Sluch MI, Vitukhnovsky AG (1997) Synth Met 91:159
53. Tanigaki N, Yase K, Kaito A (1996) Thin Solid Films 273:263
54. Yamamoto T, Hayashi Y, Yamamoto A (1978) Bull Chem Soc Jpn 51:2091
55. Hamaguchi M, Sawada H, Kyokane J, Yoshino K (1996) Chem Lett: 527
56. Schlüter AD, Wegner G (1993) Acta Polym 44:59
57. Vahlenkamp T, Wegner G (1994) Macromol Chem Phys 195:1933
58. McCarthy TF, Witteler H, Pakula T, Wegner G (1995) Macromolecules 28:8350
59. Remmers M, Schulze M, Wegner G (1996) Macromol Rapid Commun 17:239
60. Vanhee S, Rulkens R, Lehmann U, Rosenauer C, Schulze M, Köhler W, Wegner G (1996) Macromolecules 29:5136

61. Kowitz C, Wegner G (1997) Tetrahedron 53:15 553
62. Frahn J, Karakaya B, Schäfer A, Schlüter A-D (1997) Tetrahedron 53:15 459
63. Goodson FE, Wallow TI, Novak BM (1998) Macromolecules 31:2047
64. Schlüter S, Frahn J, Karakaya B, Schlüter A-D (2000) Macromol Chem Phys 201:139
65. Percec V, Pugh C, Cramer E, Okita S, Weiss R (1992) Makromol Chem, Macromol Symp 54–55:113
66. Percec V, Okita S, Weiss R (1992) Macromolecules 25:1816
67. Percec V (1993) US Patent: 5 241 044
68. Percec V, Bae J-Y, Zhao M, Hill DH (1995) Macromolecules 28:6726
69. Percec V, Zhao M, Bae J-Y, Hill DH (1996) Macromolecules 29:3727
70. Ueda M, Abe T, Awao H (1992) Macromolecules 25:5125
71. Huang J, Zhang H, Tian W, Hou J, Ma Y, Shen J, Liu S (1997) Synth Met 87:105
72. Tanigaki N, Masuda H, Kaeriyama K (1997) Polymer 38:1221
73. Wang Y, Quirk RP (1995) Macromolecules 28:3495
74. Klavetter FL, Gustafsson GG, Heeger AJ (1993) Polym Mater Sci Eng 69:153
75. Jing W-X, Kraft A, Moratti SC, Grüner J, Cacialli F, Hamer PJ, Holmes AB, Friend RH (1994) Synth Met 67:161
76. Hamaguchi M, Yoshino K (1995) Jpn J Appl Phys 34:L587
77. Yang Y, Pei Q, Heeger AJ (1996) J Appl Phys 79:934
78. Yang Y, Pei Q, Heeger AJ (1996) Synth Met 78:263
79. Cimrová V, Remmers M, Neher D, Wegner G (1996) Adv Mater 8:146
80. Cimrová V, Schmidt W, Rulkens R, Schulze M, Meyer W, Neher D (1996) Adv Mater 8:585
81. Wegner G, Neher D, Remmers M, Cimrová V, Schulze M (1996) Mater Res Soc Symp Proc 413:23
82. Chen S-A, Chao C-I (1996) Synth Met 79:93
83. Edwards A, Blumstengel S, Sokolik I, Yun H, Okamoto Y, Dorsinville R (1997) Synth Met 84:639
84. Grüner J, Remmers M, Neher D (1997) Adv Mater 9:964
85. Chao C-I, Chen S-A (1998) Appl Phys Lett 73:426
86. Annan KO, Scherf U, Müllen K (1999) Synth Met 99:9
87. Shin S-W, Park J-S, Park J-W, Kim HK (1999) Synth Met 102:1060
88. Fu Y (1997) Polym Prepr 38(1):410
89. Cimrová V, Výprachtický D, Pecka J, Kotva R (2000) Proc SPIE 3939:164
90. Kim S, Jackiw J, Robinson E, Schanze KS, Reynolds JR, Baur J, Rubner MF, Boils D (1998) Macromolecules 31:964
91. Baur JW, Kim S, Balanda PB, Reynolds JR, Rubner MF (1998) Adv Mater 10:1452
92. Wittemann M, Rehahn M (1998) Chem Commun: 623
93. Thunemann AF, Ruppelt D, Schnablegger H, Blaul J (2000) Macromolecules 33:2124
94. Hamaguchi M, Yoshino K (1997) Polym Adv Technol 8:399
95. Akagi K, Oguma J, Shirakawa H (1998) J Photopolym Sci Technol 11:249
96. Chen SH, Conger BM, Mastrangelo JC, Kende AS, Kim DU (1998) Macromolecules 31:8051
97. Park JH, Lee CH, Akagi K, Shirakawa H, Park YW (2001) Synth Met 119:633
98. Fiesel R, Huber J, Apel V, Enkelmann V, Hentsche R, Scherf U, Cabrera K (1997) Macromol Chem Phys 198:2623
99. Fiesel R, Huber J, Scherf U (1998) Enantiomer 3:383
100. Fiesel R, Scherf U (1998) Acta Polym 49:445
101. Katsis D, Chen H-MP, Chen SH, Tsutsui T (2000) Proc SPIE 4107:77

102. Taylor PN, O'Connel MJ, McNeill LA, Hall MJ, Aplin RT, Anderson HL (2000) Angew Chem Int Ed 39:3456
103. Cacialli F, Wilson JS, Michels JJ, Daniel C, Silva C, Friend RH, Severin N, Samori P, Rabe JP, O'Connell MJ, Taylor PN, Anderson HL (2002) Nat Mater 1:160
104. Baskar S, Lai Y-H, Valiyaveetil S (2001) Macromolecules 34:6255
105. Park KC, Dodd LR, Levon K, Kwei TK (1996) Macromolecules 29:7149
106. Rhee TH, Choi T, Chang EY, Suh DH (2001) Macromol Chem Phys 202:906
107. Reddinger JL, Reynolds JR (1997) Macromolecules 30:479
108. Mikroyannidis JA (2001) Macromol Chem Phys 202:2367
109. Bao Z, Chan WK, Yu L (1995) J Am Chem Soc 117:12 426
110. Bao Z, Yu L (1995) Proc SPIE 2528:210
111. Raney MB, Reynolds JR (1999) Polym Prepr 40(2):1207
112. Kaeriyama K, Tsukahata Y, Negoro S, Tanigaki N, Masuda H (1997) Synth Met 84:263
113. Jiang B, Tilley TD (2000) Polym Prepr 41(1):829
114. Birgerson J, Fahlman M, Bröms P, Salaneck WR (1996) Synth Met 80:125
115. Birgerson J, Kaeriyama K, Barta P, Bröms P, Fahlman M, Granlund T, Salaneck WR (1996) Adv Mater 8:983
116. Salaneck WR (1997) Philos Trans R Soc Lond A 355:789
117. Edwards A, Blumstengel S, Sokolik I, Dorsinville R, Yun H, Kwei TK, Okamoto Y (1997) Appl Phys Lett 70:298
118. Huang J-S, Zhang H-F, An H-Y, Tian W-J, Hou J-Y, Chen B-J, Liu S-Y, Shen J-C (1996) Chin Phys Lett 13:944
119. Scherf U (1999) J Mater Chem 9:1853
120. Grimme J, Kreyenschmidt M, Uckert F, Müllen K, Scherf U (1995) Adv Mater 7:292
121. Scherf U, Müllen K (1991) Makromol Chem Rapid Commun 12:489
122. Scherf U, Müllen K (1992) Macromolecules 25:3546
123. Scherf U, Müllen K (1995) Adv Polym Sci 123:1
124. Scherf U, Müllen K (1997) ACS Symp Ser 672:358
125. Fiesel R, Huber J, Scherf U (1996) Angew Chem Int Ed Engl 35:2111
126. Grimme J, Scherf U (1996) Macromol Chem Phys 197:2297
127. Schindler F, Jacob J, Grimsdale A, Scherf U, Müllen K, Lupton JM, Feldmann J (2005) Angew Chem Int Ed 44:1520
128. Stampfl J, Graupner W, Leising G, Scherf U (1995) J Luminesc 63:117
129. Hüber J, Müllen K, Saalbeck J, Schenk H, Scherf U, Stehlin T, Stern R (1994) Acta Polym 45:244
130. Leising G, Grem G, Leditzky G, Scherf U (1993) Proc SPIE 1910:70
131. Grüner J, Wittmann HF, Hamer PJ, Friend RH, Huber J, Scherf U, Müllen K, Moratti SC, Holmes AB (1994) Synth Met 67:181
132. Mahrt RF, Siegner U, Lemmer U, Hopmeier M, Scherf U, Heun S, Göbel EO, Müllen K, Bässler H (1995) Chem Phys Lett 240:373
133. Köhler A, Grüner J, Friend RH, Müllen K, Scherf U (1995) Chem Phys Lett 243:456
134. Yang X, Hou Y, Wang Z, Chen X, Xu Z, Xu X (2000) Thin Solid Films 363:211
135. Scherf U, Bohnen A, Müllen K (1992) Makromol Chem 193:1127
136. Haugeneder A, Lemmer U, Scherf U (2002) Chem Phys Lett 351:354
137. Tasch S, Niko A, Leising G, Scherf U (1996) Appl Phys Lett 68:1090
138. Tasch S, Niko A, Leising G, Scherf U (1996) Mater Res Soc Symp Proc 413:71
139. Stagira S, Zavelani-Rossi M, Nisoli M, DeSilvestri S, Lanzani G, Zenz C, Mataloni P, Leising G (1998) Appl Phys Lett 73:2860
140. Kallinger C, Hilmer C, Haugeneder A, Perner M, Spirkl W, Lemmer U, Feldmann J, Scherf U, Müllen K, Gombert A, Wittwer V (1998) Adv Mater 10:920

141. Riechel S, Kallinger C, Lemmer U, Feldmann J, Gombert A, Wittwer V, Scherf U (2000) Appl Phys Lett 77:2310
142. Tasch S, Gao J, Wenzl FP, Holzer L, Leising G, Heeger AJ, Scherf U, Müllen K (1999) Electrochem Solid State Lett 2:303
143. Tasch S, List EWJ, Hochfilzer C, Leising G, Schlichting P, Rohr U, Geerts Y, Scherf U, Müllen K (1997) Phys Rev B Condens Matter 56:4479
144. List EWJ, Tasch S, Hochfilzer C, Leising G, Schlichting P, Rohr U, Geerts Y, Scherf U, Müllen K (1998) Opt Mater 9:183
145. Tasch S, List EWJ, Ekström O, Graupner W, Leising G, Schlichting P, Rohr U, Geerts Y, Scherf U, Müllen K (1997) Appl Phys Lett 71:2883
146. Lupton JM (2002) Chem Phys Lett 365:366
147. Romaner L, Heimel G, Weisenhofer H, Scandiucci de Freitas P, Scherf U, Bredas J-L, Zojer E, List EJW (2004) Chem Mater 16:4667
148. Qiu S, Lu P, Liu X, Lu FS, Liu L, Ma Y, Shen J (2003) Macromolecules 36:9823
149. Patil S, Scherf U, personal communication
150. Lupton JM, Pogantsch A, Piok T, List EWJ, Patil S, Scherf U (2002) Phys Rev Lett 89:7401
151. Forster M, Scherf U (2000) Macromol Rapid Commun 21:810
152. Chmil K, Scherf U (1993) Makromol Chem Rapid Commun 14:217
153. Chmil K, Scherf U (1997) Acta Polym 48:208
154. Kirstein S, Cohen G, Davidov D, Scherf U, Klapper M, Chmil K, Müllen K (1995) Synth Met 69:415
155. Goldfinger MB, Swager TM (1994) J Am Chem Soc 116:7895
156. Tour JM, Lambda JJS (1993) J Am Chem Soc 115:4935
157. Lambda JJS, Tour JM (1994) J Am Chem Soc 116:11 723
158. Grem G, Paar C, Stampfl J, Leising G, Huber J, Scherf U (1995) Chem Mater 7:2
159. Grüner J, Hamer PJ, Friend RH, Huber H-J, Scherf U, Holmes AB (1994) Adv Mater 6:748
160. Stern R, Schenk H, Salbeck J, Stehlin T, Scherf U, Müllen K, Leising G (1999) US Patent: 5 856 434
161. Grüner J, Friend RH, Huber J, Scherf U (1996) Chem Phys Lett 251:204
162. Leclerc M (2001) J Polym Sci A Polym Chem 39:2867
163. Neher D (2001) Macromol Rapid Commun 22:1365
164. Scherf U, List EWJ (2002) Adv Mater 14:477
165. Fukuda M, Sawada K, Yoshino K (1989) Jpn J Appl Phys 28:L1433
166. Fukuda M, Sawada K, Yoshino K (1993) J Polym Sci Polym Chem 31:2465
167. Ohmori Y, Uchida K, Muro K, Yoshino K (1991) Jpn J Appl Phys 30:L1941
168. Ohmori Y, Uchida M, Morishima C, Fujii A, Yoshino K (1993) Jpn J Appl Phys 32:L1663
169. Uchida M, Ohmori Y, Morishima C, Yoshino K (1993) Synth Met 57:4168
170. Liu B, Chen Z-K, Yu W-L, Lai Y-H, Huang W (2000) Thin Solid Films 363:332
171. Advincula R, Yia C, Inaoka S (2000) Polym Prepr 41(1):846
172. Woo EP, Inbasekaran M, Shiang W, Roof GR (1997) PCT Int Patent Appl: WO97/05184
173. Inbasekaran M, Wu W, Woo EP (1998) US Patent: 5 777 070
174. Bernius MT, Inbasekaran M, Woo EP, Wu W, Wujkowski L (1999) Proc SPIE 3797:129
175. Bernius M, Inbasekaran M, Woo E, Wu W, Wujkowski L (2000) J Mater Sci Mater Electron 11:111
176. Bernius M, Inbasekaran M, O'Brien J, Wu W (2000) Adv Mater 12:1737
177. Inbasekaran M, Woo E, Bernius M, Wujkowski L (2000) Synth Met 111–112:397

178. Grice AW, Bradley DDC, Bernius MT, Inbasekaran M, Wu WW, Woo EP (1998) Appl Phys Lett 73:629
179. Grell M, Knoll W, Lupo D, Meisel A, Miteva T, Neher D, Nothofer H-G, Scherf U, Yasuda A (1999) Adv Mater 11:671
180. Klaerner G, Miller RD (1998) Macromolecules 31:2007
181. Lee SH, Tsutsui T (2000) Thin Solid Films 363:76
182. Miller RD, Klaerner G, Fuhrer T, Kreyenschmidt M, Kwak J, Lee V, Chen W-D, Scott JC (1999) Nonlinear Opt 20:269
183. Grell M, Bradley DDC, Inbasekaran M, Woo EP (1997) Adv Mater 9:798
184. Teetsov J, Fox MA (1999) J Mater Chem 9:2117
185. Grell M, Bradley DDC, Whitehead KS (2000) J Korean Phys Soc 36:331
186. Whitehead KS, Grell M, Bradley DDC, Jandke M, Strohriegl P (2000) Appl Phys Lett 76:2946
187. Whitehead KS, Grell M, Bradley DDC, Inbasekaran M, Woo EP (2000) Synth Met 111–112:181
188. Whitehead KS, Grell M, Bradley DDC, Jandke M, Strohriegl P (2000) Proc SPIE 3939:172
189. Miteva T, Meisel A, Grell M, Nothofer H-G, Lupo D, Yasuda A, Knoll W, Kloppenburg L, Bunz UHF, Scherf U, Neher D (2000) Synth Met 111–112:173
190. Nothofer H-G, Meisel A, Miteva T, Neher D, Forster M, Oda M, Lieser G, Sainova D, Yasuda A, Lupo D, Knoll W, Scherf U (2000) Macromol Symp 154:139
191. Oda M, Nothofer H-G, Lieser G, Scherf U, Meskers SCJ, Neher D (2000) Adv Mater 12:362
192. Oda M, Meskers SCJ, Nothofer HG, Scherf U, Neher D (2000) Synth Met 111–112:575
193. Nothofer H-G, Oda M, Neher D, Scherf U (2000) Proc SPIE 4107:19
194. Tang H, Fujiki M, Motonaga M, Torimitsu K (2001) Polym Prepr 42(1):440
195. Zhang J, Grimsdale AC, Müllen K, unpublished results
196. Pei Q, Yang Y (1996) J Am Chem Soc 118:7416
197. Stéphan O, Collomb V, Vial J-C, Armand M (2000) Synth Met 113:257
198. Yang Y, Pei Q (1997) J Appl Phys 81:3294
199. Kreyenschmidt M, Klaerner G, Fuhrer T, Ashenhurst J, Karg S, Chen WD, Lee VY, Scott JC, Miller RD (1998) Macromolecules 31:1099
200. Lee J-I, Klärner G, Miller RD (1999) Synth Met 101:126
201. Bliznyuk VN, Carter SA, Scott JC, Klärner G, Miller RD, Miller DC (1999) Macromolecules 32:361
202. Lee J-I, Klaerner G, Miller RD (1999) Chem Mater 11:1083
203. Pschirer NG, Byrd K, Bunz UHF (2001) Macromolecules 34:8590
204. List EWJ, Guentner R, Scanducci de Freitas P, Scherf U (2002) Adv Mater 14:374
205. Lupton JM, Craig MR, Meijer EW (2002) Appl Phys Lett 80:4489
206. Pei J, Ni J, Zhou X-H, Cao X-Y, Lai Y-H (2002) J Org Chem 67:4924
207. Zeng G, Yu W-L, Chua S-J, Huang W (2002) Macromolecules 35:6907
208. Gaal M, List EJW, Scherf U (2003) Macromolecules 36:4236
209. Weinfurtner K-H, Fujikawa H, Tokito S, Taga Y (2000) Appl Phys Lett 76:2502
210. Craig MR, de Kok MM, Hofstraat JW, Schenning APHJ, Meijer EW (2003) J Mater Chem 13:2861
211. Sainova D, Miteva T, Nothofer H-G, Scherf U, Glowacki I, Ulanski J, Fujikawa H, Neher D (2000) Appl Phys Lett 76:1810
212. Klärner G, Lee J-I, Lee VY, Chan E, Chen J-P, Nelson A, Markiewicz D, Siemens R, Scott JC, Miller RD (1999) Chem Mater 11:1800
213. Roitman DB, Antoniadis H, Helbing R, Pourmiazaie F, Sheats JR (1998) Proc SPIE 3476:232

214. Suh Y-S, Ko SW, Jang B-J, Shim H-K (2002) Opt Mater 21:109
215. Lee J, Cho H-J, Jung B-J, Cho NS, Shim H-K (2004) Macromolecules 37:8523
216. Chou C-H, Hsu S-L, Dinakaran K, Chiu M-Y, Wei K-H (2005) Macromolecules 38:745
217. Takagi K, Kunii S, Yuki Y (2005) J Polym Sci A Polym Chem 43:2119
218. Klärner G, Davey MH, Chen W-D, Scott JC, Miller RD (1998) Adv Mater 10:993
219. Klärner G, Lee J-I, Davey MH, Miller RD (1999) Adv Mater 11:115
220. Tokito S, Weinfurtner K-H, Fujikawa H, Tsutsui T, Taga Y (2001) Proc SPIE 4105:69
221. Lee J-I, Klaerner G, Davey MH, Miller RD (1999) Synth Met 102:1087
222. Becker S, Marsitzky D, Setayesh S, Müllen K, Friend RH, MacKenzie JD (2000) UK Patent Appl: GBP 0018782.3
223. Becker S, Ego C, Grimsdale AC, List EWJ, Marsitzky D, Pogantsch A, Setayesh S, Leising G, Müllen K (2002) Synth Met 125:73
224. Ego C, Marsitzky D, Becker S, Zhang J, Grimsdale AC, Müllen K, MacKenzie JD, Silva C, Friend RH (2003) J Am Chem Soc 125:437
225. Klaerner G, Miller RD, Hawker CJ (1998) Polym Prepr 39(2):1006
226. Marsitzky D, Vestberg R, Blainey P, Tang BT, Hawker CJ, Carter KR (2001) J Am Chem Soc 123:6965
227. Tang H-Z, Fujiki M, Zhang Z-B, Torimitsu K, Motonaga M (2001) Chem Commun: 2426
228. Setayesh S, Grimsdale AC, Weil T, Enkelmann V, Müllen K, Meghdadi F, List EJW, Leising G (2001) J Am Chem Soc 123:946
229. Trimpin S, Grimsdale AC, Räder HJ, Müllen K (2002) Anal Chem 74:3777
230. Jacob J, Oldridge L, Zhang J, Gaal M, List EJW, Grimsdale AC, Müllen K (2004) Curr Appl Phys 3:339
231. Oldridge L, Grimsdale AC, Müllen K, unpublished results
232. Lee J-H, Hwang D-H (2003) Chem Commun: 2836
233. Pogantsch AF, Wenzl FP, List EWJ, Leising G, Grimsdale AC, Müllen K (2002) Adv Mater 14:1061
234. List EWJ, Pogantsch A, Wenzl FP, Kim C-H, Shinar J, Loi MA, Bongiovanni G, Mura A, Setayesh S, Grimsdale AC, Nothofer HG, Müllen K, Scherf U, Leising G (2001) Mater Res Soc Symp Proc 665:C5.47.1
235. Lupton JM, Schouwink P, Keivanidis PE, Grimsdale AC, Müllen K (2003) Adv Funct Mater 13:154
236. Leclère P, Hennebicq E, Calderone A, Brocorens P, Grimsdale AC, Müllen K, Brédas JL, Lazzaroni R (2003) Prog Polym Sci 28:55
237. Jäckel F, De Feyter S, Hofkens J, Köhn F, De Schryver FC, Ego C, Grimsdale A, Müllen K (2002) Chem Phys Lett 362:534
238. Janietz S, Bradley DDC, Grell M, Giebeler C, Inbasekaran M, Woo EP (1998) Appl Phys Lett 73:2453
239. Gross M, Muller DC, Nothofer H-G, Scherf U, Neher D, Meerholz K (2000) Nature 405:861
240. Brown TM, Friend RH, Millard IS, Lacey DJ, Burroughes JH, Cacialli F (2001) Appl Phys Lett 79:174
241. Bernius M, Inbasekaran M, Woo E, Wu W, Wujkowski L (2000) Thin Solid Films 363:55
242. Chen JP, Klaerner G, Lee J-I, Markiewicz D, Lee VY, Miller RD, Scott JC (1999) Synth Met 107:129
243. Chen JP, Markiewicz D, Lee VY, Klaerner G, Miller RD, Scott JC (1999) Synth Met 107:203
244. Miteva T, Meisel A, Knoll W, Nothofer HG, Scherf U, Müller DC, Meerholz K, Yasuda A, Neher D (2001) Adv Mater 13:565

245. Müller DC, Braig T, Nothofer H-G, Arnoldi M, Gross M, Scherf U, Nuyken O, Meerholz K (2000) Chem Phys Chem 1:207
246. Raymond F, Xiao SS, Nguyen MT (2001) Polym Prepr 42(2):587
247. Xia C, Advincula RC (2001) Macromolecules 34:5854
248. Ego C, Grimsdale AC, Uckert F, Yu G, Srdanov G, Müllen K (2002) Adv Mater 14:809
249. Uckert F, Setayesh S, Müllen K (1999) Macromolecules 32:4519
250. Uckert F, Tak Y-H, Müllen K, Bässler H (2000) Adv Mater 12:905
251. Kulkarni AP, Kong X, Jenekhe SA (2004) J Phys Chem B 108:8689
252. Wu F-I, Reddy S, Shu C-F, Liu MS, Jen AK-Y (2003) Chem Mater 15:269
253. Shu C-F, Dodda R, Wu F-I, Liu MS, Jen AK-Y (2003) Macromolecules 36:6698
254. Donat-Bouillud A, Lévesque I, Tao Y, D'Iorio M, Beaupré S, Blondin P, Ranger M, Bouchard J, Leclerc M (2000) Chem Mater 2000:1931
255. Lévesque I, Donat-Bouillud A, Tao Y, D'Iorio M, Beaupré S, Blondin P, Ranger M, Bouchard J, Leclerc M (2001) Synth Met 122:79
256. Cho HN, Kim DY, Kim JK, Kim CY (1997) Synth Met 91:293
257. Ranger M, Leclerc M (1998) Can J Chem 76:1571
258. Charas A, Barbagallo N, Morgado J, Alcácer L (2001) Synth Met 122:23
259. Liu B, Yu W-L, Lai W-H, Huang W (2001) Chem Mater 13:1984
260. Kameshima H, Nemoto N, Endo T (2001) J Polym Sci A Polym Chem 39:3143
261. Yu W-L, Cao Y, Pei J, Huang W, Heeger AJ (1999) Appl Phys Lett 75:3270
262. Yu W-L, Pei J, Cao Y, Huang W, Heeger AJ (1999) Chem Commun: 1837
263. Liu B, Yu W-L, Lai Y-H, Huang W (2000) Chem Commun: 551
264. Stork M, Gaylord BS, Heeger AJ, Bazan GC (2002) Adv Mater 14:361
265. Gaylord BS, Heeger AJ, Bazan GC (2002) Proc Natl Acad Sci USA 99:10 954
266. Gaylord BS, Heeger AJ, Bazan GC (2003) J Am Chem Soc 125:896
267. Liu MS, Jiang X, Herguth P, Jen AK-Y (2001) Chem Mater 13:3820
268. Jiang X, Liu S, Zheng L, Liu M, Jen AK-Y (2000) Polym Prepr 41(1):873
269. Jiang X, Liu S, Ma H, Jen AK-Y (2000) Appl Phys Lett 76:1813
270. Millard IS (2000) Synth Met 111–112:119
271. O'Connor SJM, Towns CR, O'Dell R, Burroughes JH (2001) Proc SPIE 4105:9
272. Salbeck J (1996) Ber Bunsenges Phys Chem 100:1666
273. Kreuder W, Lupo D, Salbeck J, Schenk H, Stehlin T (1996) Eur Patent Appl: EP 707 020
274. Wu Y, Li J, Fu Y, Bo Z (2004) Org Lett 6:3485
275. Yu W-L, Pei J, Huang W, Heeger AJ (2000) Adv Mater 12:828
276. Müller CD, Falcou A, Reckefuss N, Rojahn M, Wiederhirn V, Rudati P, Frohne H, Nuyken O, Becker H, Meerholz K (2003) Nature 421:829
277. Grisorio R, Mastronilli P, Nobile CF, Romanazzi G, Surana EP, Acierno D, Amendola E (2005) Macromol Chem Phys 206:448
278. Vak D, Chun C, Lee CL, Kim J-J, Kim D-Y (2004) J Mater Chem 14:1342
279. Setayesh S, Marsitzky D, Müllen K (2000) Macromoledules 33:2016
280. Grimsdale AC, Leclère P, Lazzaroni R, MacKenzie JD, Murphy C, Setayesh S, Silva C, Friend RH, Müllen K (2002) Adv Funct Mater 12:729
281. Keivanidis PE, Jacob J, Oldridge L, Sonar P, Carbonnier B, Baluschev S, Grimsdale AC, Müllen K, Wegner G (2005) Chem Phys Chem 6:1650
282. Marsitzky D, Scott JC, Chen J-P, Lee VY, Miller RD, Setayesh S, Müllen K (2001) Adv Mater 13:1096
283. Jacob J, Sax S, Piok T, List EJW, Grimsdale AC, Müllen K (2004) J Am Chem Soc 126:6987
284. Somma E, Loppinet B, Fytas G, Setayesh S, Jacob J, Grimsdale AC, Müllen K (2004) Colloid Polym Sci 282:867

285. Kreyenschmidt M, Uckert F, Müllen K (1995) Macromolecules 28:4577
286. Stern R, Lupo D, Salbeck J, Schenk H, Stehlin T, Müllen K, Scherf U, Huber J (1996) Eur Patent Appl: EP 699 699
287. Grazulevicius JV, Strohriegl P, Pielichowski J, Pielichowski K (2003) Prog Polym Sci 28:1297
288. Morin J-F, Leclerc M, Ades D, Siove A (2005) Macromol Rapid Commun 26:761
289. Ngbilo E, Ades D, Chevrot C, Siove A (1990) Polym Bull 24:17
290. Siove A, Aboulkassim A, Faid K, Ades D (1995) Polym Int 37:171
291. Romero DB, Schaer M, Leclerc M, Adès D, Siove A, Zuppiroli L (1996) Synth Met 80:271
292. Lmimouni K, Legrand C, Chapoton A (1998) Synth Met 97:151
293. Morin J-F, Leclerc M (2001) Macromolecules 34:4680
294. Dierschke F, Grimsdale AC, Müllen K (2003) Synthesis: 2470
295. Morin J-F, Leclerc M (2002) Macromolecules 35:8413
296. Iraqi A, Wataru I (2004) Chem Mater 16:442
297. Zotti G, Schiavon G, Zecchin S, Morin J-F, Leclerc M (2002) Macromolecules 35:2122
298. Li J, Dierschke F, Wu J, Grimsdale AC, Müllen K (2006) J Mater Chem 16:96
299. Morin J-F, Boudreault P-L, Leclerc M (2003) Macromol Rapid Commun 23:1032
300. Morin J-F, Beaupre S, Leclerc M, Levesque I, D'Iorio M (2002) Appl Phys Lett 80:341
301. Patil SA, Scherf U, Kadashchuk A (2003) Adv Funct Mater 13:609
302. Dierschke F, Grimsdale AC, Müllen K (2004) Macromol Chem Phys 205:1147
303. Jenekhe SA, Chen XL (1998) Science 279:1903
304. Zhong XF, François B (1988) Makromol Chem Rapid Commun 9:411
305. Zhong XF, François B (1989) Synth Met 29:E35
306. Zhong XF, François B (1991) Makromol Chem 192:2277
307. François B, Zhong XF (1991) Synth Met 41:955
308. François B, Widawski G, Rawiso M, Cesar B (1995) Synth Met 69:463
309. Mays J, Hong K, Wang Y, Advincula RC (1999) Mater Res Soc Symp Proc 561:189
310. Widawski G, Rawiso M, François B (1994) Nature 369:387
311. Romero DB, Schaer M, Staehli JL, Zuppiroli L, Widawski G, Rawiso M, François B (1995) Solid State Commun 95:185
312. Romero DB, Schaer M, Zuppiroli L, Cesar B, Widawski G, François B (1995) Opt Eng 34:1987
313. Marsitzky D, Klapper M, Müllen K (1999) Macromolecules 32:8685
314. Marsitzky D, Brand T, Geerts Y, Klapper M, Müllen K (1998) Macromol Rapid Commun 19:385
315. Marsitzky D (1999) Funktionalisierung von konjugierten Polymeren auf der Basis von PPP, PhD Thesis, Johannes Gutenberg University, Mainz
316. Schmitt C, Nothofer H-G, Falcou A, Scherf U (2001) Macromol Rapid Commun 22:624
317. Güntner R, Asawapirom U, Forster M, Schmitt C, Stiller B, Tiersch B, Falcou A, Nothofer H-G, Scherf U (2002) Thin Solid Films 417:1
318. Leclère P, Calderone A, Marsitzky D, Francke V, Geerts Y, Müllen K, Brédas J-L, Lazzaroni R (2000) Adv Mater 12:1042
319. Surin M, Marsitzky D, Grimsdale AC, Müllen K, Lazzaroni R, Leclère P (2004) Adv Funct Mater 14:708
320. Klaerner G, Trollsås M, Heise A, Husemann M, Atthoff R, Hawker CJ, Hedrick JL, Miller RD (1999) Macromolecules 32:8227
321. Johansson DM, Grandlund T, Theander M, Inganäs O, Andersson MR (2001) Synth Met 121:1761
322. Theander M, Grandlund T, Johanson DM, Ruseckas A, Sundström V, Andersson MR, Inganäs O (2001) Adv Mater 13:323

Editor: Ullrich Scherf